



TECHNISCHE
UNIVERSITÄT
WIEN
Vienna | Austria

DIPLOMARBEIT

Exploring the Potential of Organic Cells in Building Integrated Photovoltaic Systems

unter der Leitung von

Univ.-Prof. Ardeshir Mahdavi

E 259 Abteilung für Architekturwissenschaften

Institut für Architekturwissenschaften

eingereicht an der

Technischen Universität Wien

Fakultät für Architektur und Raumplanung

von

Camilla Parrella

1526533

e1526533@student.tuwien.ac.at

Wien, November 2017

ABSTRACT

Besides the ecological advantages, the Photovoltaic plays a very important role in the daylight provision. Although the capacity of collecting energy for the use in buildings is increasing, the visual performance of the technology seems not to have the same importance. In this work the photovoltaic technologies available will be examined and evaluated in terms of both visual and ecological performance. The materials, the installation methods and the energy conversion capacity together with the efficiency and daylight calculation will demonstrate the potential of the organic solar cells. The market counts now three main technologies and, for their bad efficiency, Organic PVs are not considered a good choice. Their potential will be analyzed by evaluating a sample office building with integrated photovoltaic systems in order to see the different visual behavior of the technologies and to prove the good performance of OPVs, which will make them the best choice in the building sector's future. Two main simulations will be conducted: a thermal evaluation for the energy production and its capacity to help the building energy consumption beside a more important visual evaluation of one office room. The aim is to compute performance indicators that define the inside visual comfort and to analyze their results to see the behavior of a layer of OPVs integrated into windows. The expectation is to demonstrate that this integration will not deny the visual comfort that daylight gives and together will provide electrical energy.

Keywords

Organic photovoltaic cells, BIPV, visual comfort, daylight, energetic demand.

ACKNOWLEDGEMENTS

The process of writing a thesis includes the sharing of the knowledge acquired and in acquisition with the people that supports, helps and evaluates the work.

My process would not be the same without the passion and the competence of the professors and colleagues of Technische Universität Wien. It was a pleasure and an honor to be part of the team that in October 2015 started the Master in *Building Science and Technology*. The experience allowed me to grow up academically, professionally and humanly.

This thesis is one step of my journey towards architecture and engineering, that I chose to be the path of the definition of my personal being.

The research was supported by Univ.Prof.Dipl-Ing. A. Mahdavi, Univ.Ass.Dipl-Ing. U.Pont, Assistant Prof.Dipl-Ing. M.Schuss, Univ.Ass. F.Tahmasebi. From them I took inspiration and motivation. I certainly do not consider this as a final work, too much is still to come.

The process of writing a thesis starts with an opportunity: someone one day decided I was worthy and I deserve it. This work is for you, nothing would have happen otherwise. To Mum and Dad.

CONTENTS

1	Introduction.....	1
1.1	Overview	1
1.2	Motivation	2
1.3	Background	3
1.3.1	Overview	3
1.3.2	The Building Integrated Photovoltaic System.....	3
1.3.2.1	The BIPVT (building integrated photovoltaic thermal) system	7
1.3.3	BIPV in facades and windows.....	8
1.3.4	Photovoltaic cells: the technologies, the materials, the developments 11	
1.3.4.1	The PV production and application companies	15
1.3.5	The OPVs technology for BIPV application.....	15
1.3.5.1	Flat heterojunctions.....	16
1.3.5.2	Bulk heterojunctions.....	17
1.3.6	Transmission and transparency.....	21
1.3.7	Substrates	23
1.3.8	Production methods.....	24
1.3.8.1	Coating techniques	24
1.3.8.2	Printing techniques	24
1.3.9	Architecture of Organic Solar Cells	26
1.3.10	The integration of OPVs in buildings: companies and buildings	28
2	Method	32
2.1	Overview	32
2.2	Hypothesis.....	32
2.3	The sample office building	33
2.4	The thermal simulation: performance indicators and computation methodology	39
2.5	The visual simulation: performance indicators and computation methodology	43

3	Results	48
3.1	Overview	48
3.2	Thermal Simulation Results	48
3.2.1	Annual and Monthly Heating Demand	49
3.2.2	Annual and Monthly Cooling Demand.....	52
3.2.3	Annual and Monthly Electric Demand	58
3.2.4	Annual and Monthly Energy Production	59
3.2.5	Annual Total Demand and Energy Production Comparison	64
3.3	Visual Simulation Results	66
3.3.1	Illuminance and Uniformity	67
3.3.2	Daylight Autonomy	76
3.3.3	Daylight Glare.....	78
3.3.4	Daylight Factor	83
3.3.5	Irradiance	88
3.3.6	Color Spectrum.....	93
4	Discussion	96
5	Conclusion.....	103
6	Index.....	104
6.1	List of Figures	104
6.2	List of Tables	108
6.3	List of Equations	110
7	Literature	111
8	Appendix	116
A.	Thermal Simulation tables.....	116
B.	Visual Simulation tables and graphs.....	119

1 INTRODUCTION

1.1 Overview

The high demand of increasing the usage of renewable resources to minimize the consumption of fossil fuels and gas emissions and so the environment pollution is day by day growing, especially in the sector of building. It is, in fact, responsible of almost a third of energy consumptions, starting from the construction to the high utilization of systems that requires everyday more energy.

Providing buildings with solar and photovoltaic systems is an effective way to turn the energetic use to a different level: these systems can make the building almost self-sufficient in the energy production in a way that they are actively producing what they need and passively consuming. This helps to decrease the general consumption in buildings during their lifetime, due mostly to heating and cooling systems and to store energy spendable in other fields. The usage of photovoltaic systems to collect and provide energy, together with the idea of integrating them into building elements is not a new topic, but there have been developed new technologies and others are emerging.

Next to the roofing installation of silicon cells, which can be considered the most spread and efficient technology and combination, the integration of new cells has been performed and the organic technology is becoming more effective and so more attractive. In particular, the Building Integration of Photovoltaic Systems (BIPV) moved from roof installation to facades and windows: combining the thermal and visual performance, transparent cells integrated into the glass of windows or facades allow visual comfort in interior spaces by transmitting and absorbing daylight that both generates electricity and provides natural illumination, reducing even more the energetic demand. According with this, the development of integration into windows has also aesthetical reasons: if photovoltaic modules mounted on facades strongly influenced the architecture, the presence of thin film layers in the glazing structure does not influence the aesthetical appearance, guaranteeing to architect more design choices.

The attraction of this new possibility opened the door to a research on organic photovoltaic cells. Despite their still low efficiency, which makes them the third technology used for photovoltaic systems, they seem to be the best choice for windows integration considering their high flexibility and lightweight.

The work here presented aimed to evaluate this potential both by looking at the companies' products and simulating a virtual installation: theoretically the critics still dispute the low efficiency of organic cells but practical applications, which studied the right exposure, orientation and cell design demonstrated that they can compete with the other technologies. The steps consider a theoretical background of BIPV and organic photovoltaic materials, a close look into companies and their projects and then a representative performance analysis to concretely calculate the savings in the energetic demands and the visual comfort that the technology is able to guarantee.

1.2 Motivation

Starting from the general overview of consumptions, pollution data, greenhouse gases emergency, energy saving necessity, it has been showed that the urgency is to develop new solutions for energy provision and new smart buildings and building systems able to self-sufficiently collect it.

The photovoltaic systems are today highly used all over the world and the standards in almost every country require their presence in the new buildings. Although the wide-spread use, the cost of production and installation is still high and the market only counts one big technology which is worth using: the crystalline silicon. These cells' efficiency and durability have been long studied and developed, but it must be still considered that the lack of usage of renewable materials do not go in their favour. In this way, the demand for the organic technology is increasing. Not only the ecological importance but both the mass and economical production possibility and its properties of lightweight and transparency are considerable factors which make this technology worth improving for the future. In particular, the high versatility due to organic chemistry, the energy yield due to a positive temperature coefficient of the power conversion efficiency, the non-toxicity and low consumption of abundant absorber materials and the property of merging possibility with architecture for tenability of colors play an important role in their high consideration for application in windows. In fact, in terms of visual requirements, the performance of organic cells is higher than the others because of their transparency property. This makes them worth using in windows as a layer between the glass panes and in facades, combined with glass, as a covering material. In this way, their energetic importance is combined with the need of providing natural light inside the buildings. An artificial lighting, in fact, requires a lot of the energy collected by the PV system. If a system can provide energy but shuts out the daylight transmission, it is, in some

way, “self-harming”. The potential of organic technology is strongly connected with this peculiarity.

1.3 Background

1.3.1 Overview

The research has to start with an overview over the technology that today is mostly used and its properties, because the topic is counting many complicated factors and studies. The integration of photovoltaic systems into buildings may seem a simple idea but it has many declinations, because of its advantages that made it worth exploring and implementing. In this way not only the photovoltaic but also the solar systems started to be integrated. Additionally, the integration keeps different meanings, from the positioning of photovoltaic modules on a building element to the study of orientation, the surroundings’ shading, the cells design, their material composition and their environmental impact and efficiency.

1.3.2 The Building Integrated Photovoltaic System

“Building Integrated Photovoltaic BIPV have dual functionality: replace the conventional elements of construction and generate energy.”(Ceròn et al. 2013)

Integration of systems into buildings is exactly the replacing of materials of elements like roof, façade, shading in favor of photovoltaic modules, usually connected to the grid to share with it the energy collected. The idea of BIPV was born in late 1970s when the developments in the photovoltaic fields were increasing the efficiency of the systems and, instead of limiting the effectiveness of the use in buildings to the mere positioning of panels on the roof tops, they have been rethought as constructive elements. In this way the integration is not equivalent to a simple addition, but the photovoltaic system influences actively the performance of the building. In fact, part of the incident solar radiation beam is directly converted into electricity by the PV cells, before transmitting through the envelope and, in the case of semi-transparent modules, it changes the visible transmittance of light, the internal visual comfort and the artificial lighting demand.

As mentioned above, the most diffuse integration techniques nowadays are in:

- roofing elements: replacing of tiles or installation of modules (flat or sloped) on flat roofs;

- facades: curtain walling, replacing of glass elements in favor of PV transparent modules, external cladding elements in ventilated facades;
- shadings: installation of modules or cells arrows on shading devices, mostly sun-oriented, situated to avoid internal overheating, so in the best position to catch the highest sunlight amount;
- windows: film layer of very thin cells integrated outside or inside the glazing structure.

The techniques are expressed in chronological order: the introduction of semi-transparent PV modules in BIPV designs is the latest discover, due to the corresponding need of development of adequate cells. It has complicated the analysis of building energy performance, because the potential of daylight provision causes a heat transfer increasing and so a higher energetic demand for cooling.

As BIPV can make use of the building envelope for solar collection providing an efficient way of reducing building energy consumption, the best integration is achieved when the system design is taken into consideration in the building design stage. This leads to a better aesthetical quality of the entire building architecture, achieved a good composition between materials, together with a previous analysis of the actual building demands and energy consumptions, which helps to install the right PV power.

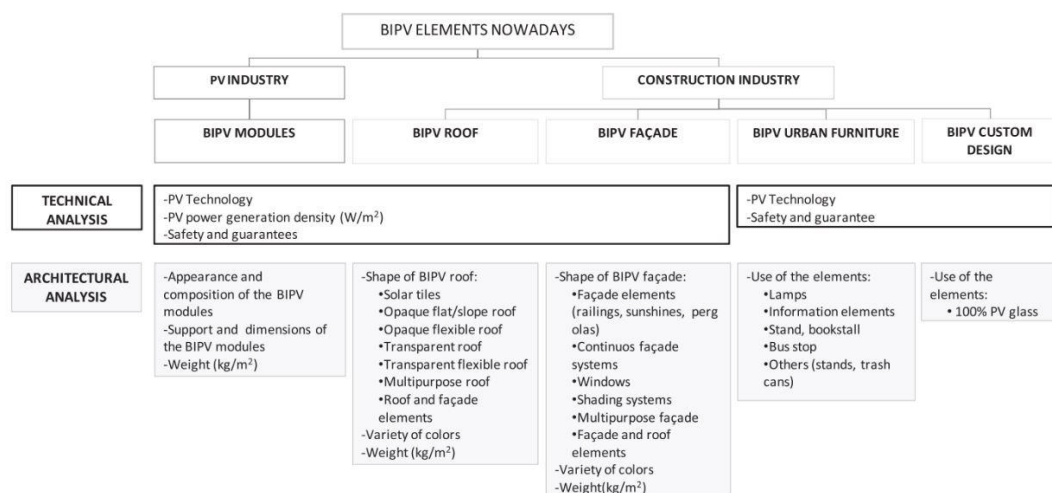


Figure 1 BIPV elements summary.

Fig.1 reassumes the BIPV elements and underlines the architectural elements that can 'host' the PV modules and other diffuse application outside the building sector.

The analysis of the building needs is not the only factor to consider when installing BIPV systems: in order for the system to work at its best, it is necessary to combine

it with the right panel orientation, the surroundings analysis, to avoid other buildings or nature shading effect, and the temperature distribution of the location, which can negatively affect the modules performance. It is true that the energy collection of BIPV can help to decrease the consumption, but it is also true that it must be quantified depending on all the factors expressed above.

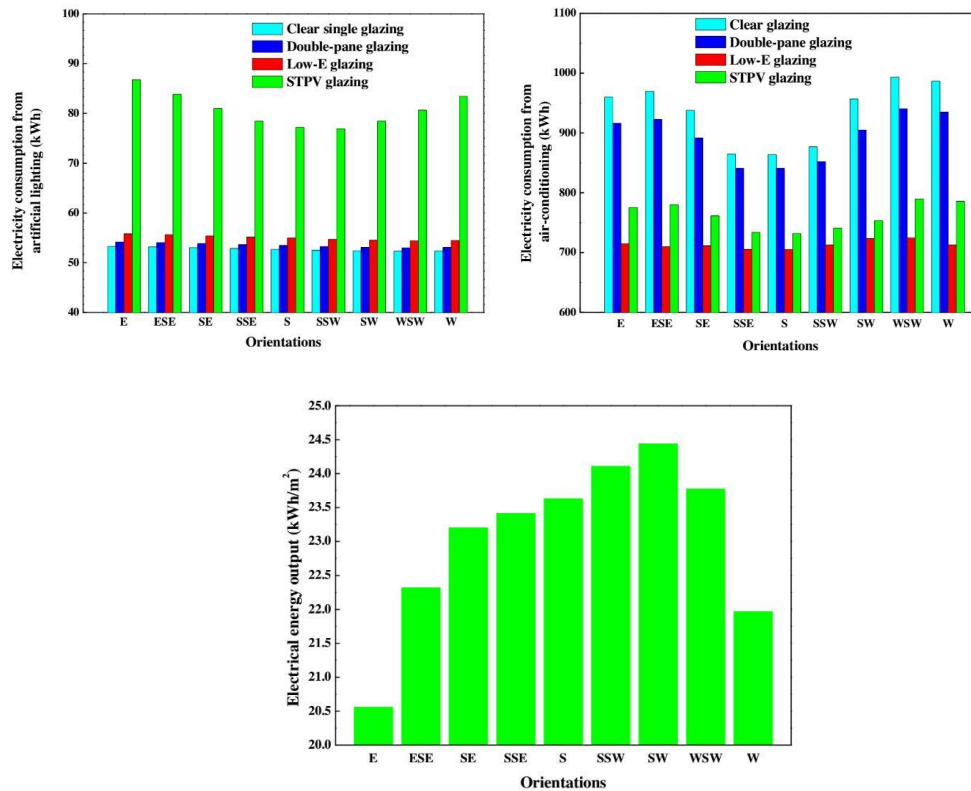


Figure 2 Panels orientation influence on electrical consumptions: electrical consumption for air conditioning, for lighting and total electrical energy output. Example of a building in Hong Kong.

An example from a research conducted over an office building in Hong Kong by Zhang, Lu, Peng and Song, which has window BIPV integration of semi-transparent photovoltaic (STPV) cells, is here proposed to show the importance of a good system design. Fig.2 above give an overview on the impact that the orientation of BIPV system has on the annual Air Conditioning and artificial lighting consumptions. It is possible to clearly see the difference of PV efficiency in energetic power outputs for different window orientations: for the case of Hong Kong it is better to install the system on the SW windows, in order to obtain the best energetic performance. This concept is to take into consideration for the BIPV in windows but also in facades and shading devices; moreover, it has also to be considered the orientation in the case of positioning sloped PV modules on flat roof. In case of windows, the orientation has an impact not only on the energy collection but also on the daylight provision.

Regarding the temperature influence on efficiency, Kontinen first and Skoplaki then described the effect, saying that: “High operating temperatures have a negative effect both on the efficiency and lifetime of the PV system. On one side, the PV efficiency decreases practically linearly with increasing of T_{mod} and on the other side, the PV lifetime is strongly influenced by high operating temperatures, due to the large number of temperature-induced degradation effects, such as diffusion of impurities and dopants in the solar cell material, diffusion of moisture and contaminates in the encapsulant as well as thermal oxidation of the cell or encapsulant” (“*Experimental investigation of a low cost passive strategy to improve the performance of Building Integrated Photovoltaic systems*”, 2014).

Considering the design and the elements of integration is one side of the BIPV technology analysis; on the other side, the differences between PV cells play an equally important role in the performance efficiency. The market of PV system is lead by the silicon-based cells (mono and multi-crystalline), which are suitable for mostly all the integration techniques as they can be installed as modules and as layers very easily and they are high efficient and high reliable. In 2013, Cerón, Caamaño-Martín and Neila studied the utilization's distribution of different PV cells technologies in BIPV and grouped them into the following charts.

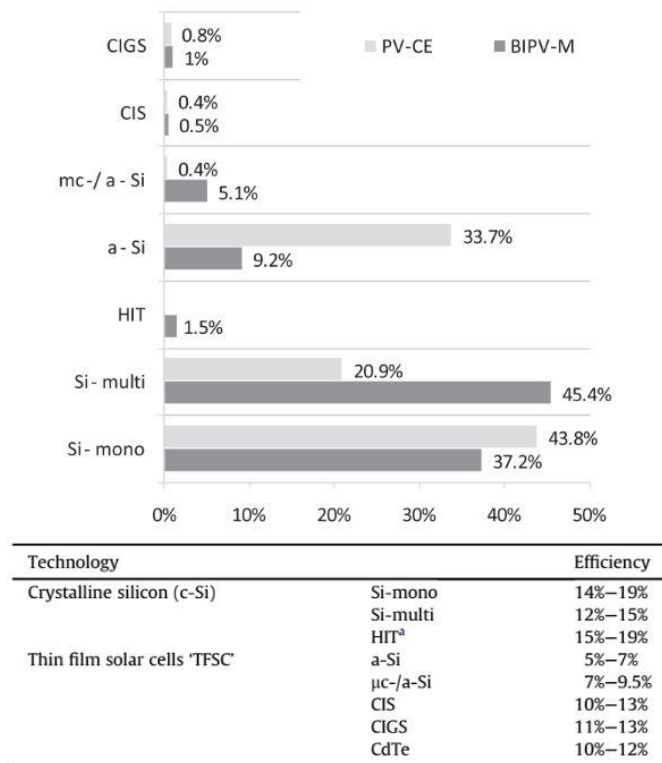


Figure 3 Cells utilization's distribution and efficiency differences of photovoltaic technologies.

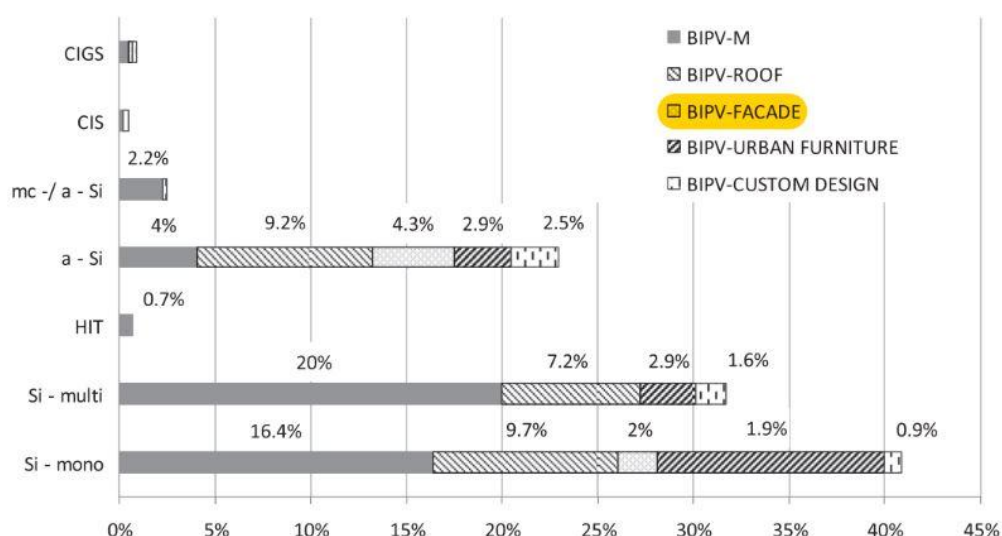


Figure 4 Diffusion of PV integration methods divided by elements of the building.

They took into consideration crystalline cells and thin-film cells: the first ones are mostly installed in mono and multi structure as modules in roof and other urban applications, while the second ones, especially the amorphous silicon (a-Si), are more suitable for facades for their construction possibilities of large size, small thickness and transparency. Their review was rather exhaustive considering the BIPV market of that year, but during the years this latter has seen the developments of other technologies, such as the dye sensitized cells and the organic cells in the group of thin-film, which have taken place step by step next to the more spread and traditional crystalline ones.

1.3.2.1 The BIPVT (building integrated photovoltaic thermal) system

The necessity of decreasing the energy consumption is strongly connected with the HVAC but also to other building systems, for example the hot-water one. The further development of the BIPV is the BIPVT, where the energetic needs meet the thermal ones: the energy collected by the photovoltaic modules is meant to be use for the functioning of the hot-water system. The aim is to provide to the building both electrical and thermal power, in order to satisfy the need of electricity and hot water. As most of the thermal systems, the BIPVT systems are installed on the roof top, although configurations for facades, walls and windows integrations have also been explored. These systems can be either semi-transparent or opaque, as the PV ones, according to the necessity of providing or not daylight.

BIPVT systems are efficient for both air and water-based thermal systems, but due to easier construction and operation of PVT with air heat extraction rather than with water heat extraction, the former has more extensively been studied as an alternative and cost effective solution to building integrated photovoltaic (BiPV) systems.

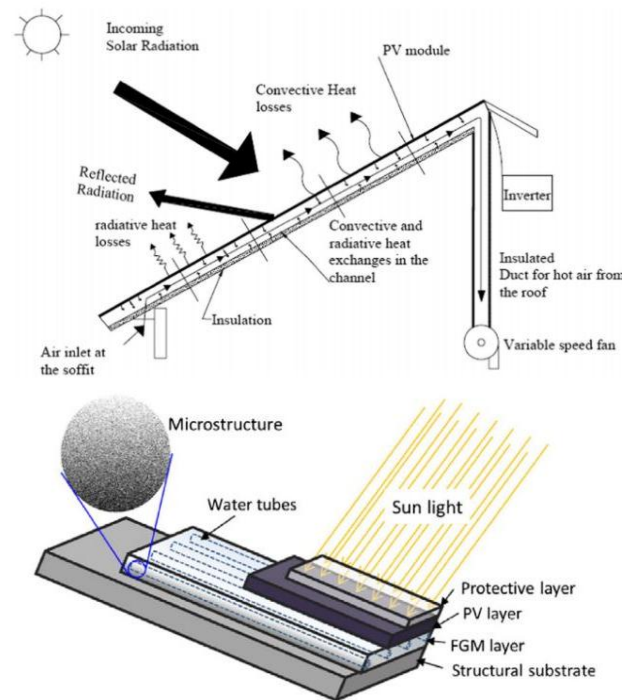


Figure 5 Example of a BIPVT module's structure.

Fig.5 above represents respectively an air-based and water-based system installed on roof top. The photovoltaic is connected to the fan on one side and to the water collector on the other to provide charge to the system.

1.3.3 BIPV in facades and windows

This research aims at evaluating the visual and thermal performance of organic cells so it is necessary to understand deeply the integration in façades and windows. The attraction of these two BIPV systems is mostly due to their optical properties, which provide visual comfort to occupants of interior spaces. Moreover, they have become increasingly attractive also because they allow more choices in terms of facades' design thanks to the variability of integration. In terms of energetic performance, Lu and Law found that the BIPV window has the potential to reduce over 65% of the total heat gain when compared with a conventional clear glass window. The integration into facades and windows is generally made as in the figures below.

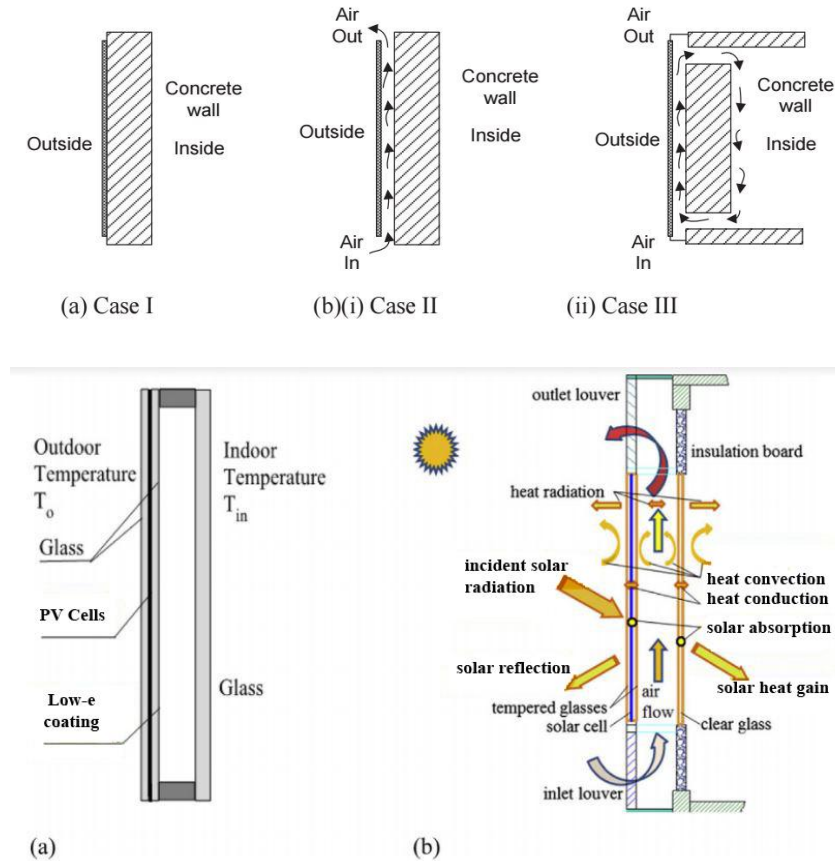


Figure 6 PV Integration mode on facades and windows (a). Three different positions cases. Heat behavior in the case of a window integration (b).

In the case of wall BIPV, different solutions can be found, depending on the wall structure desired (normal wall, ventilated-wall, BIPVT wall attached as a ventilated facade with indoor airflow used to cool the PV panel).

In the case of window BIPV, the PV layer is usually integrated on the outside to better catch the sunlight and the glazing structure can be easily customized.

The analysis of these BIPV systems will be here conducted over different representative examples and last technologies development, which can at best explain the working concept and advantages.

First, it has to be considered that, in the case of windows, the typical figure-of-merit of a solar cell, energy conversion efficiency and the relation between transmittance and efficiency are not sufficient parameters to define the overall thermal-optical performance of the system. In fact, there is a widespread presence of good-working window systems which have nominally low cell efficiency. Then, it is important to have in mind that as solar radiation is partly converted into electricity, the daylight

illuminance in the interior spaces will decrease: in this way it should be expected a balance between the efficiency power that cells can theoretically have and the one actually installed to allow a beneficial visual comfort.

Chae, Kim, Park and Shin in their report presented an approach to evaluate the performance of semi-transparent BIPV in window. In particular they used for the simulation hydrogenated amorphous silicon, which is one of the most used materials in case of façade and window integration. They grouped the reasons of this spread use, which prove the potential of the material, as followed:

- a-Si:H solar cells can be easily fabricated on the glass windows in a large scale;
- -extremely thin layer thickness from 100 nm to 250 nm is all that is required for sunlight absorption which does not add more weight on the glasses;
- -the transparency of the film can be easily controlled by changing the thickness of a-Si:H layers and the surface morphology.

Mostly all of the window integrations up to now have this technology applied. This is a well performing material but it must be considered that it shows a performance decrease in front of high environment temperatures, so it is suitable mostly for non-tropic and non-equatorial climates. Additionally the level of transparency that can be reached are still low. Fig. 7 below shows the achievements for solar modules in 2014.

Solar module	Transparency (%) 400-800 nm	Efficiency (%)
a-Si:H (our)	20	6.5
Schott	10	5.2
SunTech	10	4.5
Smile Solar	10	7.1
Sun Well [7]	20	6.3
Tianwei [8]	20	4.9

Figure 7 Comparison of the efficiency and transparency of aSi semitransparent solar modules (2014).

The research of Zhang, Lu, Peng, Song, already mentioned above about the Hong Kong windows efficiency, is here recalled to analyze the solutions they found for high temperature climate and how they performs. They saw that, comparing the a-Si semi-transparent photovoltaic (STPV) case with the low-e coating glazing, the thermal performance was better in the second case. In fact, “the Low-E coating can block most of the incident long-wave radiation so that it can reduce not only the solar heat gain of windows in cooling dominated area but the heat loss from inward

in cold climate region as well.” (*Comparison of the overall energy performance of semi-transparent photovoltaic windows and common energy-efficient windows in Hong Kong*, 2016). And this is better than the performance of STPV, which are not good in reducing the window heat loss.

Directly connected to this semitransparent cells’ defect, there has been a discover that corrects this behavior. The so called ‘Smart Window’, well described in the works of Connelly, Wu, Chen, Lei, develops the concentrating PV (CPV), which uses an integrated thermotropic membrane layer capable of reducing the loss in presence of high temperature. The design of the window is comprised of a glazing cover laminated with a thermotropic layer with solar cells optically coupled around the edges of the glazing. This layer varies the proportion of light transmitted through it and scattered from it depending on the heat that it is subjected to. The authors specify that “the solar cells are normally attached to the rear of a glass or some other transparent cover with a diffuse reflective surface provided in the spaces between the cells.” (*Design and development of a reflective membrane for a novel Building Integrated Concentrating Photovoltaic (BICPV) ‘Smart Window’ system*, 2016). They also add that “this approach can achieve close to 100% optical efficiency and generate uniform solar radiation on the solar cell surface”.

The advantage of this technology is so explained: “This novel CPV can be thought of as an electricity-generating smart window or glazed facade as this system will respond automatically to the climate, varying the balance of solar energy reflected to the PV for electricity generation and transmitted through the system into the building to provide light and heat. It therefore offers the potential to optimize energy consumption in buildings.” (*Design and development of a reflective membrane for a novel Building Integrated Concentrating Photovoltaic (BICPV) ‘Smart Window’ system*, 2016).

1.3.4 Photovoltaic cells: the technologies, the materials, the developments

As already underlined, the silicon-based cells lead and has lead the market of photovoltaic for a long time, since the development of the first cell in 1950s. The world of solar cells however is more complicated, and “silicon-based” embraces a technology which considers many different materials and production processes.

The basic distinction for photovoltaic cells is made by their structure: they can be crystalline or thin-film.

The first group contains monocrystalline and multicrystalline cells: their difference stands in the silicon molecules crystal structure. Monocrystalline cells have been the first produced. Their shape is a wafer cut with round edges, produced with the Czochralski method. Their high efficiency is the results of a very long and precise process, which accepts no material impurities. This specific requirement of high silicon purity, necessary to obtain a perfect crystalline structure, had to face the fact that silicon availability was decreasing and its price was growing. This forced to find a solution and multicrystalline cells started to be produced. In this case a block casting with a large crystal grain structure avoided costly pulling process needed for monocrystalline cells. Their shape is different from the others: instead of single wafer cuts, the cells are combined in modules, which allow keeping a high standard of efficiency, with square edges. Multicrystalline (or polycrystalline) cells are now more spread in the module production than the monocrystalline ones: their advantages stand not only in lower capital costs, but also in higher throughput, less sensitivity to the quality of the silicon feedstock used and higher packing density, thanks to the rectangular shape.

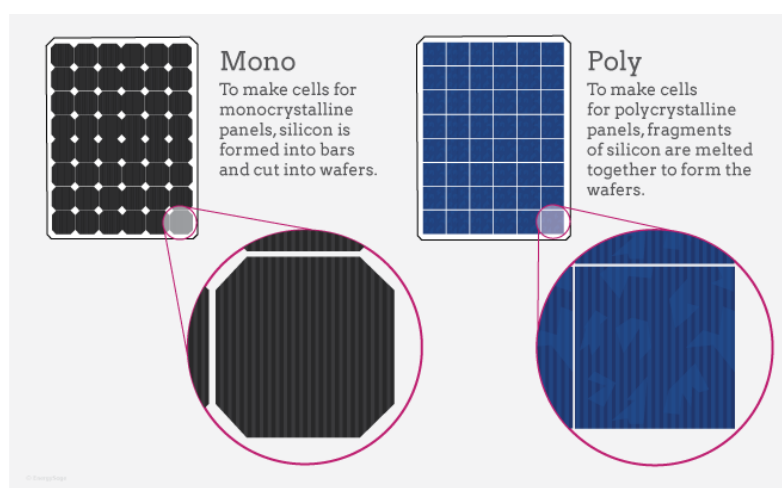


Figure 8 Mono and Poly crystalline cells design's differences.

Next to these crystalline structures, it has been developed also the thin-film technology, where semiconductor materials are deposited on a substrate. The process of deposition of active layer on a support can happen in both the liquid and gas phases: in the first case the respective substrate is brought into contact with a metal melt (Cu, Al, Sn, In) saturated with silicon and, by lowering the temperature of the melt, supersaturation occurs and silicon is deposited, while in the second case, a mixture of H and Si is decomposed thermally at the hot surface of the substrate. These kinds of cells have the advantage of requiring very few amount of silicon: the

need of a substrate, which can vary between low quality silicon and glass, graphite and ceramics, is justified by the necessity of providing a mechanical support due to the reduced thickness of the active layer (5-50 μm). The choice of this support has to be conducted carefully as inexpensive materials usually contain a high level of impurities which causes the migration of these impurities from the substrates into the active Si-layer at high temperatures, influencing negatively the efficiency of the cells. In this way, the deposition on glass and the further processing of cells need to be done at temperature below 600°C, which is its melting point. The other support materials most of times present an insulator material in order to avoid the situation of impurities influence described above. The most common thin-film technology used for photovoltaic cells for buildings is the amorphous silicon (a-Si). It is an alloy of silicon with hydrogen; its process of deposition is mainly the chemical, where diluted SiH_4 with hydrogen is deposited on substrate at temperatures below 500°C. Improvements of solar cells now have to rely mostly on device design. Hydrogen controls the structure of the film and it can be diluted with silicon in different amounts; at very high dilution (<90%), however, a transition to the microcrystalline state of the material occurs.

To sum up, in the table below it is described an example of the performance of these three different cells produced by Ausind Solar, together with their lifetime expectation.


	Monocrystalline Panels	Polycrystalline Panels	Thin Film Panels
Type			
Efficiency	14% – 18% cell efficiency	12% – 14% cell efficiency	5% – 6% cell efficiency
Temperature Tolerance	0% +5%	-5% +5%	-3% +3%
Life Time	25-30 year life span	20-25 year life span	15-20 year life span
Durability	Hail resistant 25 year P & M	25 year P & M warranty	25 year P & M warranty

Figure 9 Comparison between main silicon PV structures. Products of Ausind..

All these cells are suitable for the use in buildings, as already said. What make them available for that is their efficiency level, which provides good power energy conversion and high energy collection amounts, their lifetime expectation, that

assures a long performance, their good production method, various and reliable, their module configuration, which allows the use as panels on roof and facades and their thin layer alternative configuration, which allows the use on windows. The production processes, moreover, have been improved through the years, making them cheaper, more effective and faster in the large production of cells and panels.

The only negative note in this picture seems to be the inorganic material nature and its availability as a not renewable resource. These two aspects increase the development of other materials in the photovoltaics production since 1990s.

Although through the years some other compounds have been tested, such as copper indium diselenide, cadmium telluride and some others III-V compounds, for the specific use in buildings, dye sensitized cells and organic cells are the most important alternatives.

Dye sensitized solar cells (DSSC) can be considered organic-inorganic hybrid cells. Nanocrystalline TiO_2 is coated on a transparent conducting oxide (TCO). Their photovoltaic mechanism is based on a fast regenerative photoelectrochemical process and the dye element, responsible for the light absorption, is absorbed onto the TiO_2 surface, making these cells different from the ones described above. What makes this technology particularly suitable for building applications is their transparency possibility in different degrees. However, the efficiency of these cells is strongly connected to the thickness of the TiO_2 and it affects the transparency: in fact, as the electron of the active material becomes thicker to improve the efficiency, the light transmittance possibility rapidly decreases. To overcome this problem, different combinations of thickness have been tried and still are: up to now the efficiency is around 10%. Their use is focused on facades and windows; an example of integration in façade of transparent and colored cells is provided below.

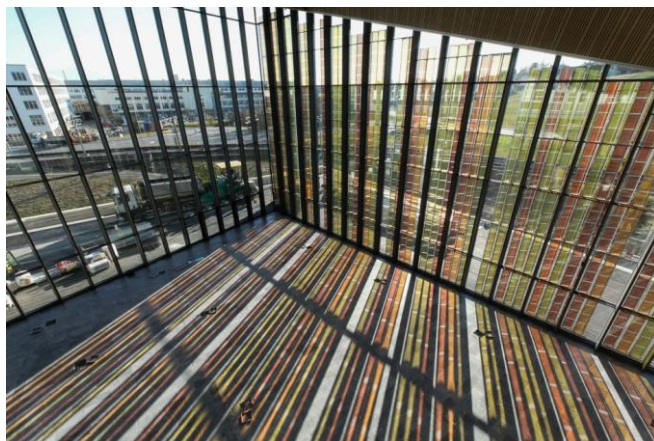


Figure 10 Integration of DSC. Example of SwissTech Convention Centre in Switzerland.

1.3.4.1 The PV production and application companies

In 2016 the following companies resulted to be the most involved in the photovoltaic production and projects supporting of building integration. Most of them are born in Asia, especially in China, but operate all over the world. The products are mostly monocrystalline and polycrystalline cells and the projects regard residential and commercial buildings together with plant installation to support other energy production systems, as wind power plants, or stand alone plants to collect solar energy.

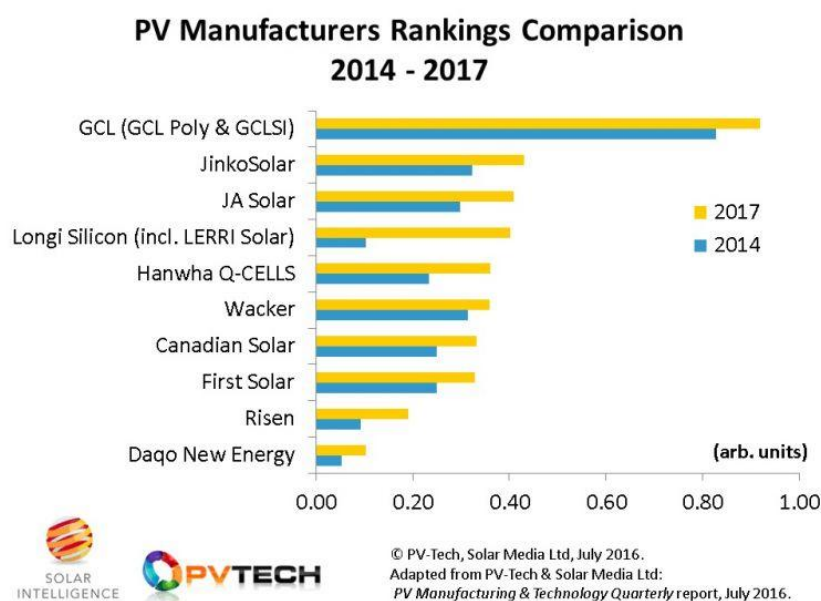


Figure 11 PV Manufacturers Rankings Comparison up to July 2016 by First Solar.

1.3.5 The OPVs technology for BIPV application

The basic working technology of organic solar cells is based on active materials which need to be able to absorb a photon of sunlight and to make the electrons of this photon reach them to convert it into energy. The structure is implemented with two different materials for a donor and an acceptor, both elements of the cell. Once the incident photon reaches the cell, in fact, an exciton is generated: this exciton needs to be split into a hole polaron in the donor and an electron polaron in the acceptor. The energy necessary for this charge separation is provided by the offset between the LUMOs (lowest unoccupied molecular orbitals) and the HOMOs (highest occupied molecular orbitals) of the materials. The charge separation can happen in the donor or in the acceptor materials, depending on the absorption area of the photon: for an exciton in the donor, the exciton splitting results in the injection

of an electron into the LUMO of the acceptor, while the hole remains in the HOMO of the donor; vice versa for an exciton in the acceptor. What is important for organic cells materials is to have a low-bandgap (defined as the distance, the “gap”, between the LUMO and the HOMO of the active material) in order to perform at best. Donors and acceptors can be combined in two different structures, called junctions. Here below the flat and bulk heterojunctions are further described in order to understand the structure of a cell.

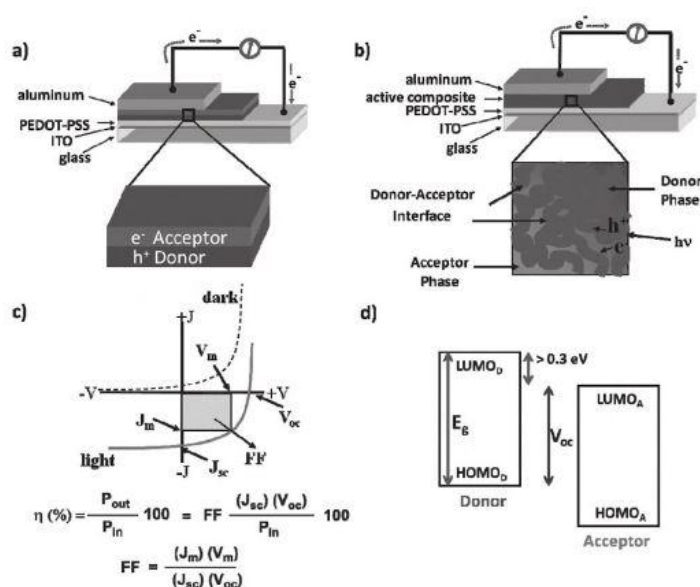


Figure 12 Donor and Acceptor working structure. Position into the cell (a). Donor-Acceptor junction (b). Mathematical explanation of the working method of the junction (c). HOMO and LUMO interface (d).

1.3.5.1 Flat heterojunctions

All efficient photovoltaic systems are based on the combination of two materials, a donor and an acceptor, since only the junction between these two provides sufficient driving force to split the typically strongly bound excitons generated by photon absorption. The first layered cell that introduced this kind of structure was developed by Tang and was conceptually simple: a thin layer of donor molecules was deposited onto a transparent front electrode (usually indium-tin oxide film on a glass substrate) and a thin film of acceptor molecules was evaporated on top. The result was a so-called “bilayer” cell, with a configuration of a well-defined planar interface. The solar cell was finalized by thermal evaporation of a metallic top electrode

(aluminum or calcium), necessary to allow ohmic (barrier-free electrical contact) extraction of electrons from the LUMO of acceptor.

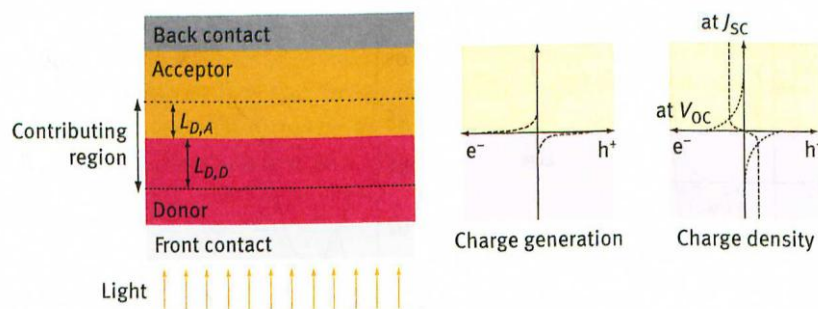


Figure 13 Flat heterojunction structure.

With this configuration only a small region in close proximity to the donor-acceptor interface can act as charge generator: the organic semiconductors, in fact, have typically low exciton diffusion lengths (on the order of few nanometers) and this leads to a huge loss of charge generation possibilities for excitons that are generated out of the active small region and cannot diffuse to reach the heterojunction. Moreover the layered structure forbids the electronic contact with the electron-collecting electrode for the donor and with the hole-collecting electrode for the acceptor.

1.3.5.2 Bulk heterojunctions

Differently than flat heterojunctions, donor and acceptor are processed together to form a mixed film rather than a layered structure. This is called bulk heterojunction since donor-acceptor heterojunctions are present throughout the whole film rather than only at one defined interface.

“Bulk heterojunctions are commonly realized either by co-evaporation of donor and acceptor materials or by deposition of a thin mixed film ratio. The phase separation between donor and acceptor can be partly controlled via processing parameters, such as the evaporation rate or the solution concentration, the substrate temperature, potential post-treatments like thermal or solvent annealing, solvent additives, and most importantly material’s properties like their tendency to crystallize or their hydrophobicity. However, direct control down to the nanometer scale is not possible so that the donor-acceptor morphology can be only indirectly adjusted and experimentally optimized.” (Schmidt-Mende and Weickert 2016)

Often in cases of polymeric donors combined with fullerene acceptors the phase separation is not as clear as indicated. Many materials show differently pronounced tendency to crystallize and this leads to formation of amorphous and crystalline regions and of mixed phases, where the materials are deeply mixed on molecular level. In the spread production of organic solar cells the crystallinity cannot be completely controlled, resulting in the presence of defect states: they reduce the exciton diffusion length of the cell to few nanometers. These defects are frequent in the solution-based deposition methods, like printing or blade coating (which are the most interesting in terms of commercialization of organic photovoltaics).

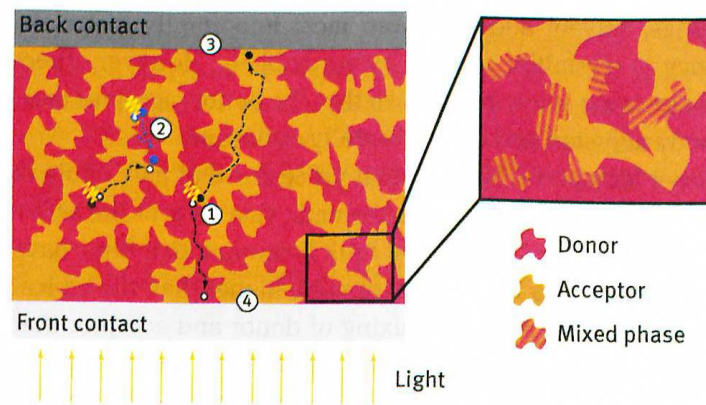


Figure 14 Bulk heterojunction structure.

The different processes of exciton diffusion, charge separation and charge transport define the efficiency of the cell and depend on the material's properties and on the internal morphology. The internal quantum efficiency of a bulk heterojunction determines the potential of incident photon conversion into electrical power and is defined by the following equation:

$$\eta_{IQE} = \eta_{ED} * \eta_{CS} * \eta_{CC} \quad (1)$$

η_{ED} : efficiency at which excitons diffuse through the material and reach a donor-acceptor heterojunction within their lifetime;

η_{CS} : efficiency of charge separation once an exciton reaches the heterojunction;

η_{CC} : efficiency for charge collection at the external electrodes, which is reduced in the case there is non-geminate recombination in the active layer.

The power conversion efficiency (PCE) of an organic solar cell is determined by three different parameters and is expressed with the following equation

$$\eta [\%] = (J_{sc} * V_{oc} * FF) / (P_{in}) \quad (2)$$

J_{sc} : short-circuit current density;

V_{oc} : open-circuit voltage;

FF : fill factor (determines the maximum power);

P_{in} : input power (incoming light intensity, whose spectrum is close to AM1.5)¹

As said above, necessary characteristics for a donor component regard the electronic requirements of low bandgap for high J_{sc} , correct positioning of frontier energy levels for high V_{oc} , sufficient driving force for exciton dissociation and the morphological requirements of optimal mixing with fullerenes, a certain degree of crystallinity and high charge carrier mobility.

“To achieve high J_{sc} the active layer needs to absorb sunlight broadly and intensely across the solar spectrum (from the UV/vis into the near infrared (NIR)) because J_{sc} is proportional to the product of spectral absorption breadth and absorption intensity of the active layer. Considering that most fullerenes primarily absorb in the UV, and often to a lesser degree in the visible region of the solar spectrum, an important design principle for novel donor materials is to lower the bandgap, allowing absorption of longer wavelength light, and thus high J_{sc} . Often polymers with a bandgap lower than poly(3-hexylthiophene) (P3HT), which is still considered the benchmark for conjugated polymers and has a bandgap of 1.9 eV, are called low-bandgap. Mixing of donor materials with the fullerene acceptor at favorable ratios is also beneficial for high J_{sc} because, in combination with the fact that fullerenes do not absorb in the NIR, the absorption coefficients of donor materials in the visible spectra are generally considerably higher than for fullerenes.” (Richter and Rand, 2016)

The bulk heterojunction (BHJ) is currently the dominant organic solar cell geometry, since it offers advantage of single-solution processing step to form the active layer, which is easily adaptable for large-scale fabrication at low temperature and ambient pressure using minimal energy.

Common donor and acceptor materials

Regarding donor materials, P3HT (poly(3-hexylthiophene)) is become the benchmark polymer for polymer-PCBM bulk heterojunction devices, thanks to its good performance. Furthermore its tendency to crystallize helps the morphology

¹ AM1.5 stands for „air mass 1.25“ that is a path through 1.5 times the thickness of the atmosphere achieved for solar incidence at an angle of 48.2°

formation of P3HT-PCBM bulk heterojunction, most commonly active material used for organic solar cells.

However its efficiency is limited due to the large bandgap of about 2 eV. To overcome the limit new low-bandgap materials have been investigated, as PCDTBT which has become widespread for its improving PCE >7%.

Considering the acceptors, fullerenes C_{60} and C_{70} and derivatives are mostly used since they are soluble in the same solvents as the conjugated polymers. Especially C_{70} in combination with small bandgap donors is spread due to its higher light extinction in the visible range. The picture below sums up the most common active materials for donors and acceptors, indicating also their chemical structures.

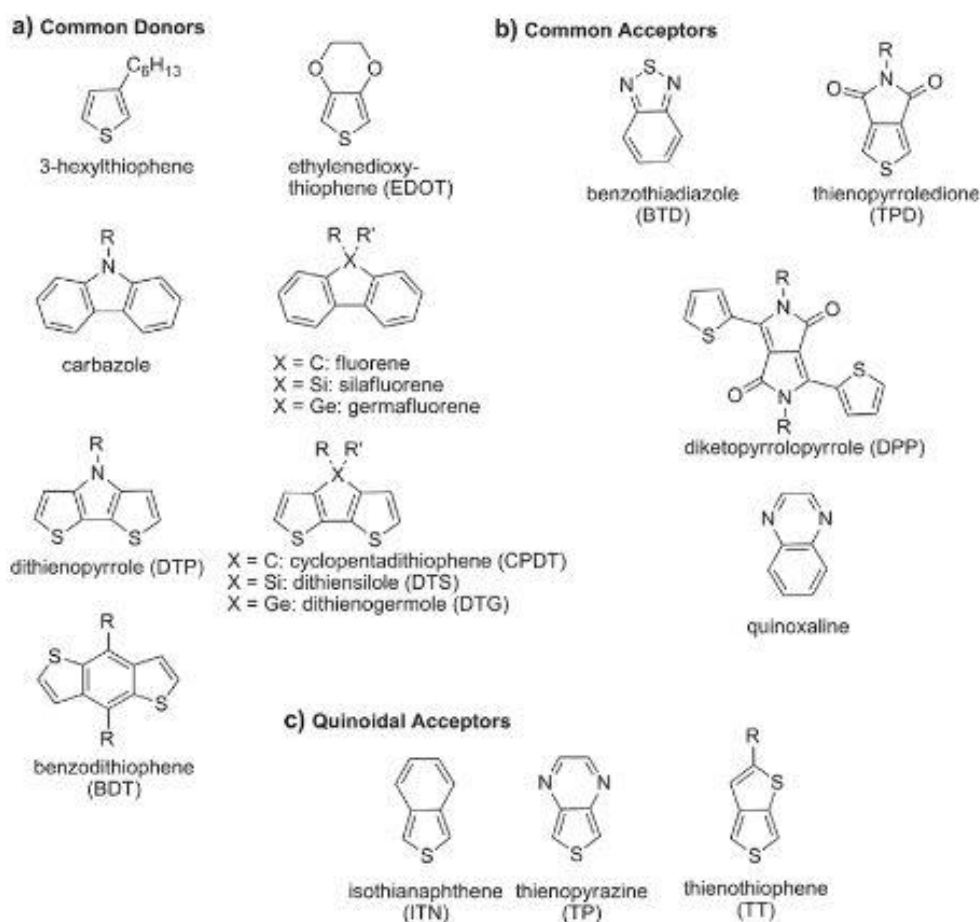


Figure 15 Common donor and acceptor materials for OPVs.

1.3.6 Transmission and transparency

Together with the substrate and the transparent conductor both the interference effects, due to the active film thickness, and the potential presence of a reflecting top contact affects the amount of light that can couple into the cell.

In order to reach a good degree of light transmission (to get transparency of cells) it is necessary to:

- find materials that show only weak absorption in the wavelength region of interest (visible and near IR range);
- reduce the reflectivity of the transparent contact.

The first requirement is addressed by using thinner films, but as this implies higher resistances it is necessary to find the right balance optimization. Thicknesses in the range of the wavelength interference effects significantly influence the transmittance of the film. The second requirement is solvable by matching the index between the conducting film and substrate and by using anti-reflection coatings on the front side of the substrate.

The most common configuration for a good transparency is formed by a first layer deposited on top of the substrate of a transparent conducting oxide (TCO) with indium-tin-oxide coating which assures an excellent electrical conductivity and high optical transparency. Although this good performance, it is an expensive material which needs to be deposited in vacuum under high temperature so it is tried to be replaced by other promising behaved vacuum-free semitransparent electrodes, like PEDOT:PSS, tin- and zinc-based oxides, stacked metal-oxide/metal/metal-oxide films, silver nanowires, graphene or carbon nanotubes and other nanomaterials.

PEDOT:PSS is often used as a hole-selective layer. It can be deposited easily as ink by roll-to-roll techniques, such as rotary screen printing as it allows the deposition of sufficiently thick layers. As an electron-selective layer, ZnO is a preferred material, as it also allows the formulation as ink and deposition from solution. Up to now the transparency of organic cells can reach 50-60% with decreasing efficiency as it increases, as already said. Below, figure 17 shows the development of transparency and efficiency for the products of Heliatek company.

Electrode [Ref]	T (%) ^b	R _{sheet} (Ω/sq)	σ _{ac} /σ _{opt} ratio ^c	Advantages	Issues
ITO [165]	83	8.5	227	Well-established process/mechanically robust/easy patternability	Indium price fluctuation/poor flexibility
FTO [166]	83	13	149	Relatively low cost among TCOs	Surface roughness
AZO [167]	88	10	285	Low work function (if needed)/relatively low cost	Weak to corrosive chemical environment, relatively low mechanical hardness
Thin metal [98] (Ag, 12 nm)	45	6	64	High sheet conductance/flexibility possible	High reflectance (low transmittance). Need to find the uniform growth condition for thin metal
D/M/D ^d					
ZnS/Ag/WO ₃ [18]	85	14	159	Optical tuning possible by layer structure variation/high conductance/flexibility	Optical design can be non-trivial/Spectral dependence of T/trilayer structure may increase the overall fabrication cost
MoO ₃ /Ag/MoO ₃ [19]	78	6	229		
Ag-NWs [111]	80	10	159	High sheet conductance/flexibility possible/solution-processable	Difficult to control surface roughness
PEDOT:PSS [78] (vapor-phase growth [93])	86 (85)	150 (58)	16 (38)	High flexibility/solution-processable/low roughness	Relatively low conductivity/condition to enhance conductivity still under development/relatively poor stability
CNTs [149]	70	50	19	High flexibility	Limited sheet conductance
Graphene [158]	90	30	116	High flexibility/relatively good sheet conductance	Related processes are not yet mature and still under development

Figure 16 Transparency properties of main diffuse OPVs materials.

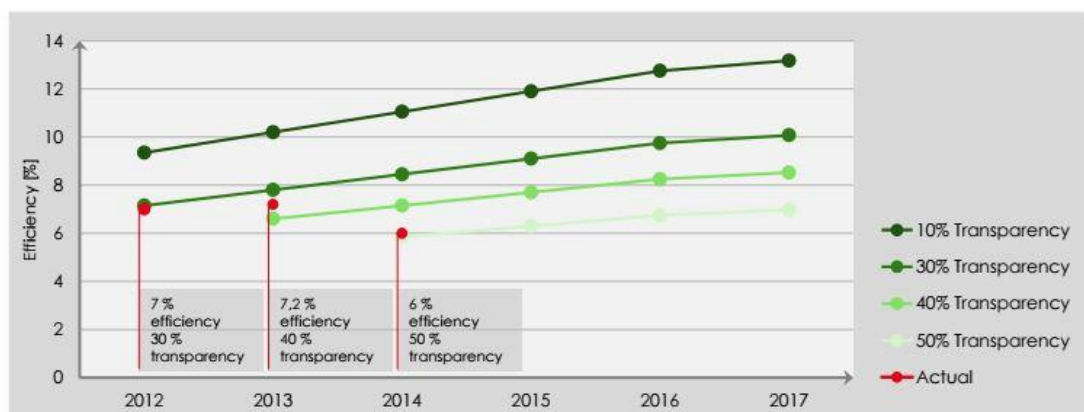


Figure 17 OPVs efficiency and transparency comparison. Heliatek products in 2016.

1.3.7 Substrates

Substrates are the cells base for all the layers that need to be deposited on top. In case of semitransparent solar cells, the transparent substrate is combined with a transparent electrode which can be placed either on its top, on its bottom or on both sides. Substrates should have the property of low birefringence to improve the transmission.

In case of semitransparent solar cells for building application it makes sense to use glass substrates, especially for window cases. Glass is stable and reliable for the use as substrate and it is ideal as barrier for moisture and oxygen which threaten its performance. Moreover, as glass is highly transparent for visible light, it allows efficient in-coupling of light into the active semiconductor layer. Compared to plastic substrates, it assures many optical advantages, as being highly transparent over the visible spectrum, possessing a high homogeneity of the refractive index and exhibiting a high UV resistance; additionally it provides also thermal advantages as high temperature stability, high dimensional stability, high chemical resistance and a low thermal expansion coefficient. In particular its good barrier properties can significantly decrease the cost and improve the lifetime of the solar cells, as in such cases an additional barrier layer will not be required. When needed, plate glass can become flexible because its thickness can be reduced to several hundred micrometers (ultra-thin glass sheets) allowing superior performances to plastic films.

Although all these advantages, it is not possible to use roll-to-roll processing with glass substrates; as the potential of organic cells is strongly connected to the mass production, printable flexible substrates are needed for low-cost production of solar cells.

Flexible transparent foils are required to fulfill several requirements in order to be comparable to glass performances: they need to be thermally stable to withstand all processing steps (including high-temperature deposition and solvents), should expand little on heating, should have a high surface quality with a smooth and ideally defect free layer (normally a planarizing coating is applied to improve the smoothness and the surface hardness to prevent easy scratching), should not internally deform under roll-to-roll casting and should not age and get brittle.

The most common flexible substrate is polyethylene terephthalate (PET) followed by polyethylene naphthalate (PEN). PET is a very cheap and common material: its degradation, mainly attributed to a catalyzing effect of the -COOH ends, by hydrolysis and brittleness (which leads to cracking) can be improved and stabilized

over time through additives. Additionally as the active layers, which are deposited consecutively on top of the substrate, are also prone to photodegradation and photooxidation, the substrate should act as a barrier avoiding oxygen and moisture diffusion into the active films.

1.3.8 Production methods

1.3.8.1 Coating techniques

Coating is noncontact methodology allowing fabrication of very even layers with minimal physical damage and stress. The film is the result of constant feeding of ink to a standing meniscus between the “coating head” and the moving substrate. The most common techniques in this category are the knife coating and the slot-die coating.

The first method is suitable for continuous coating of large unpatterned areas and can be performed at high speed, thanks to the stationary “knife”, which is a blade through which the wet film is formed on the web. The thickness of this film is defined by the distance between the web and the knife.

With the second method the thickness can be controlled with higher precision, as it is defined by the web speed, the width of the coated area and the pumping rate. The ink is supplied through a slot in the coating head, which is typically fed with a pump to ensure control over the flow. Slot-die coating is currently the most widely used technique for layer processing in organic solar cells and has mainly been used for hole-blocking layers, active layers and electron-blocking layers.

1.3.8.2 Printing techniques

Printing technique implies by definition the transfer through physical contact of the carrier of a motif and a substrate and so it is a 2-dimensional patterning method.

The screen printing is the mostly spread printing method and can be performed roll-to-roll. As a squeegee moves relative to the screen in the presence of ink, the latter is pushed through the open area of the screen and onto the substrate. This method allows the formations of very thick wet layers (10-500µm) and thus also very thick dry films although the technique is only useful for rather viscous inks with thixotropic (shear thinning) properties, as low-viscosity inks will simply pass through the mesh by gravity. For its roll-to-roll performance two techniques can be used: flat-bed screen printing and rotary screen printing.

Flat-bed screen printing is a step-wise process where the screen is lowered upon the substrate followed by passing of a squeegee, which ensures the transfer of the motif by pushing the ink through the unfilled parts of the mesh. After raising the screen, the web is moved forward and the process starts again.

In rotary screen printing the screen is folded into a tube that rotates with the same speed as the web. The squeegee is, in this case, stationary and is placed inside the screen, which allows for continuous printing of the screen motif upon each rotation. As the ink is situated inside the screen it is much less exposed to the surroundings compared to flat-bed. Although this, it is considerably more expensive than the other methods described and it is difficult to operate. Compared to the first technique, rotary screen printing is by far superior for its speed, the edge definition/resolution as well as the wet thickness; moreover it is a true roll-to-roll technique and it is particularly useful for printing of front and back electrodes, active layers and PEDOT:PSS.

Worth developing are also the flexoprinting and gravure printing for their potential of very high processing speeds which makes them good for especially for the PEDOT:PSS production. In flexoprinting the ink is transferred from a relief on the printing plate, usually made out of rubber, which is continuously supplied with ink. Gravure printing, opposed to the flexo technique, transfers the ink through tiny engraved cavities forming a pattern in the gravure cylinder. The web is brought into contact with this cylinder by pressure of another cylinder and the ink is transferred through surface tension. This method is suitable for low-viscosity inks.

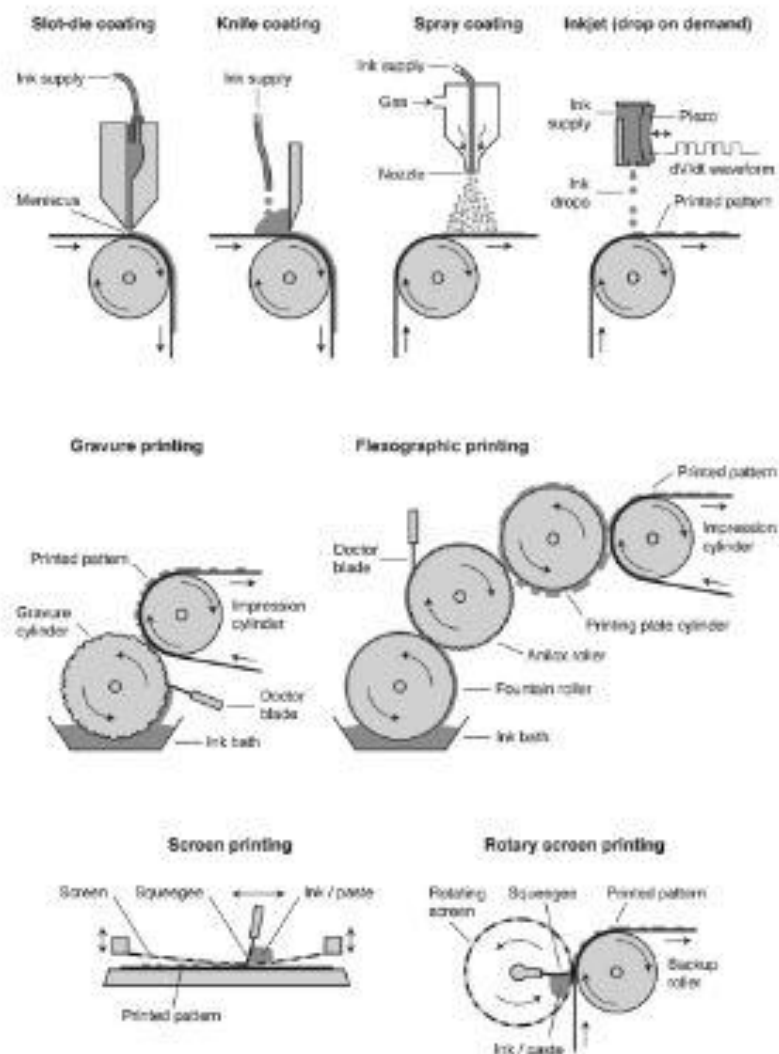


Figure 18 Main production techniques for OPVs.

1.3.9 Architecture of Organic Solar Cells

The design structure of a “conventional” organic solar cell is made to receive the light through the substrate feature a transparent conductive electrode upon it, which collects and transports the holes. This transparent electrode needs to cover the whole substrate in order to collect all the photogenerated holes, and in case of insufficient selectivity for holes another layer is applied on top of the electrode, called hole transport layer (HTL). The following layer is composed by the photoactive material, which is the bulk heterojunction as already described. Proceeding in the layered structure there is placed an optional electron transport layer (ETL), followed by the back contact which ends the cell structure and is meant to extract and transport the electrons. The position of the HTL and ETL can be

inverted to get an “inverse” organic solar cell with the advantage of improving the oxidation resistance, thanks to the metal back contact high work function.

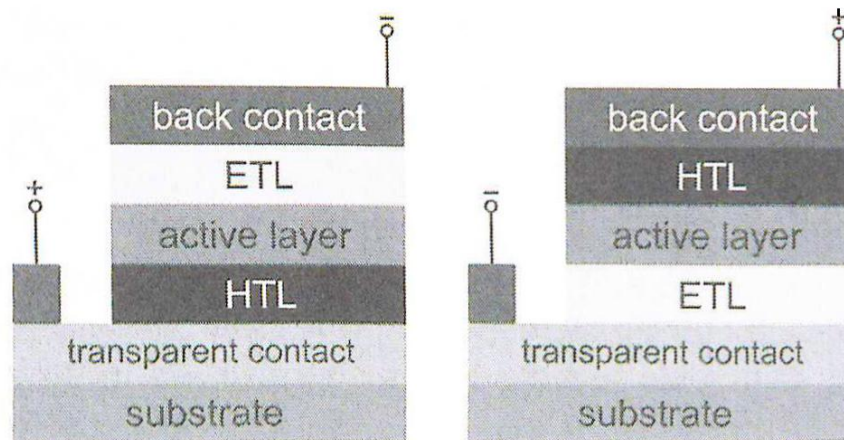


Figure 19 Architecture of an OPV cell. Normal structure and Inverse structure.

Once set that, there are two different ways to build up the solar module: the interconnection between the cells can be parallel, where the collected currents from each cell are added up, or serial, which is normally more efficient. Typically silicon solar modules are built up by connecting each separate cell through wires, due to the limited size of Si ingots. On the contrary, organic modules made of soluble components allow a whole on one and same substrate building up, which is called “monolithic”. The advantage of this configuration is that it does not require any time-consuming; the disadvantage is that each layer needs to be deposited and structured subsequently and the risk is to damage the underlying layers upon the structuring process. Furthermore in this design there is an area for serial interconnection every two cells which does not contribute to the power conversion.

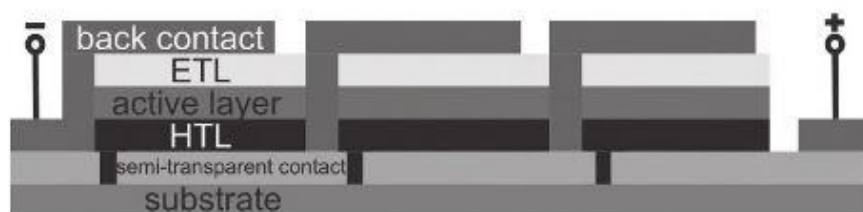


Figure 20 Cells distribution on a substrate.

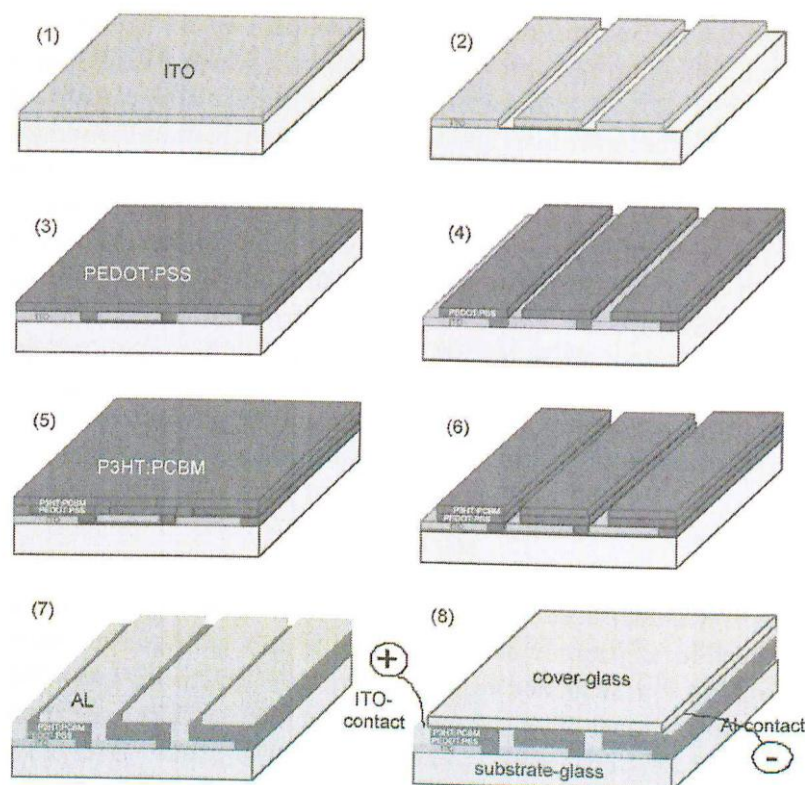


Figure 21 Cell structure mounted layer by layer.

The maximum efficiency of a monolithic solar module depends both on the active materials and on the geometric design of the module. In fact, the cell efficiency is function of the solar cell length and of the dissipative power losses. The solar cell length is, however, limited by the current generation and the sheet resistance of the lower conductive charge collecting electrode: the necessary balance between all these elements, decreases the efficiency of the cell.

1.3.10 The integration of OPVs in buildings: companies and buildings

As explained until now, the importance of developing organic cells for photovoltaic systems has been recognized by many companies, from the one that were already active in the sector of production to new ones, aiming at introducing them into the market. Although the good intention of all these companies, only few of them have been able up to now to concretely install the cells into buildings. This is due to the fact that it is still an emerging technology so the installation costs, together with the production ones, are still high, waiting for a spread which can assure a decrease. Many companies are looking at the performance of dye-sensitized cells and have not turned yet to the analysis of organic ones; some others embraced the challenge

and try to implement and evaluate them. The most notable for the developments in their researches are Belectric, Solarmer, Heliatek, Solaronix and Mitsubishi Chemical Corporation: they have not only studied the chemical composition of cells to improve the performance, but also produced specimens and have come to the practical application into buildings and to the analysis of the performance since 2014.

For this study, the focus is on the work done by Heliatek, Mitsubishi Chemical Corporation and on Belectric's research.

Heliatek is a German company, grown up from the academic environment of the Technical University of Dresden, and is now one of the leading companies in the world for the production and installation of organic cells in buildings. Their organic technology is embedded in 'Heliapfilm' cells, produced by roll-to-roll process, which does not use solvents as the other printing-based processes do, and integrated successfully into glass, concrete, steel. Heliapfilm are multilayer, organic molecule-based solar cells with doped transport layers; the active layers are only around 250 nm thick. They are able to absorb the light also in the infrared range while keeping a thin layer. Most important, they are holding the world record of power conversion efficiency of 13.22% (for opaque cells), which is obviously reduced in application but still competitive with 7-8%. The transparency currently available reaches 30 to 50%. By using several layers of the molecule, Heliatek ensures that its film produces energy even during periods of low-level sunlight.

Heliapfilm are ultra-light, with an extremely low weight of less than 1 kg/m², flexible, less than 1 mm thin, printable in customizable length up to 2 m, likely to be sandwiched between layers of glass in office windows or integrated into facades. Additionally, their technology is combined with the environmental valency, as HeliapFilm do not put additional pressure on resources of the rare earth metals often used in photovoltaic technologies and this makes it even more ecological and competitive.

"With our HeliapFilm, we are clearly executing our strategy to provide de-carbonized, de-centralized energy generation directly on buildings all over the world" says Thibaud Le Séguillon, Heliatek chief executive.

Strong of this achievement, the company started in 2014 the first project of installation of its cells into the company headquarter building. The project was a success, as the photovoltaic system is well working and achieves performances comparable to the common silicon cells.

The company, after the success of this project, raised the scientific interest and the following year provided HeliFilm for the world's most powerful and Asia's largest BIOPV installation: the government of Singapore required organic cells for the photovoltaic system of two buildings of the Clean Tech Park. HeliFilm have been implemented with various building materials, within and on glass, on steel and on curved polycarbonate and several versions have been used, full power opaque and transparent with different colors. The strength of the German technology could be proved particularly in this project, because it can face and solve a problem where conventional silicon cells have never succeeded: as the temperature rises, photovoltaic cells become less efficient, but this does not happen in case of HeliFilm organic cells, as their performance is not affected by increasing temperature. This fact makes them the most qualified cells for the use in the project and opens a new window in the market of photovoltaic cells as they can now cover a wider range of countries for the building integration.

Mitsubishi Chemical Corporation, or Mitsubishi Chemical Holdings, is a Japanese company which covers the business from energetic to chemical and health care fields by developing sustainable products and materials. In the case of photovoltaic cells production, it achieved in September 2012 a world record of 11.7% conversion efficiency for organic thin-film single cells. The organic photovoltaic modules that have been developing are thin sheets, which can be bent or rounded into various shapes. They are flexible and lightweight; they can be painted and can reach different levels of transparency. The production is made with continuous coating process, which is similar to the printing one but it spares energy and it is suitable for mass production. Although the good performance and potential demonstrated, the company keeps the research profile and it is not involved into building integration project. The only exception is represented by the Zero Energy Building in Yokohama, where Taisei Corporation required OPVs for façade integration. In 2014 the building was inaugurated and it saw the presence of three wall covering organic cells, together with roof panels. The solar panel portion of the window is only 2mm thick. These cells have a power conversion efficiency of 5% but their extension is notable, as they cover more than 50% of the entire exterior surface. The rooftop and wall solar panels generate all the power the zero-energy building needs and, although it is still grid-connected, it can send as well as draw power. This building stresses the performance of organic cells by combining them into a sustainable building which is able to be self-sufficient thanks also to the photovoltaic system.

As the aim of this research focuses on looking to the thermal and visual performance of OPVs, the applications evaluated are the ones regarding the facades and windows. Other integration possibilities, conducted and performed by these companies (concrete and steel integration, opaque cells), will not be further developed.

The third important company, worth mentioning for the project of BIPV already conducted, is the German Belectric. It takes care of different photovoltaic systems and cells for various applications, from buildings to vehicles. The most important application in terms of organic cells is in the African Peace and Security building in Addis Ababa, Ethiopia. The German government financed the project of a building for international meetings and Belectric was asked to design the photovoltaic system. The combination of flexible organic solar modules and a stainless steel cable construction from Carl Stahl has allowed the realization of a solar project of this magnitude for the very first time: 445 individual transparent blue modules, using Merck's silicon OPV active material, were installed on the roof structure directly underneath the membrane dome above the Peace and Security Building's interior, held in place by a sophisticated cable mesh construction. The modules have a 75% light transmission and are able to supply sufficient electricity to power the LED lighting system inside the building.

In 2015 Belectric have also worked in Expo Milan 2015, with the installation of very similar organic photovoltaic cells in the German Pavillion. The company designed energy-generating solar trees, meant to connect the interior and exterior space, the architecture and exhibition, and also to provide shade during the sunny months of the EXPO.

2 METHOD

2.1 Overview

The motivation of the study starts from the background. The research conducted showed that the photovoltaic market still needs more research and development, but most of all it needs concrete facts that demonstrate the real performances that all the products can give. The crystalline cells behavior is widely known and it has been proved in many situations; what is need now is the same strong and complete documentation for the other technologies, in particular the organic one. In fact, until now it has not been demonstrated properly their performance and their potential.

In this way, this research over the potential of OPVs in BIPV is conducted specifically in windows and facades according to their properties. The steps of the analysis aim to explain the thermal and visual performance of a office room with two windows with hypothetical OPVs performing. The simulation will help to prove that although most of the producing companies do not have installed this technology on real buildings, the potential is high and further concrete demonstration in buildings is worth.

2.2 Hypothesis

The background research has opened to the thinking that the market of photovoltaics is not settled but active in the development of new cells following the new technologies. It was also underlined that there is a strong need of ecological reflection together with the necessity of expanding the production methods and decreasing their costs. All this leads to the motivation of understand more about the organic photovoltaic cells and their role into the PV family. Thanks to these thoughts and, most important, the irrefutable facts presented until now, it is possible to formulate the following hypothesis:

“The organic solar cells will replace the silicon technology in the building integrated photovoltaic system for their good visual performance and increasing efficiency.”

This work will try to answer to this formulation in a positive way.

2.3 The sample office building

The building used for the computation and evaluation of organic photovoltaic cells is a reference sample office building, defined in the European Commission Joule project REVIS and further refined in the International Energy Agency Solar Heating and Cooling (IEA SHC) program Task 27 (Performance of solar façade components). This building model has already been used in some other simulation projects for thermal and visual evaluations.

The main dimensions of the model are taken without massive changes, as well as the thermal zones division. The information about the structure, the materials and their properties and the building systems and loads has been instead customized.

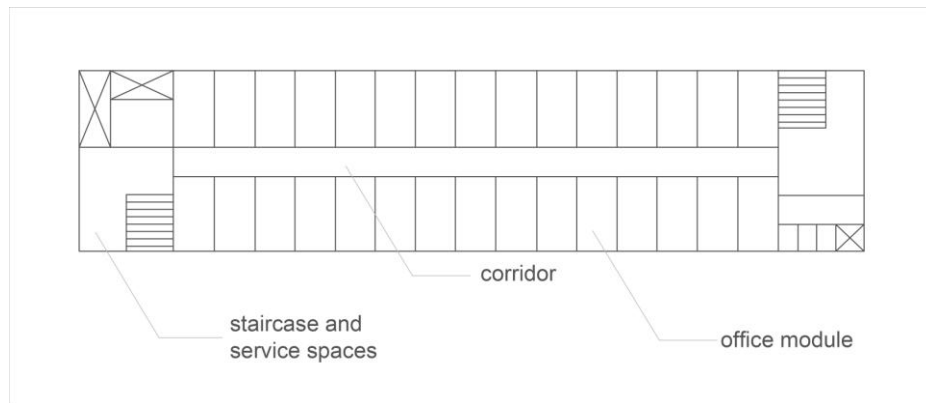


Figure 22 General plan of the sample building

The building is made of 30 office rooms for each of the five floors, separated by a corridor which connects also two service spaces placed at the short sides of the building. The orientation is set first to South then the model will be turned of 90° to face East and West for the performance comparison of the behavior under different solar conditions.

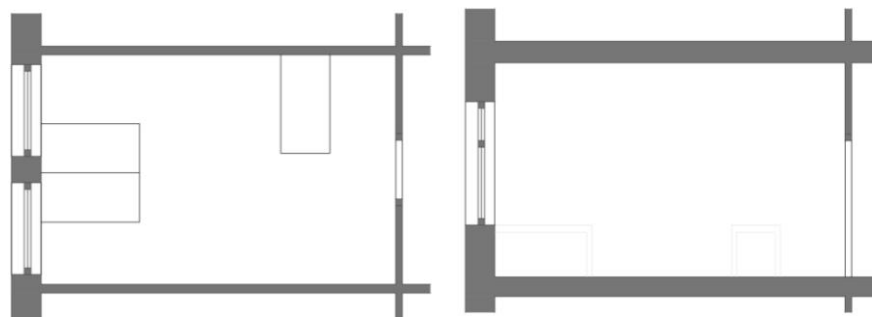


Figure 23 Plan and Section of the sample office room

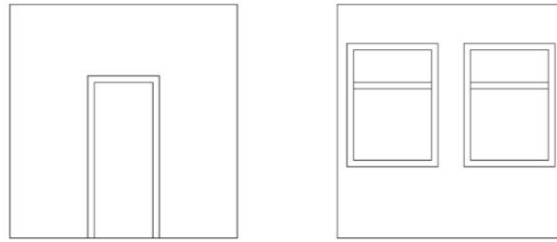


Figure 24 Prospects from outside and from inside of the room

Table 1 Building materials' properties.

	Roughness	Thickness [m]	Conductivity [W/mK]	Density [kg/m³]	Specific Heat [J/kgK]
Concrete (FG,FR,EW)	rough	0.25	2.5	2400	1000
Concrete (PS)	rough	0.2	2.5	2400	1000
Concrete (PW)	rough	0.1	0.6	1500	1000
Mortar (EW, PS, FG)	rough	0.02	1.05	1800	1000
Gypsum Plaster for interior (PW, EW)	smooth	0.015	0.18	600	1000
Gypsum Plaster for exterior (EW)	medium rough	0.015	0.57	1300	1000
Gypsum Board (FR, PS)	medium rough	0.015	0.21	700	1090
ConcreteScreed (FG)	rough	0.04	1.1	1800	1080
Concrete Screed (PS)	rough	0.03	1.1	1800	1080
Bitumen Screed (FR)	medium smooth	0.04	0.7	2100	1000
EPS (PS)	medium rough	0.03	0.038	17	1210
Rock Wool (FG)	medium rough	0.1	0.04	90	1210
Rock Wool (FR)	medium rough	0.15	0.039	120	1210
Rock Wool (EW)	medium rough	0.15	0.04	120	1210
Linoleum (FG, PS)	medium smooth	0.01	0.17	1200	1400
Sand and Gravel (FG)	very rough	0.2	2	1700	1000
Sand and Gravel (FR)	very rough	0.04	2	1700	1000
Aluminium (W)	medium smooth	0.1	160	2800	1000
Polyurethan (FG, FR)	medium smooth	0.001	0.21	1300	1800
Wood (D)	medium smooth	0.025	0.15	608	1000

*FG: floor to ground; FR: flat roof; EW: external wall; PS: partition slab; PW: partition wall; W: window; D: door.

Table 2 Normal double glazing structure's properties.

	Clear Glass	Argon Gas Fill	Frame	Divider
Thickness [m]	0.003	0.013	0.07	0.07
Optical Data Type	/	/	/	/
Solar Transmittance	0.74	/	/	/
Front Side Solar Reflectance	0.09	/	/	/
Back Side Solar Reflectance	0.1	/	/	/
Visible Transmittance	0.82	/	/	/
Front Side Visible Reflectance	0.11	/	/	/
Back Side Visible Reflectance	0.12	/	/	/
Infrared Transmittance	0	/	/	/
Front Side IR Hemispherical Emissivity	0.84	/	/	/
Back Side IR Hemispherical Emissivity	0.2	/	/	/
Conductivity [W/mK]	0.9	/	/	
Outside Projection	/	/	0.03	0.03
Inside Projection	/	/	0.03	0.03
Ratio	/	/	1	/
Number of Dividers	/	/	/	1 (horizontal)
U-value [$\text{m}^2\text{K/W}$]	/	/	2.2	2.2
Solar Absorptance	/	/	0.7	0.7
Visible Absorptance	/	/	0.7	0.7
Thermal Hemispherical Emissivity			0.9	0.9

The main structure is concrete based; the materials are taken from the OENorm B 8110-7 and the building components are set to meet the required thermal transmittance coefficients as in the standard ISO 6946.

Table 3 Constructive elements' properties.

	Thickness [m]	Construction Layers	U-value² [W/m²K]
Floor to Ground (FG)	0.621	linoleum, mortar, screed, thermal insulation, water insulation, concrete, gravel	0.4
Partition Slab (PS)	0.305	linoleum, mortar, screed, acoustical insulation, concrete, gypsum board	0.9
External Wall (EW)	0.45	plaster, mortar, thermal insulation, concrete, plaster	0.35
Partition Wall (PW)	0.13	plaster, concrete, plaster	/
Window (W)	0.019	double glazing, PVC-aluminium frame	1.7
Door (D)	0.05	wood board	/
PV film	0.001	organic thin film	
Flat Roof (FR)	0.498	sand and gravel, drainage board, screed, thermal insulation, water insulation, concrete, vapor barrier, gypsum board	0.2

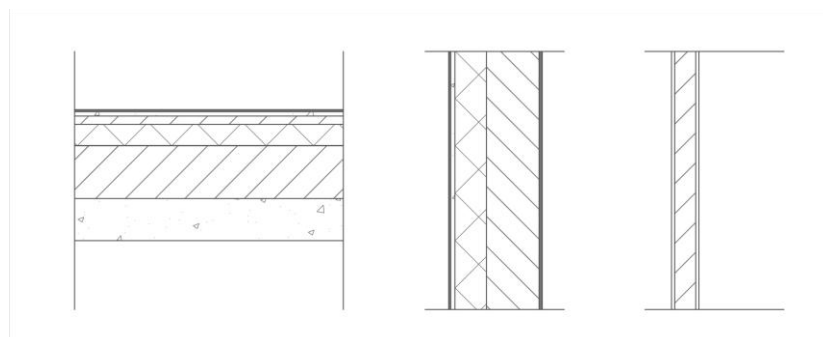


Figure 25 Constructive structures. Floor to ground. External wall. Partition wall

² According to the requirement expressed in the norm EN ISO 6946.

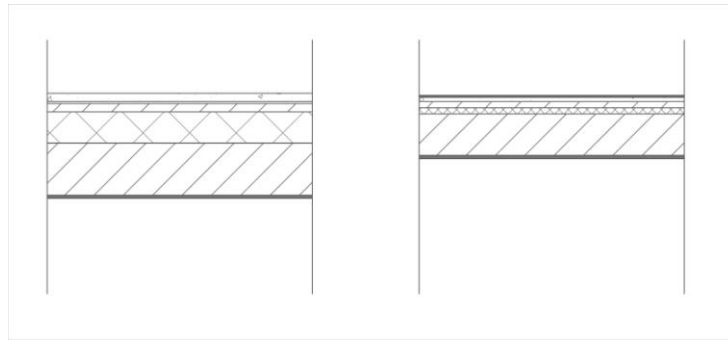


Figure 26 Constructive structures. Flat roof. Partition slab.

The internal loads are calculated according to the equipment already set in the reference model:

- 170 W for offices thermal zones;
- 20 W for services thermal zone.

The assumptions made regard the occupancy and the lighting are:

- 3 people for each office room are counted, according to three working position available;
- 8 W/m² of lighting power for each office room, according to the performance of recessed, parabolic louver and non-vented luminaries to meet the requirements for office illuminance of 500 lux;
- 4 W/m² of lighting power for the service spaces, for a total of 25 luminaries in the corridor and 8 luminaries for each stair space.

The ventilation is mechanical and controlled by a HVAC system: the natural ventilation is not set in this model in order to simplify the calculation. The HVAC system settings are as followed:

- the thermostat is set to 20°C for heating and 25°C for cooling;
- the infiltration rate is equal to 0.3 h⁻¹;
- the outdoor air method set for calculations is “flow/person” with a value of 0.00708 m³/s.

The photovoltaic system made of organic solar cells is placed on south windows, in the first case, in the second case on the east and in the third evaluation on west windows, considering the E/W orientation. The cells are applied as a layer of the glazing structure, for a total active area of 1.16 m², which corresponds to the 87.8% of the total single window area. The cells are structured in one array, made of two

strings of 3 modules of cells and connected to an inverter for the energy conversion from DC to AC.

The model is evaluated for the thermal simulation in three different ways:

- Model without PV system integrated;
- Model with OPV system integrated;
- Model with a-Si PV system integrated.

The model is evaluated for the visual simulation in two different ways:

- Model without PV system integrated;
- Model with OPV system integrated.

The cells properties are here presented.

Table 4 Photovoltaic cells' properties.

	a-Si:H	OPV
Technology	Amorphous silicon thin film cells	Organic solar cells
Efficiency	~7%	~10%
Visual transmittance (according to the efficiency)	~30%	~30%
Substrate	Glass	Glass
Active material	Amorphous silicon	Polymer-PCBM
Short Circuit Current	1.5 A	1.11 A
Open Circuit Voltage	58 V	41.1 V
Maximum Power	58 W	30 W
Nominal Current	1.27 A	0.95 A
Operating Temperature Range	-40 to 82 °C	-40 to 85 °C
Dimensions	58*56*0.4 mm	2000*322*1 mm
Weight	0.5 kg	0.8 kg

Both the PV systems are made of thin-film cells, so they can be integrated in the same way. The visual transmittance is equally set and the efficiency is referred to it. It has to be noted that organic cells could reach higher transmittance percentages (50%), while aSi could not. To keep the performance even, the value is set as 30% for both of the cell technologies. Accordingly, the difference in OPV and aSi efficiency is justified by the choice of evaluating cells with the same transmittance.

2.4 The thermal simulation: performance indicators and computation methodology

A thermal evaluation of the building is performed to strength the visual analysis and as a basis for understanding the general building's behavior. The data needed for this evaluation are according to the geometry and the thermal environment in which the building is inserted. The main dimensions and the position of doors and windows are needed to build the model. The data about the thermal environment include the weather data about the geographical location, the definition of the position of the building in the city ('City', 'Suburbs', 'Country'), the structure of the building components and their properties, systems' settings for heating and cooling.

The sample office building is modeled in Sketch Up through the Plugin of OpenStudio, defining the main dimensions, the position of windows and doors, the building envelope and the thermal zones. The weather data corresponding to the cities of Addis Ababa, Singapore, Stuttgart, San Francisco and Tokyo are used to perform different models according to different climate conditions.

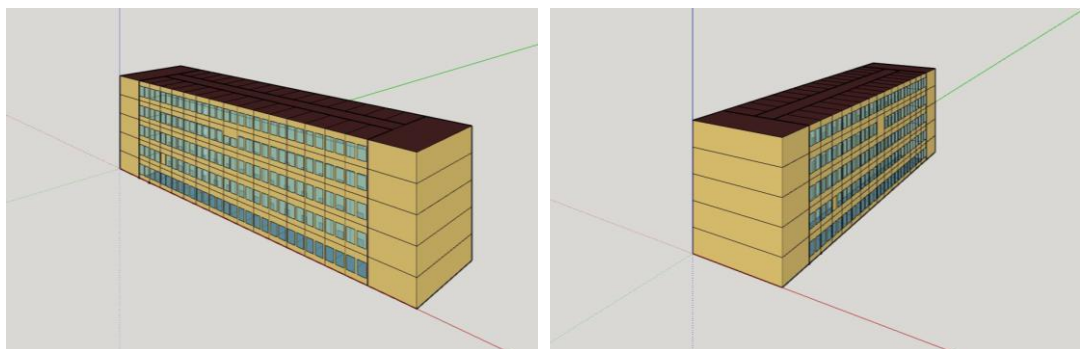


Figure 27 Models' orientation. To South on the left; to East and West on the right.

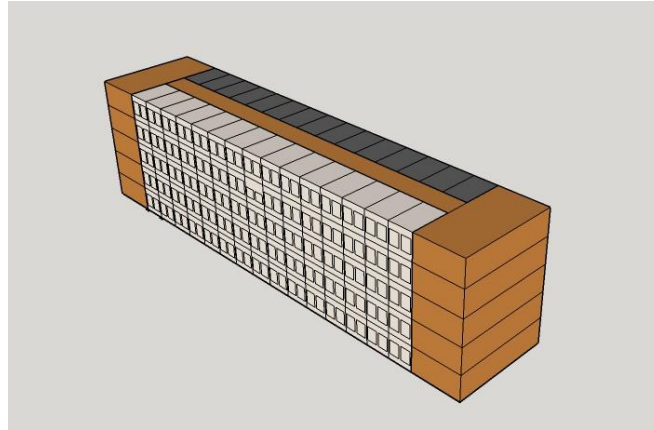


Figure 28 Thermal zones distribution

The model of the office building exported as an .idf file from OpenStudio is opened in EnergyPlus for the thermal computation. It is there completed with the missing information about the thermal environment and structure properties.

Table 5 Energy Plus settings. Building position and simulation period.

Field	Object
Building Terrain	City
Timestep (number of timesteps per hour)	6
Run Period	Annual, from 01/01 to 31/12
Solar Distribution	Full Exterior

The informations about ground temperature and properties have to be modeled directly in EnergyPlus. An object is created in the field of “Site: Ground Temperature: Undisturbed: Finite Difference” to define soil properties; then another field is added about the “Surface Property: Other Side Condition Model” to define the type of modeling. Both these objects are then inserted in the object related to the slab conditions “Site: Ground Domain: Slab”.

The system properties are connected to a schedule time setting, so it is necessary to set the schedules according to the system to control. In this case six compact schedules are created for HVAC, lighting, occupancy, equipment, activity level, zone infiltration and photovoltaic inverter. Most of them have been imported from the database of EnergyPlus Schedules, where are already set for different building

functions. Each Schedule Compact has to be connected to a limit, set in the field “ScheduleTypeLimits”.

The thermal evaluation is obtained by the computation of thermal performance indicators which will give an overview over the energy consumption and the thermal demand of the building. The outputs needed and set in the field “Output:Variable” are:

- Heating Demand: “Zone Ideal Loads Supply Air Total Heating Energy”, annually and monthly calculated;
- Cooling Demand: “Zone Ideal Loads Supply Air Total Cooling Energy”, annually and monthly calculated;
- Lighting Electric Energy Consumption: “Zone Lights Electric Energy”, annually and monthly calculated;
- Electric Equipment Energy Consumption: “Zone Electric Equipment Electric Energy” , annually and monthly calculated;
- Energy Produced by Photovoltaic System: “Facility Total Electric Demand Power”, annually and monthly calculated.

All these indicators are computed by the software through the data inserted as described above. The differences in the two photovoltaic systems’ efficiency will be of course visible in the energy production results.

The unit set for the computation results is kWh (the energy results will be converted from Joule to kWh); the values will be then converted to kWh/m² to be more easily compared. The model is now set and together with all the other information counts the following fields:

```
[0001] SimulationControl
[0001] Building
[0001] Timestep
[0001] RunPeriod
[0001] Site:GroundTemperature:Undisturbed:FiniteDifference
[0001] Site:GroundDomain:Slab
[0003] ScheduleTypeLimits
[0007] Schedule:Compact
[0020] Material
[0001] WindowMaterial:Glazing
[0001] WindowMaterial:Gas
[0007] Construction
[0001] GlobalGeometryRules
[0003] Zone
[0590] BuildingSurface:Detailed
[0596] FenestrationSurface:Detailed
[0001] WindowProperty:FrameAndDivider
[0282] InternalMass
[0001] SurfaceProperty:OtherSideConditionsModel
[0003] People
[0003] Lights
[0003] ElectricEquipment
[0003] ZoneInfiltration:DesignFlowRate
[0001] HVAC:emplate:Thermostat
[0003] HVAC:emplate:Zone:IdealLoadsAirSystem
[0144] Generator:Photovoltaic
[0001] PhotovoltaicPerformance:Simple
[0001] PhotovoltaicPerformance:EquivalentOne-Diode
[0005] ElectricLoadCenter:Generators
[0005] ElectricLoadCenter:Inverter:Simple
[0005] ElectricLoadCenter:Distribution
[0001] Output:VariableDictionary
[0001] Output:Table:SummaryReports
[0001] OutputControl:Table:Style
[0005] Output:Variable
```

Figure 29 Energy Plus final elements' list for the simulation.

EnergyPlus is now ready to compute the model and calculate the indicators. Each weather data file corresponds to a different model, so it will be performed five simulations and get different values. The results are collected in a .xls file and summed up in a HTML page.

Table 6 Model cases for thermal simulation.

Model Name	Model Orientation	PV system integrated	Total Floor Area [m²]	Total Glazing Area [m²]	Total Glazing Area with PV integrated [m²]
NS	North/South	-	4261.75	612.0	0
EW	East/West	-	4261.75	612.0	0
OPV_S	North/South	OPV on south façade	4261.75	612.0	269.28
OPV_E	East/West	OPV on east façade	4261.75	612.0	269.28
OPV_W	East/West	OPV on west façade	4261.75	612.0	269.28
aSi_S	North/South	aSi on south façade	4261.75	612.0	269.28
aSi_E	East/West	aSi on east façade	4261.75	612.0	269.28
aSi_W	East/West	aSi on west facade	4261.75	612.0	269.28

2.5 The visual simulation: performance indicators and computation methodology

The potential of the structural integration of photovoltaic cells into glazing and facades designs has to be supported by a visual comfort evaluation: the light design possibility cannot stand alone in terms of potential, the comfort inside the buildings and the rooms must be satisfactory in order for it to be functional and usable.

The visual simulation of the sample office room works in this way to analyze the comfort situation inside provided by the only daylight. The artificial lighting will not be taken into consideration (with the only exception of UGR calculation), because it is an additional element which is not useful in the understanding of the performance of the photovoltaic cells in daylight transmission. The evaluation is run for two different design situations:

- a classic double glazing structure, with standard 88% total light transmission;
- a double glazing structure with organic photovoltaic layer integrated, with 50% total light transmission.

The differences in the results will be compared and analyzed to see if both of them can satisfy the comfort standards.

The simulation runs around the computation of the following performance indicators:

- Illuminance at workplane, defined as the amount of light that reaches one square meter;
- Uniformity at workplane, defined as the illuminance distribution into the room;
- Daylight Glare of the total space, defined as the possibility of having glare problems due to a too high daylight amount;
- Daylight Autonomy, defined as the percentage of hours per day in which the standard requirements for illuminance are satisfied;
- Daylight Factor, defined as the ratio of daylight inside the room to the light level outside;
- Irradiance of the sun on windows, defined as the sunlight power incident on the windows;
- Color Spectrum, defined as the color temperature and Color Rendering Index of the inside daylight.

These will give a specific overview on the quality and quantity of daylight coming into the room. As already done for the thermal evaluation, the data are collected for

five different cities in order to see the differences given to the location of buildings. For this simulation the model is only facing South.

The softwares used for this analysis are SketchUp 2017 and Radiance. The building is drawn in SketchUp and three main scenes are defined, as in Fig. 30. With the help of the Radiance Plugin, the materials of each surface are defined. Once this is set, the drawing is imported into Radiance to compute the performance indicators.



Figure 30 Scene-images for the simulation. Scene 1, Scene 2, Scene 3

Export
Render
Sky
Views
Materials
log

Export Options

path: c:/Model11_AA/
scene: Scene_1.rif
mode: by layer ☐ triangulate

Views select all

☒ Scene 1
☒ Scene 2
☒ Scene 3

Render Options

quality: medium
detail: medium
varia: high
img x: 1324
img y: 592
type: normal
render:

Sky

location: San Francisco, USA
sky cmd: gensky 3 21 12:0 -c 37.7700 -o 122.4100 -m 120.0
north: 0.00

cancel
export

Figure 31 Radiance Plugin for SketchUp. Settings for building export into Radiance.

In order to have interesting and comparable results the skies for the simulation are set as overcast: this is the situation when not direct sunlight is incident to the building surface. This will better help to evaluate the potential of photovoltaic in diffuse light situations rather than direct sunlight.

The computation is based on a grid of 24 points set at a height of 0.8 m from the floor level (workplane height). As the grid shown below, the software calculates the values on the points for each day of the months in the working hours, from 08.00 to 16.00. The months chosen are according to seasons' beginning on midday, because this is when the sun height differences stand.

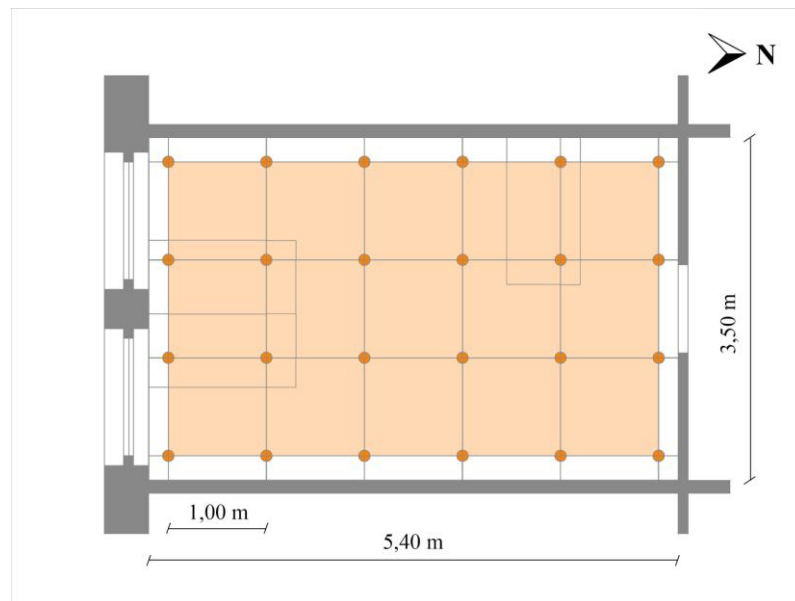


Figure 32 Distribution of calculation points at workplane height (0.8 m)

Table 7 Radiance settings. Sky settings for each city.

Sky settings*	AddisAbaba_0321_1200	# gensky 3 21 12:00 -c -a 9.005401 -o 38.76 # Local solar time: 11.83 # Solar altitude and azimuth: 80.2 -15.6 # Ground ambient level: 32.9 void brightfunc skyfunc 2 skybr skybright.cal 0 3 2 4.24e+001 6.59e+000
	AddisAbaba_0621_1200	skyfunc glow skyglow 0 0 4 1.000 1.000 1.000 0 skyglow source sky 0 0 4 0 0 1 180
	AddisAbaba_0923_1200	skyfunc glow groundglow 0 0 4 1.000 1.000 1.000 0 groundglow source ground 0 0 4 0 0 -1 180
	AddisAbaba_1221_1200	

*the sky settings are repeated for each city considered: San Francisco, Singapore, Stuttgart, Tokyo.

As the calculation needs to evaluate the interior visual comfort, the data are based also on the internal reflections on room surfaces. Here below are grouped the materials used with their reflection, specularity and roughness properties. In the case of glass, the values are different between the model cases with and without OPVs. The reflection is equal to 0.96 for the normal double glazing structure, while the value of 0.6 is for the integration of photovoltaics.

Table 8 Radiance settings. Covering materials' properties.

Covering material	Color	Red reflection	Green reflection	Blue reflection	Specularity	Roughness
Plaster (walls)	White	0.72	0.72	0.72	0	0
Gypsum board (ceiling)	White	0.87	0.87	0.87	0	0
Linoleum (floor)	Light brown	0.309	0.165	0.08	0	0
Glass (window)	-	0.96 / 0.6	0.96 / 0.6	0.96 / 0.6	-	-
Wood (door and tables)	Light brown	0.544	0.362	0.208	0	0

The computation of the indicators have considered the elements just described: no additional furniture or equipment has been taken into consideration.

Here below are listed the Radiance commands used for the computation of all the indicators, except for illuminance, where a script was written in Python and then called with the software for a quicker and more precise simulation:

- Sky generation: *gensky*;
- Glare computation: *findglare*, *glarendx*;
- Picture generation *rpict*, *falsecolor*;
- Daylight factor computation: *dayfact*.

For Daylight Factor, the Radiance computation is accompanied by a manual calculation in order to have a more precise results comparison.

For the remaining performance indicators, the computation is done by using the information already computed with Radiance inserted in the following formulas:

- Uniformity [%]: E_{\min} / E_{av} ;
- Daylight Autonomy [%]: **(total hours with $E < 500\text{lux}$ / total hours) *100.**

Irradiance and Color Spectrum have been empirically evaluated, by analyzing the skies and the sunlight power and height information already known and available for latitudes and longitudes desired. They are necessary to complete the general overview over the performance that the OPVs provide in every situation, although it is not a deep and precise analysis about the specific daylight entering the room in the present calculation.

Table 9 Model cases for visual simulation.

Model Name	Model Orientation	PV system integrated	Total Floor Area [m²]	Total Glazing Area [m²]	Total Glazing Area with PV integrated [m²]
Model 1	South	-	18.9	4.08	0
Model 2	South	OPV on south façade	18.9	4.08	3.59

3 RESULTS

3.1 Overview

The simulations return a lot of results, here divided per performance indicators. The importance of each indicator for the thermal and visual comfort and so the necessity of being precise made the computation very long.

First, the thermal simulation results are presented: the main focus is on the photovoltaic performance and on the differences between the two technologies considered.

For the visual simulation, the accent is put on the performance of the OPVs and the evaluation of the inside comfort that they provide. A positive response for each indicator is required as, more than their electrical efficiency, the capacity of guaranteeing a good natural illumination is fundamental.

3.2 Thermal Simulation Results

Here below are presented the results of the thermal simulation, conducted with EnergyPlus as already explained before. The results are organized in tables and graphs to be more readable. The performance indicators computed are the following:

- Heating demand of the total building, annually expressed;
- Cooling demand of the total building, monthly expressed;
- Electric demand of the total building, monthly expressed;
- Energy production amount by photovoltaic system, monthly expressed.

The results are presented in kWh and weighted by m^2 for an easier presentation: in fact, many of them, if not weighted, would be too big to be read in graphs and understandable in comparisons. Each model is here presented according to the different weather data, orientation and photovoltaic system used in the simulation. The main comparison, shown in the end, focus on the efficiency of the OPV and the a-Si cells in their energy production meant to decrease the total energetic demand of the building.

3.2.1 Annual and Monthly Heating Demand

The heating demand is generally very low or practically inexistent: this is due to the warm climate condition of the majority of the cities involved in the evaluation. The only case which keeps heating demand under every situation and building orientation is in the city of Stuttgart and Tokyo. The annual temperatures in there differ a lot from the other cases. The only cases, instead, which do not need heating are Addis Ababa and Singapore: again here, the reason has to be search in the typical hot climate of the region.

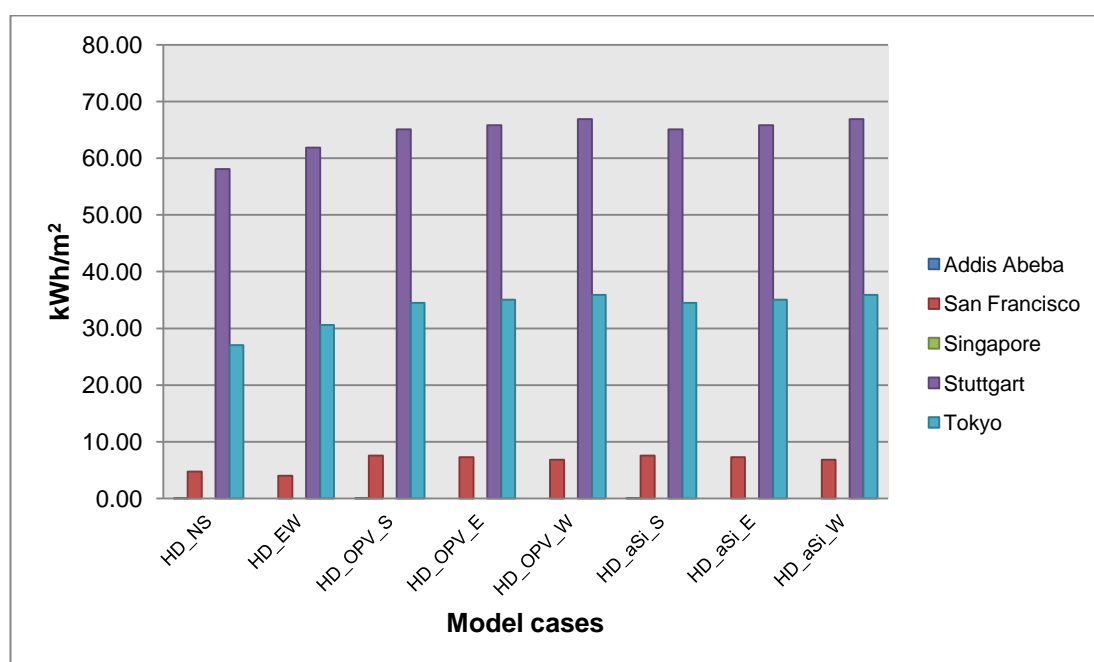


Figure 33 Annual Heating Demand summary (HD: heating demand; NS: north-south orientation; EW: east-west orientation; OPV: organic photovoltaics; aSi: amorphous silicon photovoltaics.)

Table 10 Annual Heating Demand summary.

Annual Heating Demand [kWh/m ²]								
	HD_NS	HD_EW	HD_OPV_S	HD_OPV_E	HD_OPV_W	HD_aSi_S	HD_aSi_E	HD_aSi_W
Addis Ababa	0.00	0.00	0.00	0.00	0.00	0.00	0.00	0.00
San Francisco	4.75	4.01	7.60	7.29	6.83	7.60	7.29	6.83
Singapore	0.00	0.00	0.00	0.00	0.00	0.00	0.00	0.00
Stuttgart	58.07	61.86	65.06	65.83	66.89	65.06	65.83	66.89
Tokyo	27.04	30.8	34.51	35.08	35.89	34.51	35.08	35.89

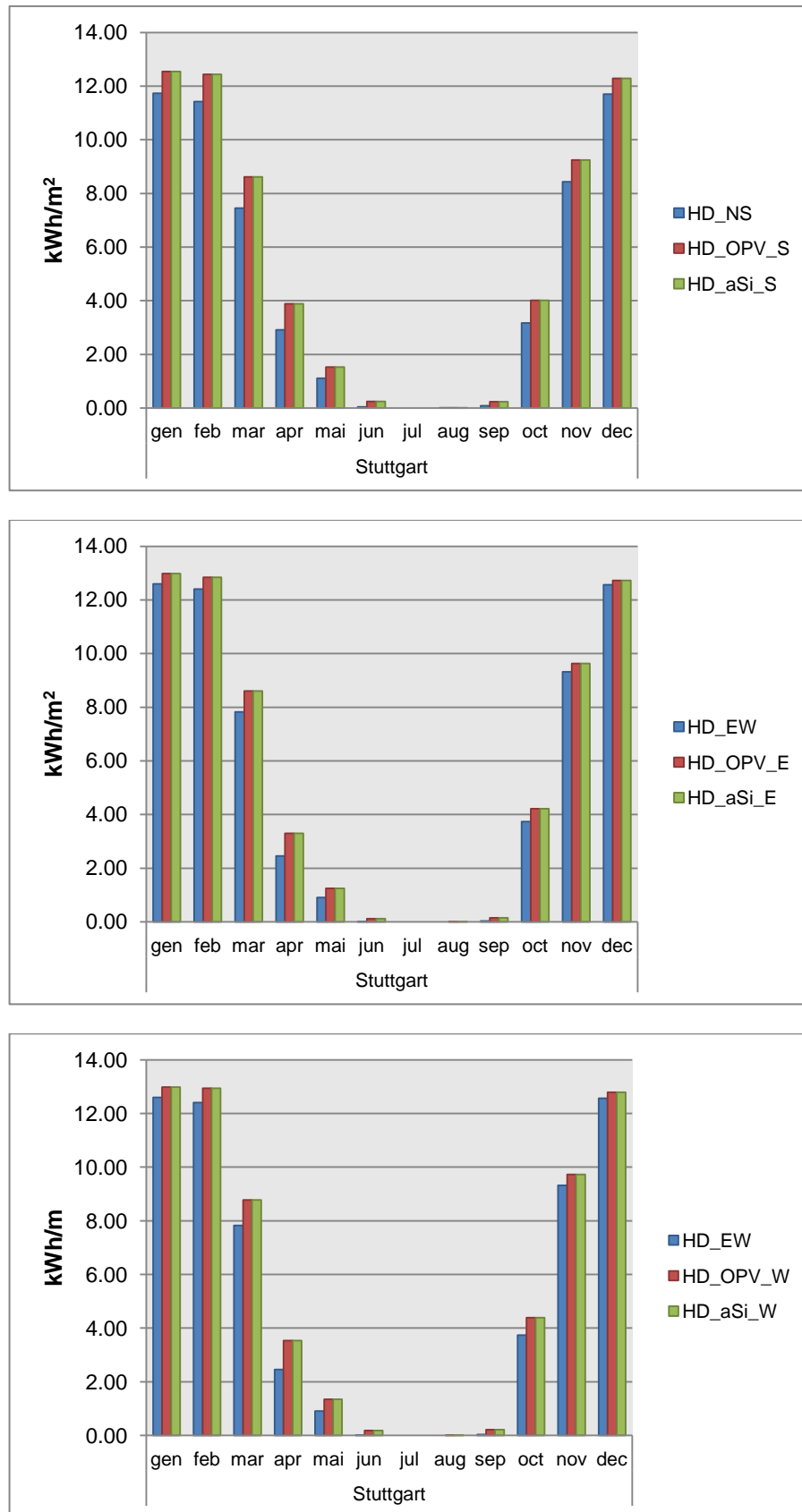


Figure 34 Annual heating demand for Stuttgart model cases.

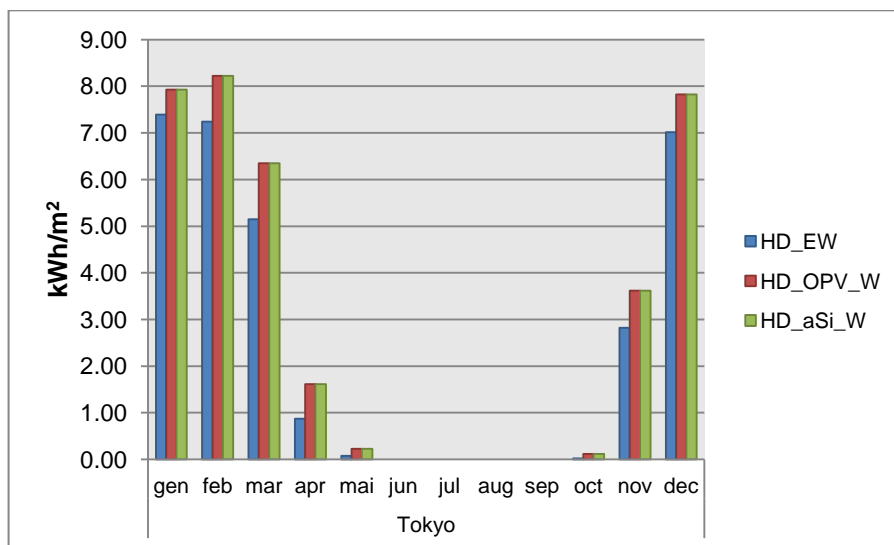
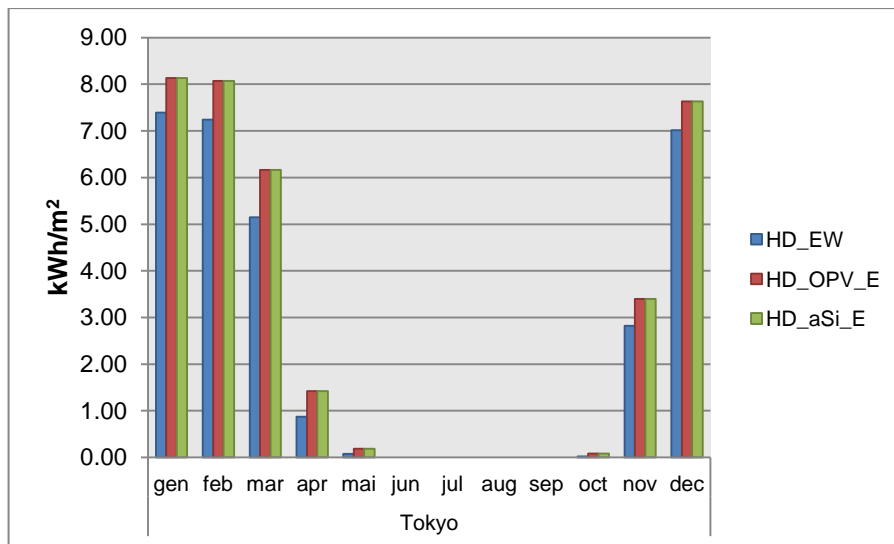
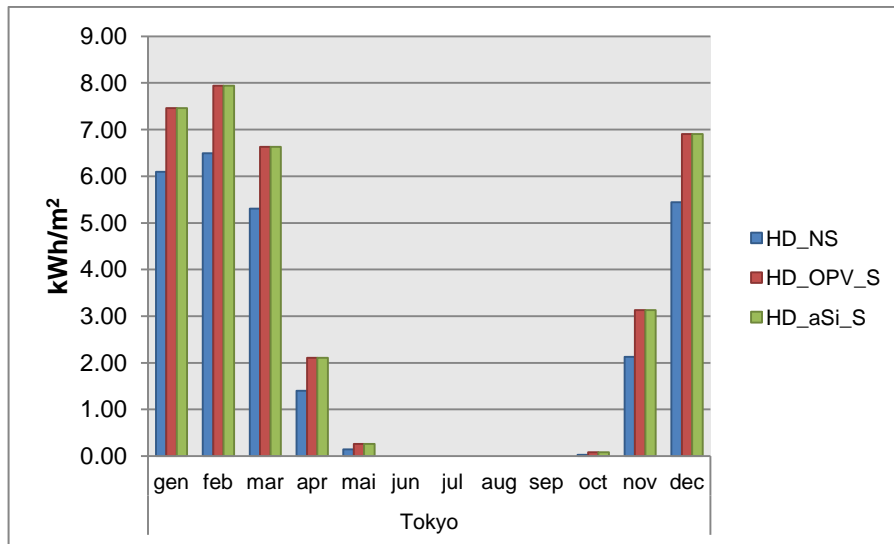


Figure 35 Annual heating demand for Tokyo model cases.

3.2.2 Annual and Monthly Cooling Demand

The cooling demand has an opposite behavior to the heating one, as it is low for Stuttgart and very high for Singapore climate, for example. The reason is again connected to the very warm temperatures of the cities considered: as expected, the highest values are for the Singapore models. In this way, the building configuration does not help really much, because two big windows for each office room are directly exposed to the sun, without any shading device.

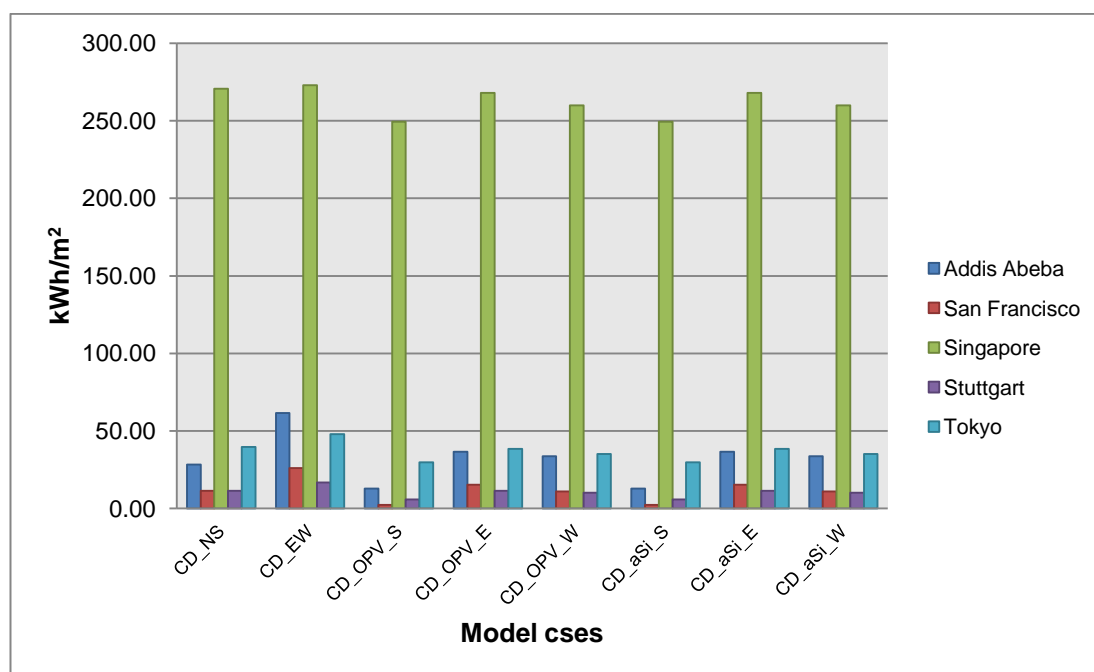


Figure 36 Annual Cooling Demand summary (CD: cooling demand; NS: north-south orientation; EW: east-west orientation; OPV: organic photovoltaics; aSi: amorphous silicon photovoltaics)

Table 11 Annual Cooling Demand summary.

Annual Cooling Demand [kWh/m ²]								
	CD_NS	CD_EW	CD_OPV_S	CD_OPV_E	CD_OPV_W	CD_aSi_S	CD_aSi_E	CD_aSi_W
Addis Ababa	28.39	61.59	12.87	36.61	33.71	12.87	36.61	33.71
San Francisco	11.37	26.07	2.42	15.39	11.10	2.42	15.39	11.10
Singapore	270.59	272.82	249.30	267.92	259.87	249.30	267.92	259.87
Stuttgart	11.40	16.87	5.93	11.52	10.09	5.93	11.52	10.09
Tokyo	39.68	47.92	29.81	38.37	35.14	29.81	38.37	35.14

Here below the monthly results are presented for each city, considering for each building orientation the presence of photovoltaic.

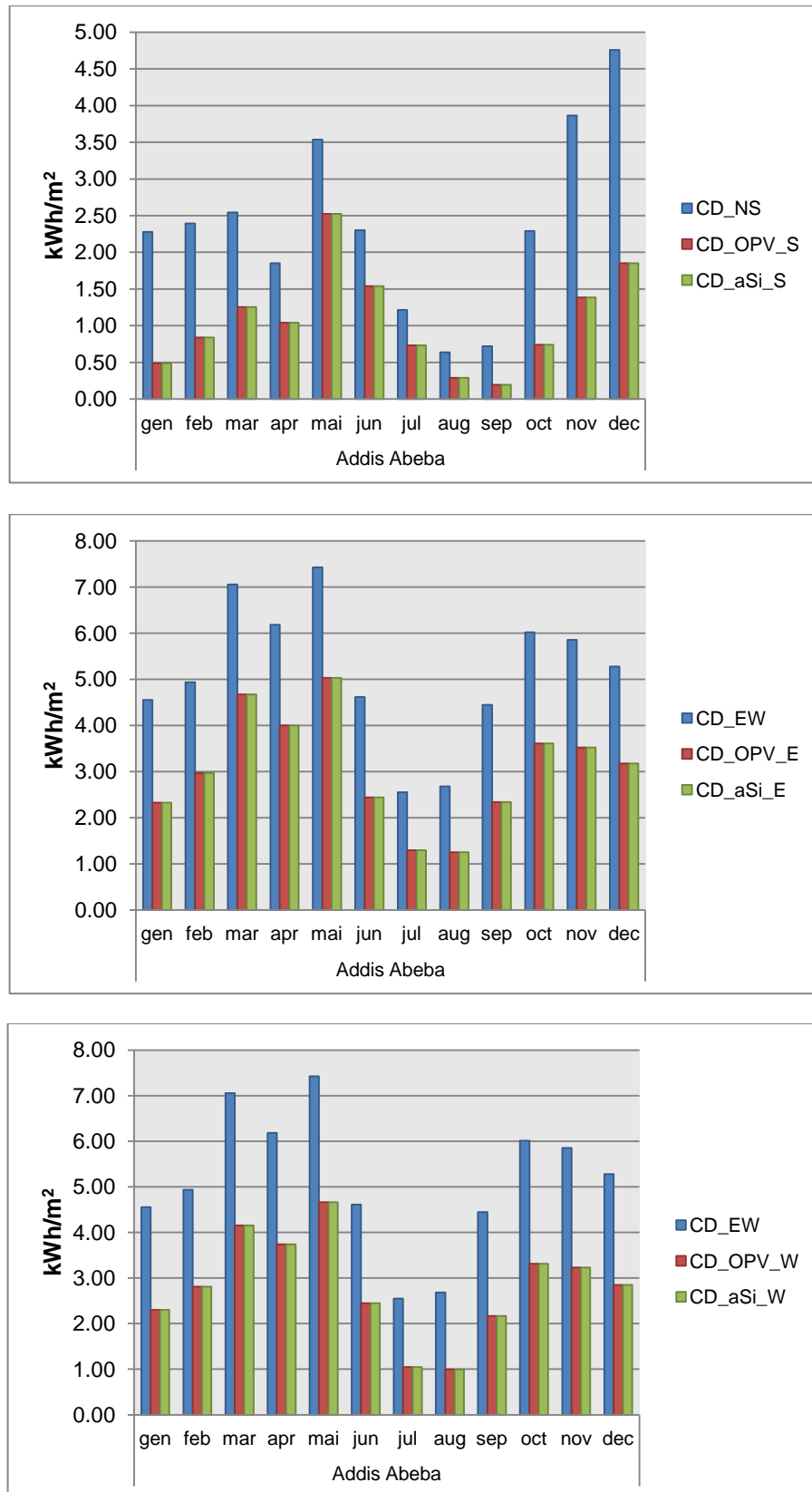


Figure 37 Annual cooling demand for Addis Abeba model cases.

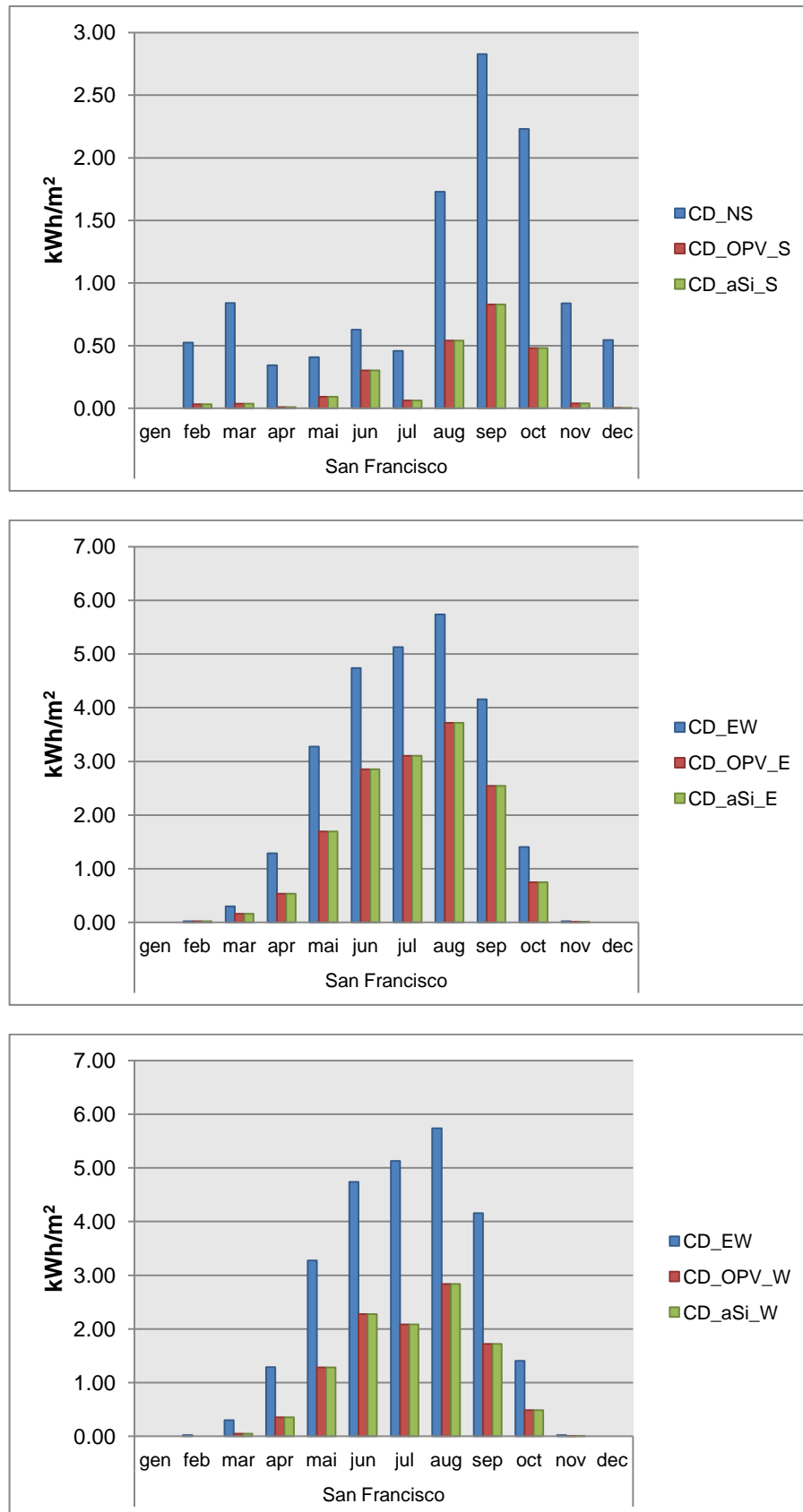


Figure 38 Annual cooling demand for San Francisco model cases.

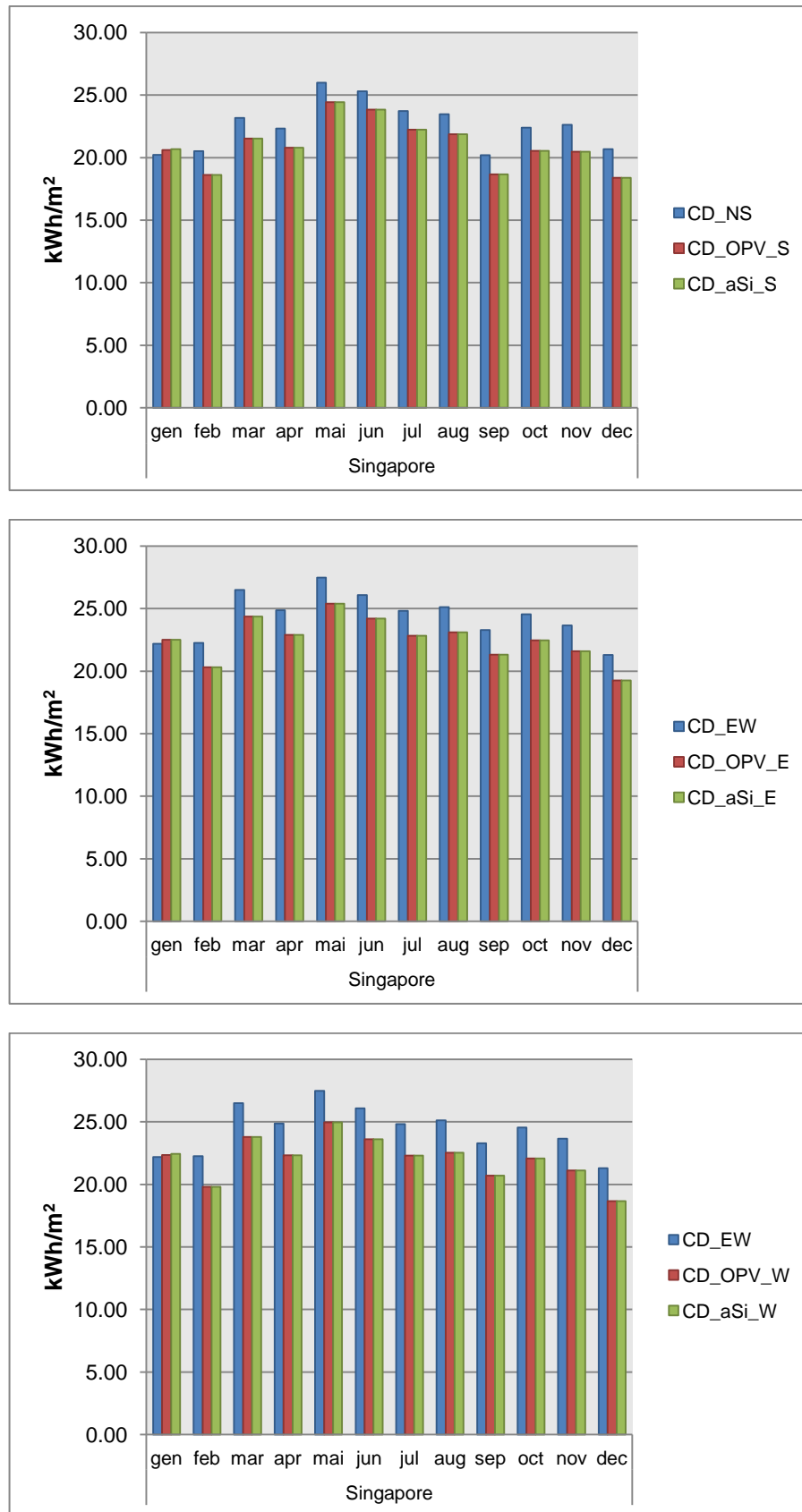


Figure 39 Annual cooling demand for Singapore model cases.

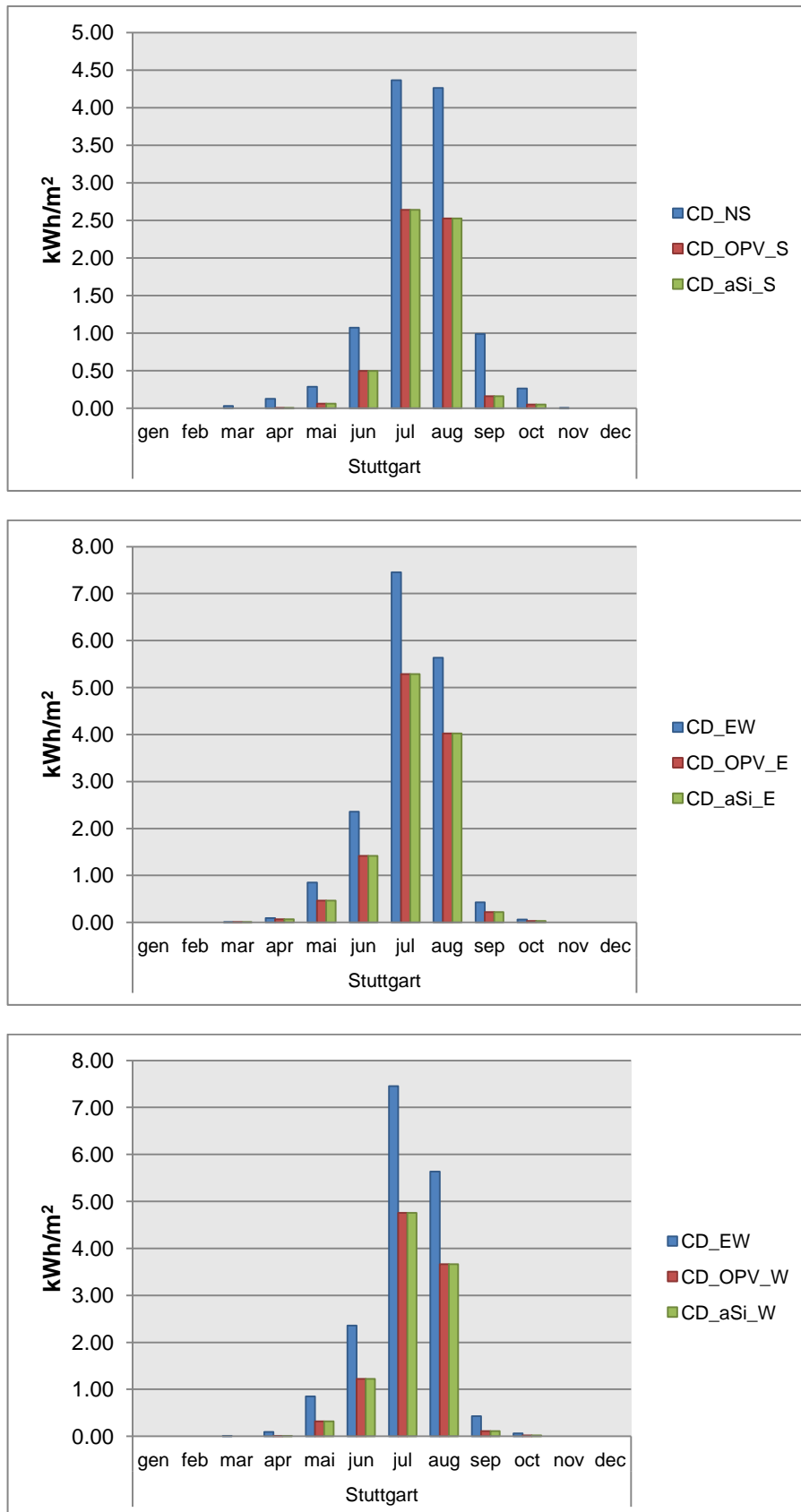


Figure 40 Annual cooling demand for Stuttgart model cases.

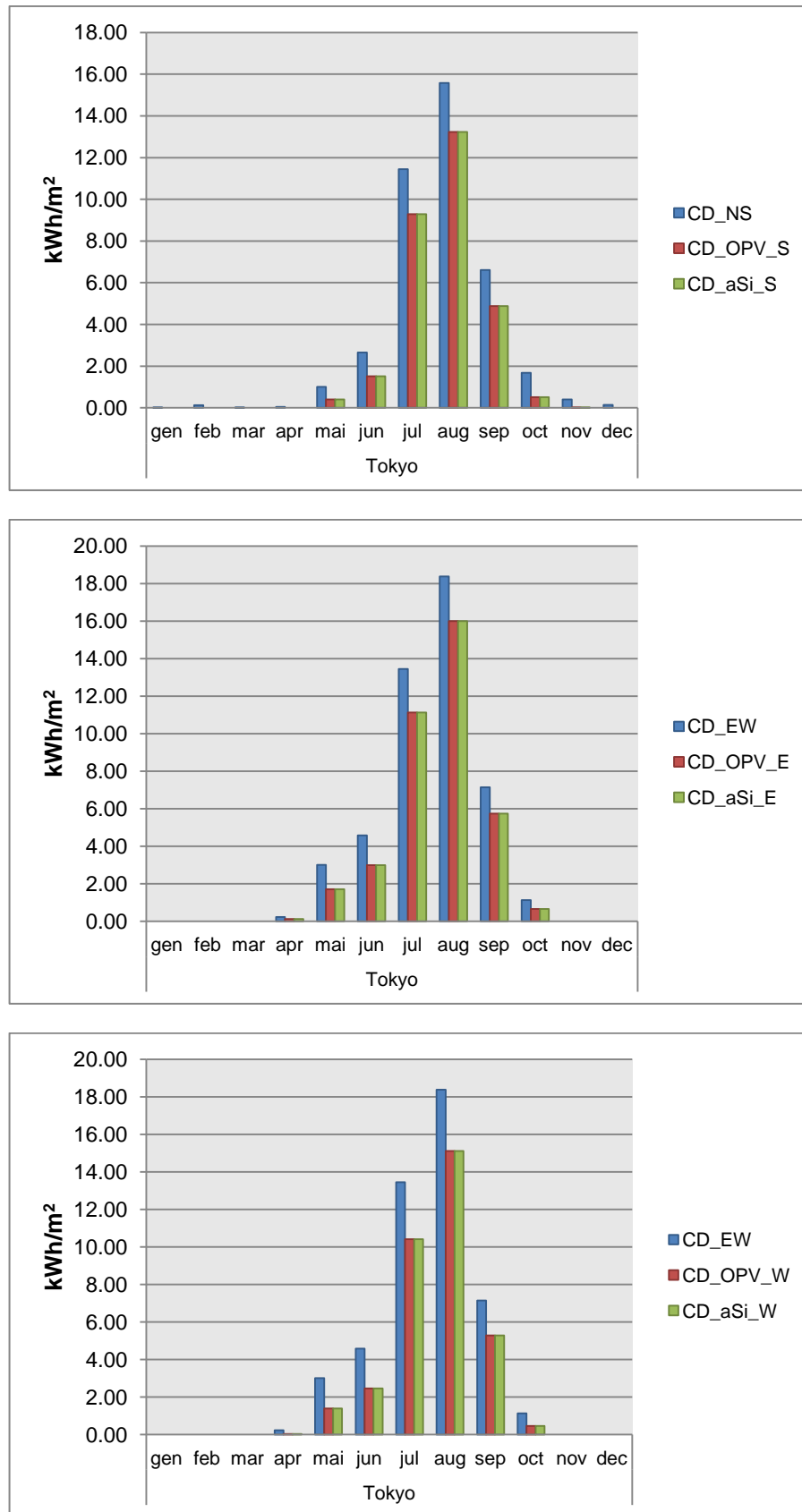
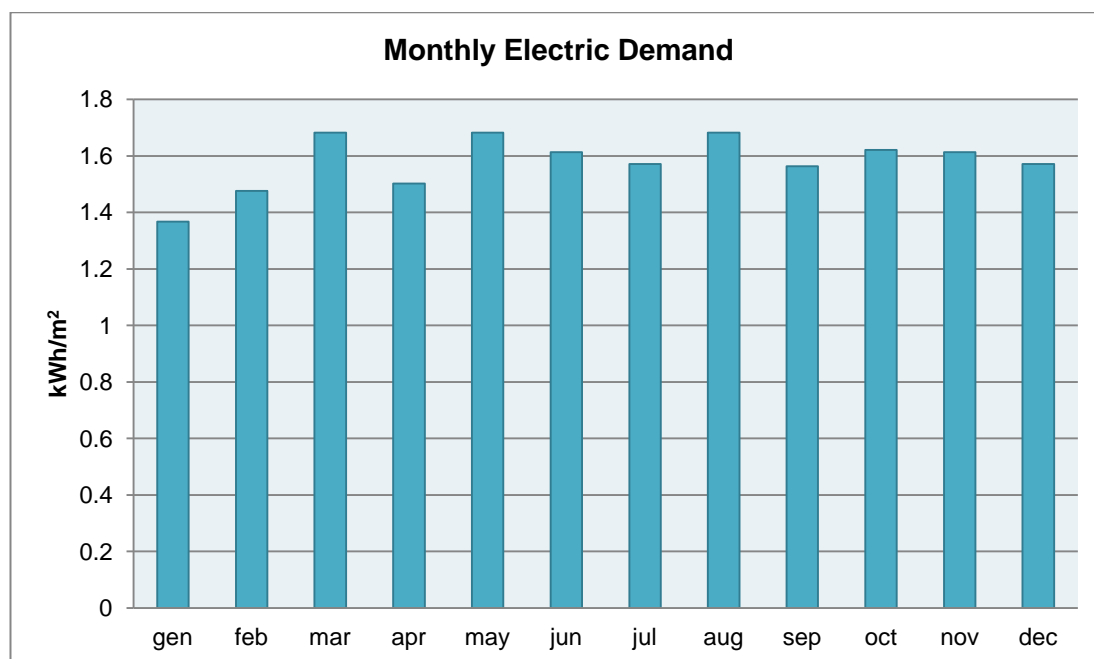


Figure 41 Annual cooling demand for Tokyo model cases.

3.2.3 Annual and Monthly Electric Demand

The electric demand remains constant for all the situations and different conditions, because it is not connected to outside factors and sun influence, but it only depends on the internal electric equipment and lighting power demands. The results are expressed in kWh and kWh/m², annually and monthly.

Table 12 Month Electric Demand summary.



Month Electric Demand		
	kWh	kWh/m ²
<i>gen</i>	6316.96	1.368
<i>feb</i>	6822.26	1.476
<i>mar</i>	7773.15	1.681
<i>apr</i>	6943.01	1.502
<i>may</i>	7773.15	1.681
<i>jun</i>	7456.19	1.613
<i>jul</i>	7259.97	1.570
<i>aug</i>	7773.15	1.681
<i>sep</i>	7223.75	1.562
<i>oct</i>	7492.41	1.621
<i>nov</i>	7456.19	1.613
<i>dec</i>	7259.97	1.570
Annual	87550.18	18.94

3.2.4 Annual and Monthly Energy Production

The models with photovoltaic cells integrated count on an amount of energy production, in the sense that the energy collected by the systems is used to decrease the energetic demand of the building. Considering the orientation and the type of PV integrated (OPV or a-Si) they differently affect the building demand.

The impact of the orientation is clearly visible already from the annual values, as the south oriented models collect more solar energy than the others, with the only exceptions of Singapore and Addis Ababa. In these cases, the reason is connected to the geographical position of the two cities, which are placed closer to the Equator than the other cities, and so the sun height is more perpendicular to the building.

Generally, the results show a positive response as all the models could collect a good amount of energy.

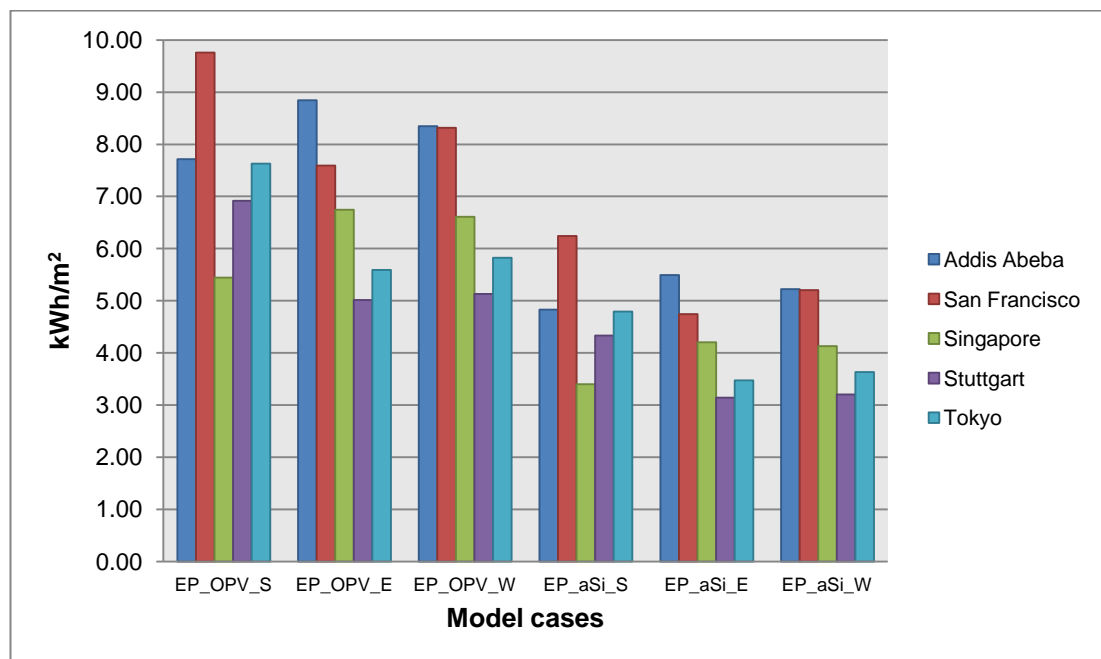


Figure 42 Annual Energy Production per floor area by PVs summary (EP: energy production; NS: north-south orientation; EW: east-west orientation; OPV: organic photovoltaics; aSi: amorphous silicon photovoltaics).

Table 13 Annual Energy Production summary.

Annual Energy Production [kWh/m ²]						
	EP_OPV_S	EP_OPV_E	EP_OPV_W	EP_aSi_S	EP_aSi_E	EP_aSi_W
Addis Ababa	7.72	8.84	8.35	4.83	5.49	5.22
San Francisco	9.76	7.59	8.32	6.24	4.75	5.21
Singapore	5.44	6.75	6.61	3.40	4.20	4.13
Stuttgart	6.92	5.01	5.13	4.33	3.14	3.20
Tokyo	7.63	5.59	5.83	4.79	3.47	3.63

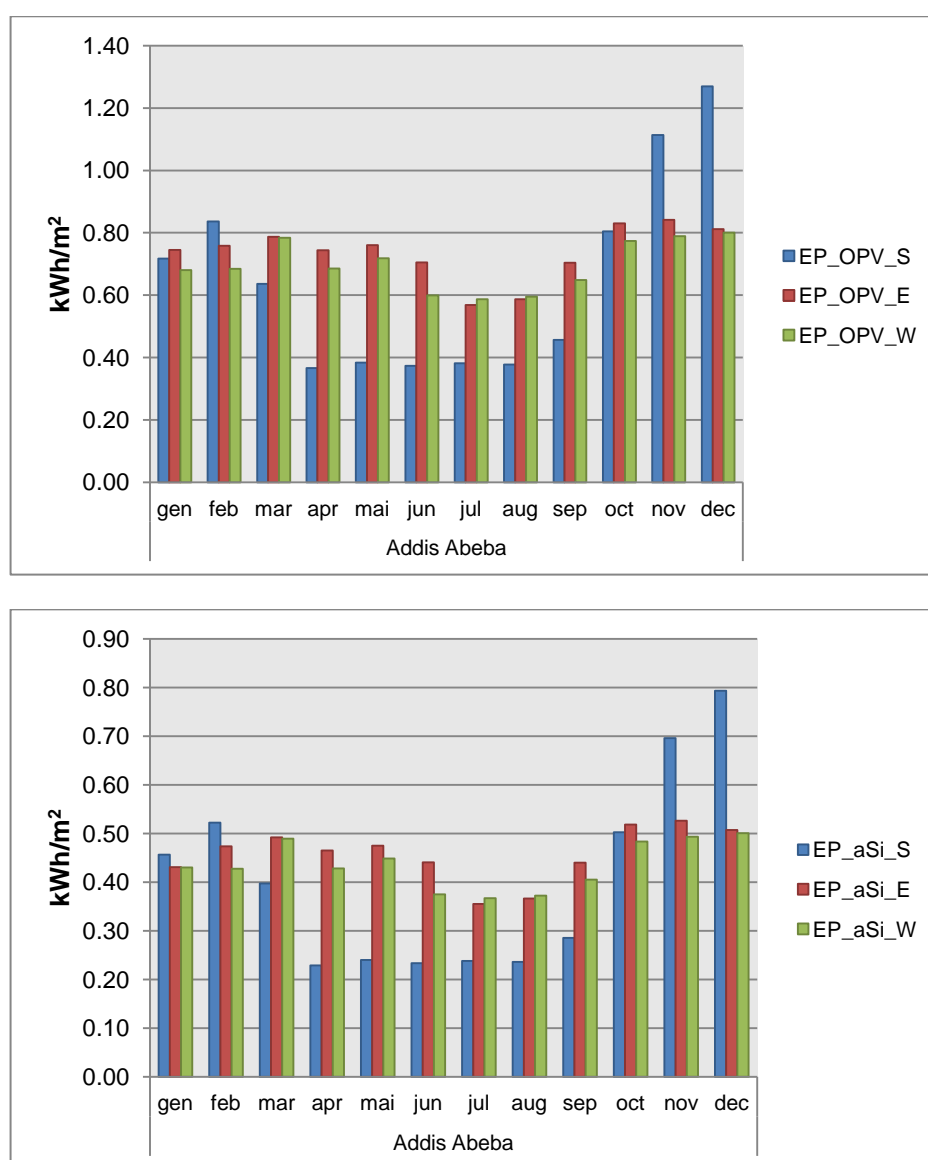


Figure 43 Annual energy production for Addis Ababa model cases.

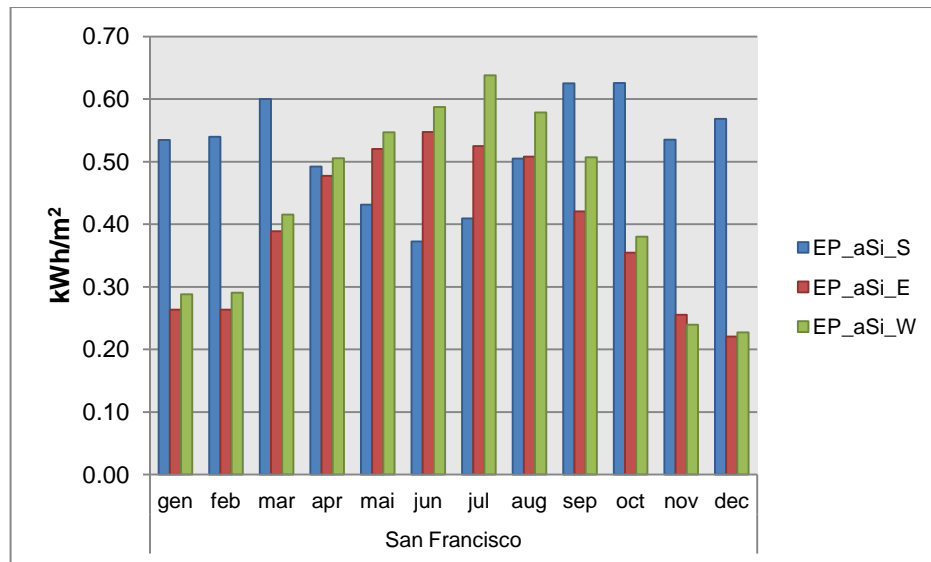
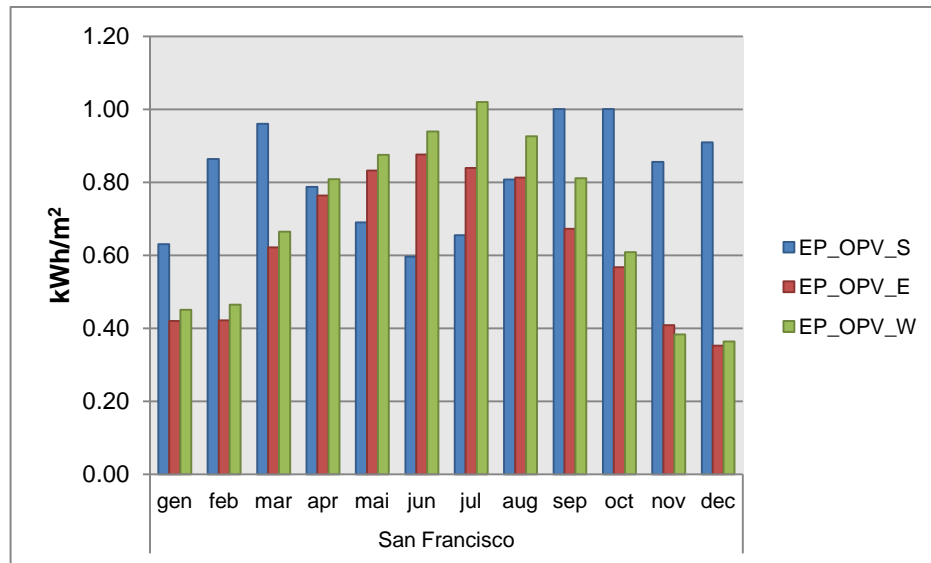


Figure 44 Annual energy production for San Francisco model cases.

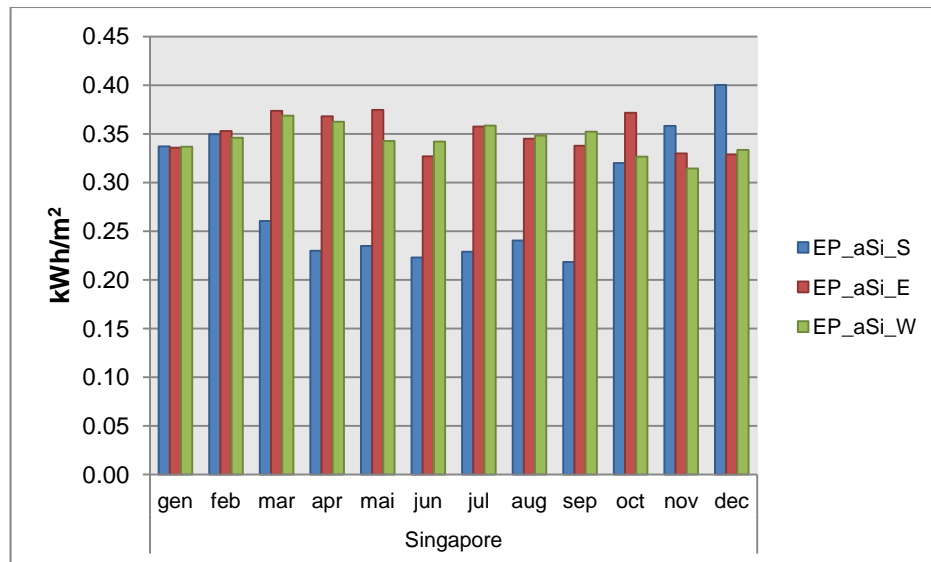
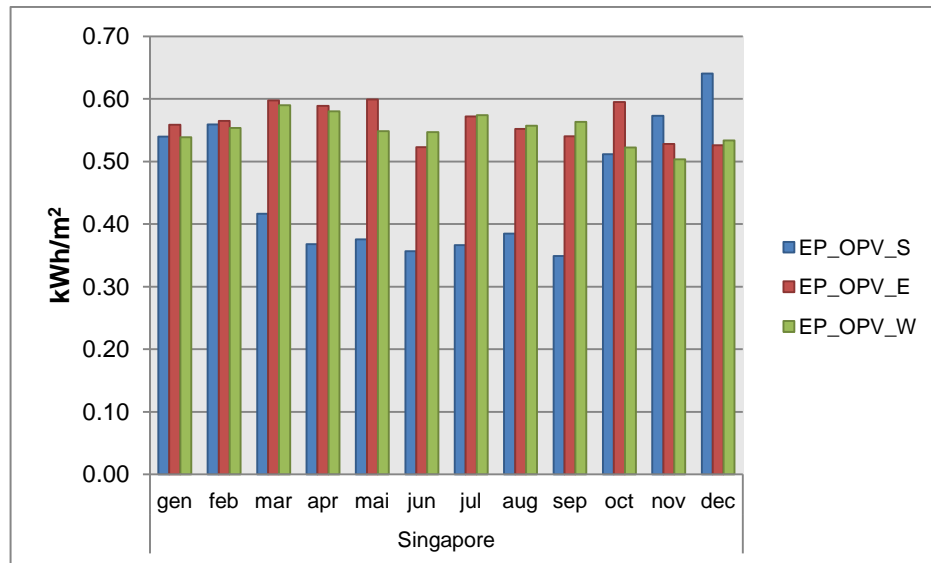


Figure 45 Annual energy production for Singapore model cases.

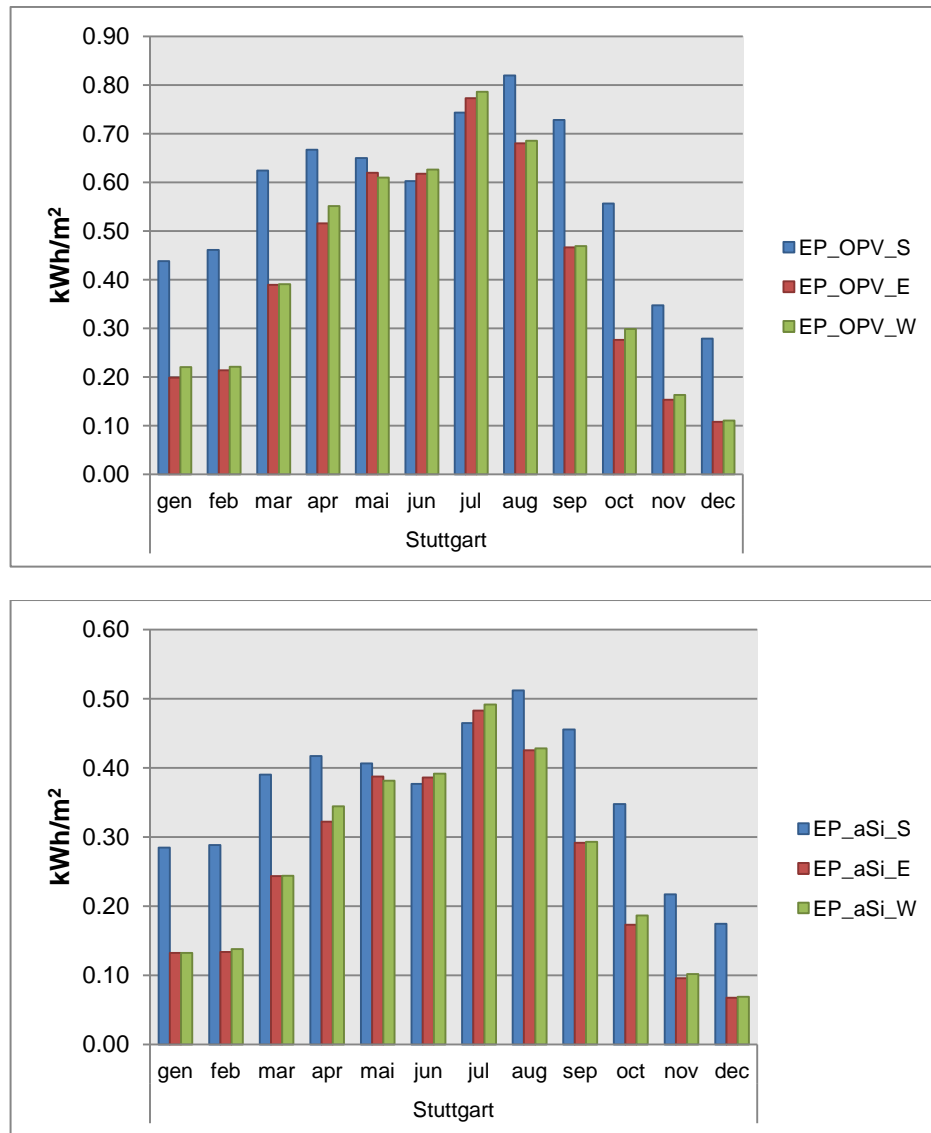


Figure 46 Annual energy production for Stuttgart model cases.

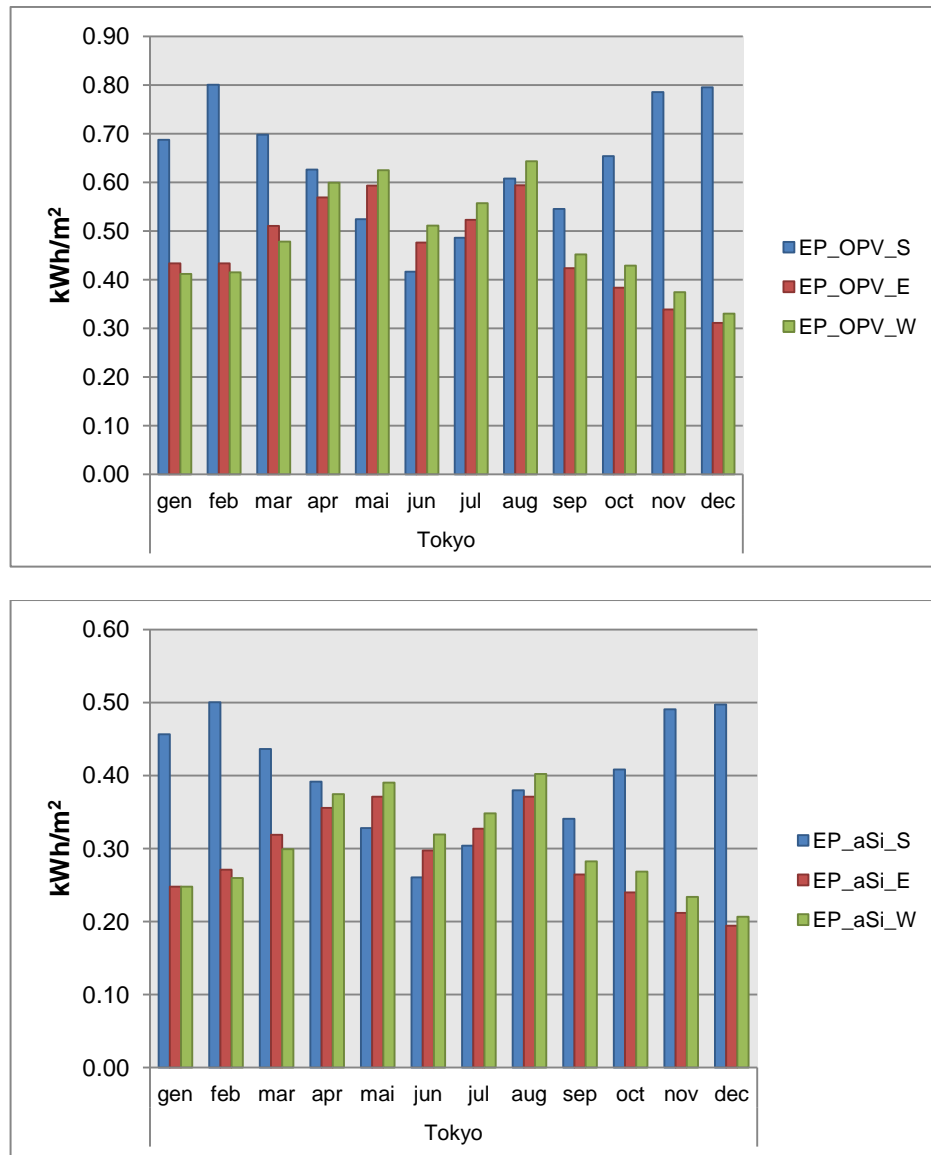


Figure 47 Annual energy production for Tokyo model cases.

3.2.5 Annual Total Demand and Energy Production Comparison

As it is visible from the graphs below, the PV energy production is not high enough to cover a significant amount of the building demand, considered as the sum of the heating, cooling and energetic. In very few cases, it reaches the third of the total demand, but generally it is very limited. Although that, it is however always positive and helpful, even if in a minimum amount. The case of Singapore seems to be singular, looking at the totality of the results: in fact, only in this case, it can be said that the PV system does not affect in almost any way the total demand. The reason may be connected both to the great entity of cooling demand, that the building has

in Singapore, and to the peculiarity of the PV systems, which maybe are not the most efficient choice for the type of building in that region.

Table 14 Annual total demand and energy production comparison. (*EP: energy production; TD: total demand; NS: north-south orientation; EW: east-west orientation; OPV: organic photovoltaics; aSi: amorphous silicon photovoltaics*).

Annual Total Demand and Energy Production [kWh/m ²]								
	EP_NS	EP_EW	EP_OPV_S	EP_OPV_E	EP_OPV_W	EP_aSi_S	EP_aSi_E	EP_aSi_W
Addis Ababa	-	-	7.71	8.84	8.34	4.83	5.49	5.22
San Francisco	-	-	9.75	7.59	8.31	6.23	4.74	5.20
Singapore	-	-	5.44	6.74	6.61	3.40	4.20	4.13
Stuttgart	-	-	6.91	5.01	5.13	4.33	3.14	3.20
Tokyo	-	-	7.62	5.59	5.82	4.79	3.47	3.63
	TD_NS	TD_EW	TD_OPV_S	TD_OPV_E	TD_OPV_W	TD_aSi_S	TD_aSi_E	TD_aSi_W
Addis Ababa	47.34	80.53	31.82	55.56	52.65	31.82	55.56	52.65
San Francisco	56.70	49.03	28.96	41.63	36.86	28.96	41.63	36.86
Singapore	289.54	291.76	294.17	316.59	316.40	294.17	316.59	316.40
Stuttgart	172.86	186.74	164.42	181.21	179.79	164.42	181.21	179.79
Tokyo	127.20	140.60	117.16	130.86	127.63	117.16	130.86	127.63

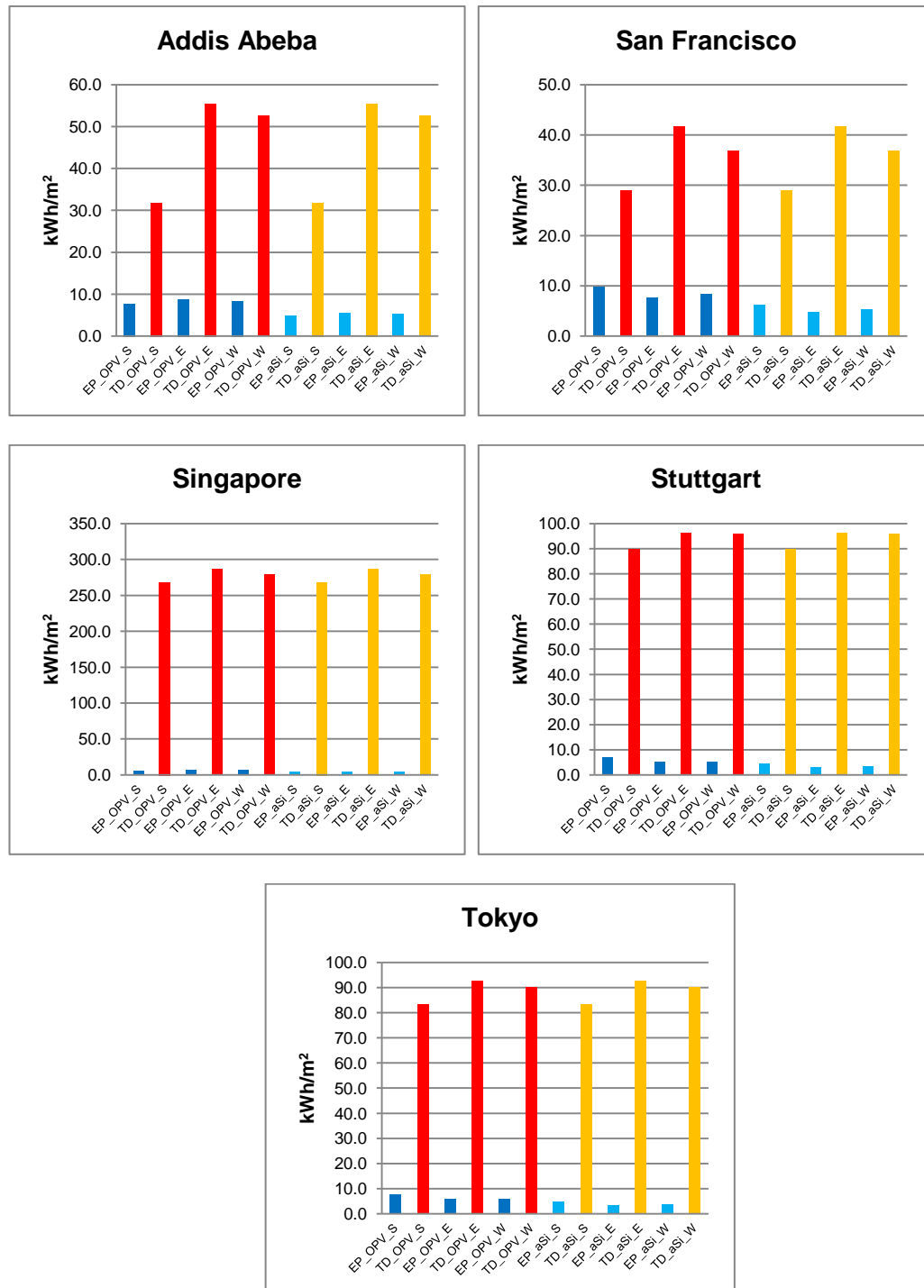


Figure 48 Total energetic demand for each building case compared to PV energy production. Blue and red columns: building cases with OPVs. Orange and light blue columns: building cases with aSi.

3.3 Visual Simulation Results

The results about the visual simulation will be listed by performance indicator in order to better have an overview over all them, while the discussion about their quality and the final comments will be expressed later. The indicators will be:

- Illuminance and Uniformity;
- Daylight Glare;
- Daylight Autonomy;
- Daylight Factor;
- Irradiance;
- Color Spectrum.

3.3.1 Illuminance and Uniformity

The computation of illuminance returns a long list of values, one for each point of the grid for every hour of every day. The graphs below summarize them and indicate the differences at workplane height, obtained for the model cases without (red) and with the photovoltaic layer integrated (orange): on the y-axis there are the illuminance values related to the specific model, while on the x-axis are shown the hours of the days, from 8:00 to 16:00. The results express illuminance average values of all grid points per hour of the day (E_{av}).

The EN 12464-1 defines the standard values for inside illumination for office buildings as follows:

- Illuminance > 500 lux for working areas;
- Illuminance > 150-250 lux for background;
- minimum illuminance on walls = 75 lux;
- minimum illuminance on ceiling = 50 lux;
- Uniformity >10%.

Additionally the minimum and mean illuminance values have been averaged for considered days to compute uniformity results. Here, together with the illuminance values, are presented the uniformity percentages that help to understand the light distribution in the room. Low uniformity values express an uneven distribution.

The graphs are divided by city: the results correspond to the months March, June, September and December. First there are the graphs about illuminance, after an example for the city of Singapore is shown about the uniformity results.

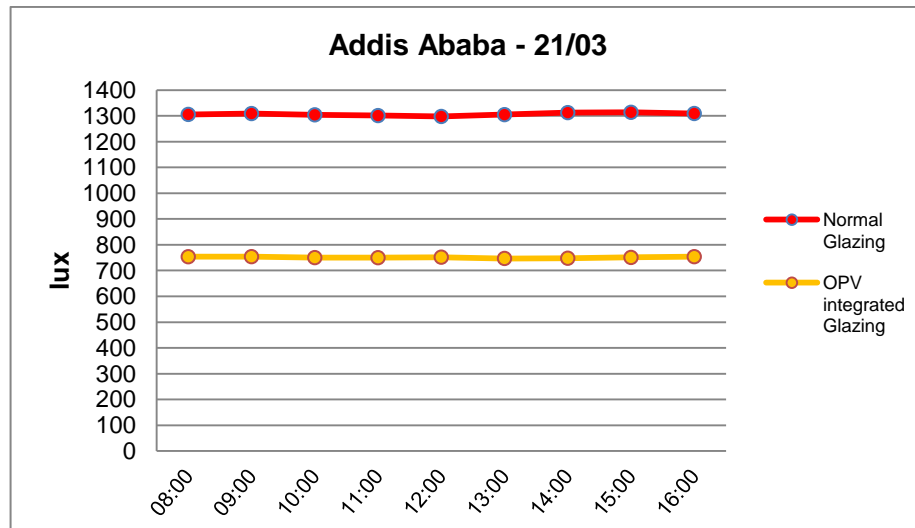


Figure 49 Average illuminance for model case without OPVs (above) and with OPVs (below).

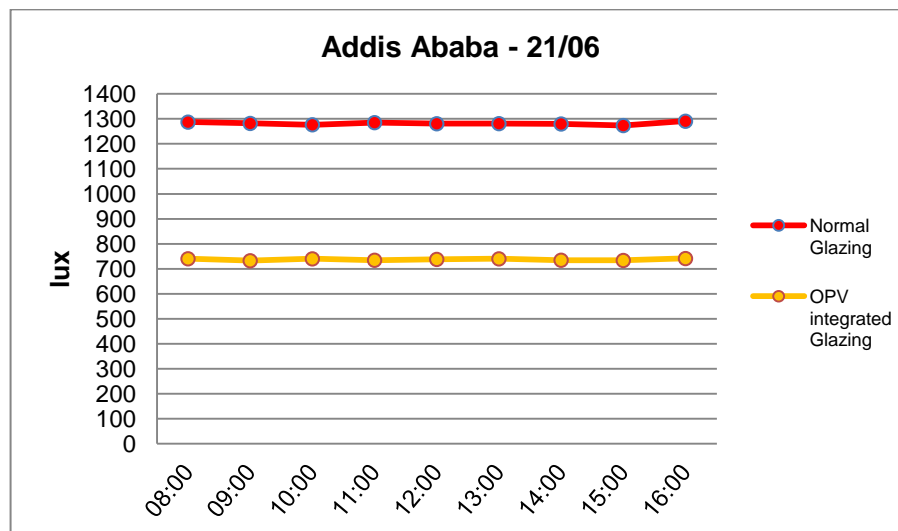


Figure 50 Average illuminance for model case without OPVs (above) and with OPVs (below).

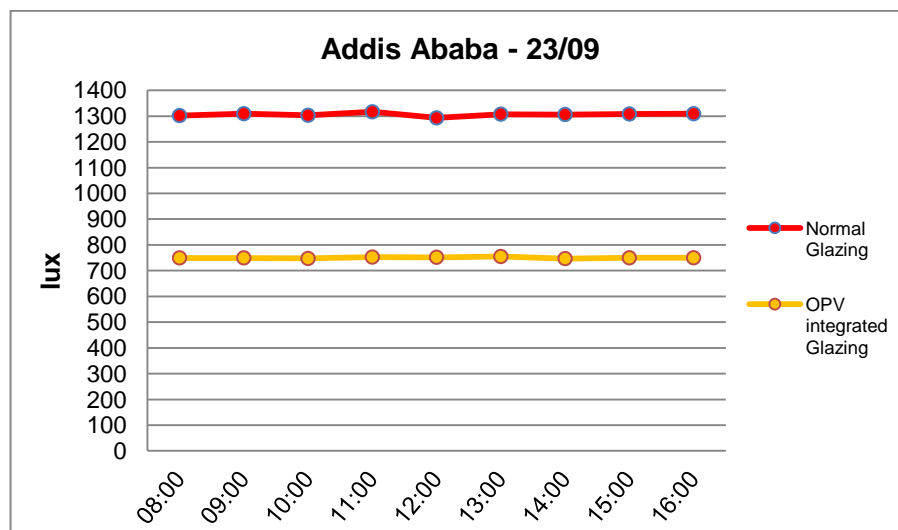


Figure 51 Average illuminance for model case without OPVs (above) and with OPVs (below).

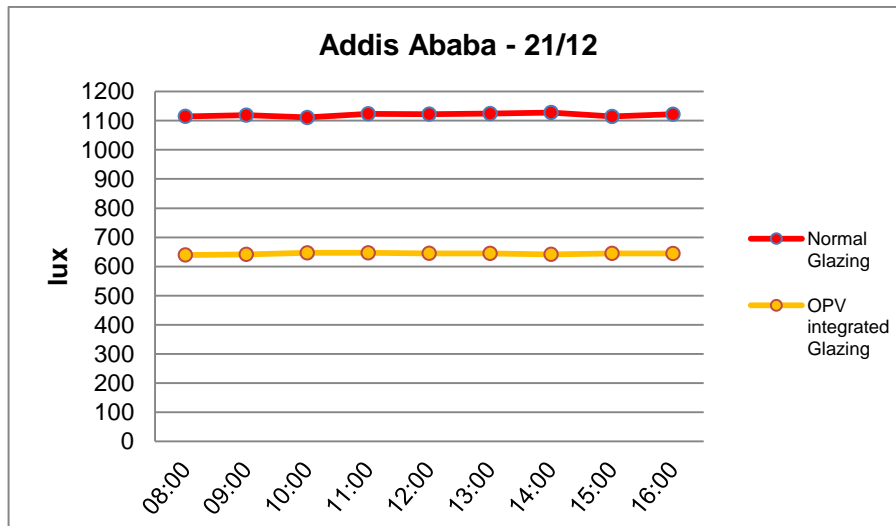


Figure 52 Average illuminance for model case without OPVs (above) and with OPVs (below).

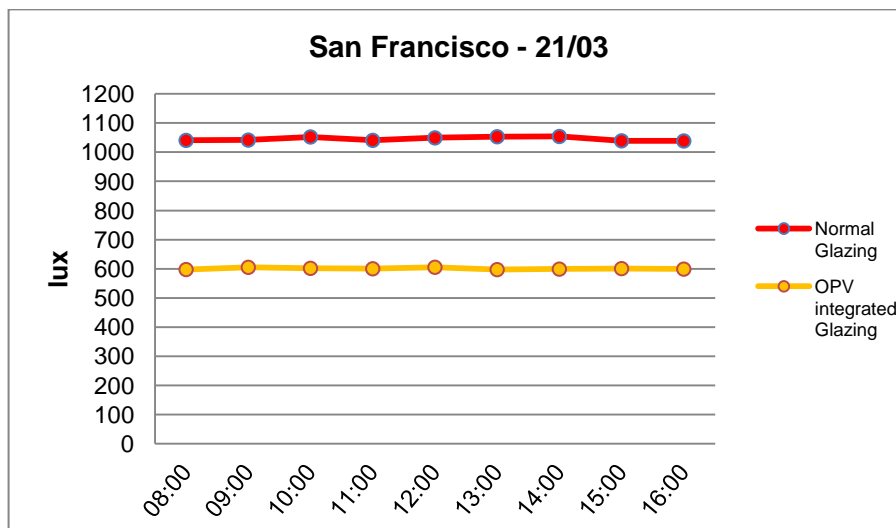


Figure 53 Average illuminance for model case without OPVs (above) and with OPVs (below).

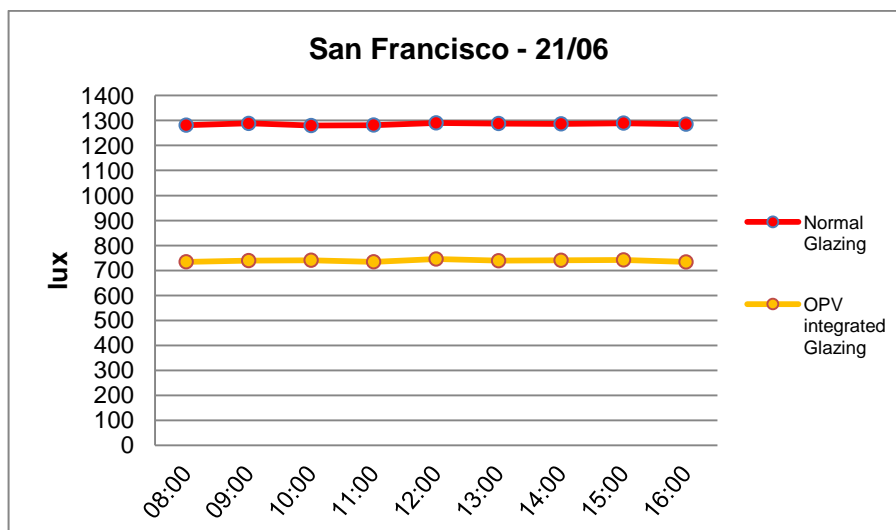


Figure 54 Average illuminance for model case without OPVs (above) and with OPVs (below).

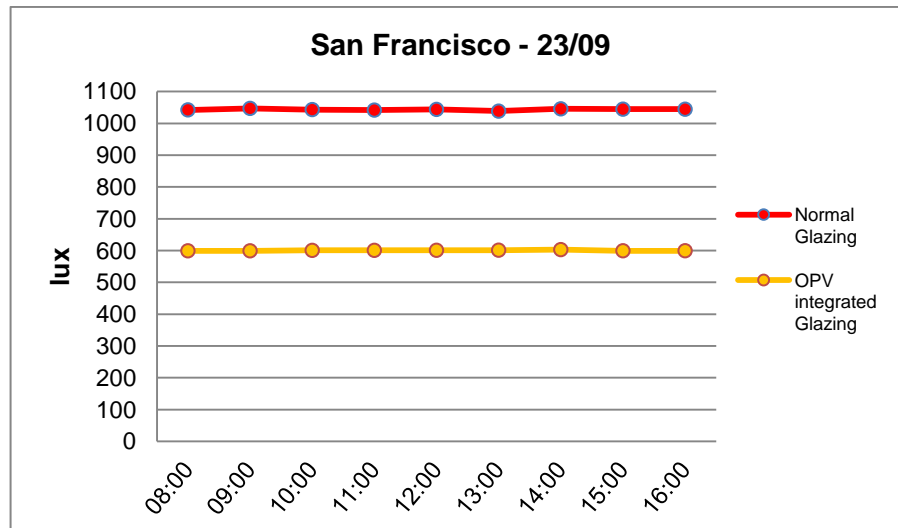


Figure 55 Average illuminance for model case without OPVs (above) and with OPVs (below).

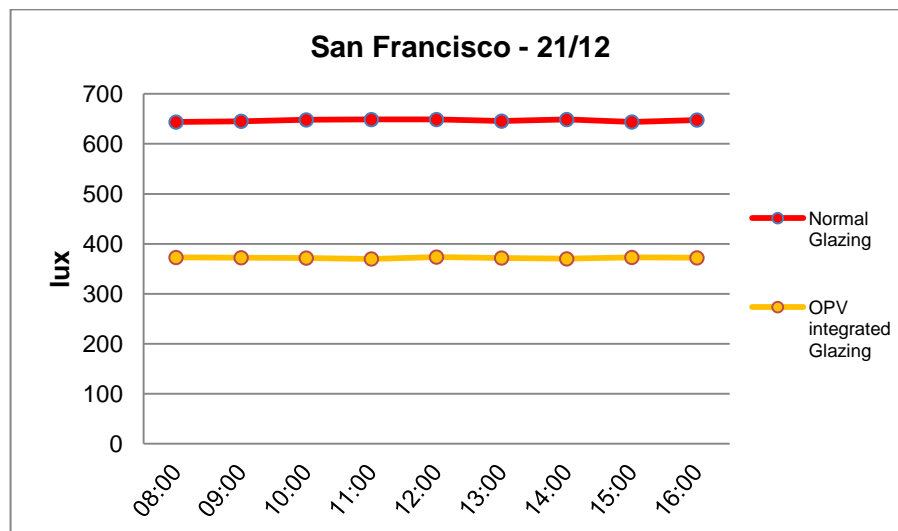


Figure 56 Average illuminance for model case without OPVs (above) and with OPVs (below).

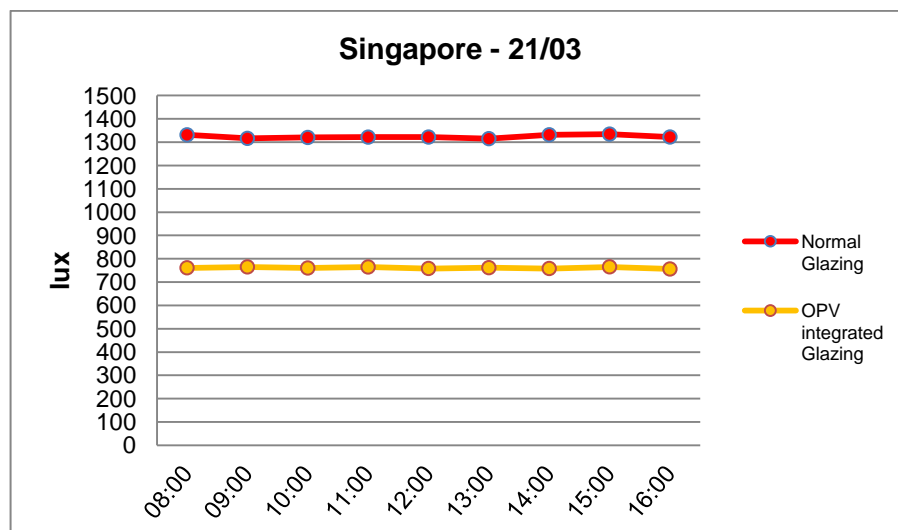


Figure 57 Average illuminance for model case without OPVs (above) and with OPVs (below).

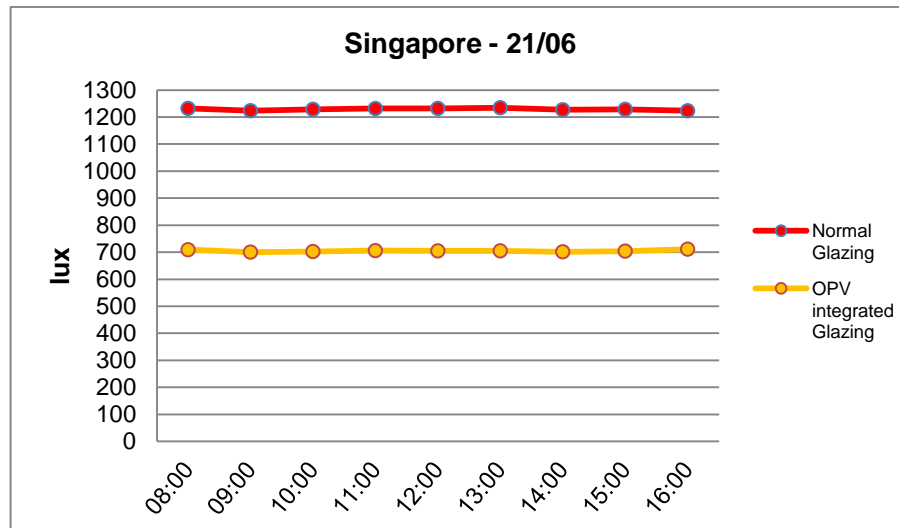


Figure 58 Average illuminance for model case without OPVs (above) and with OPVs (below).

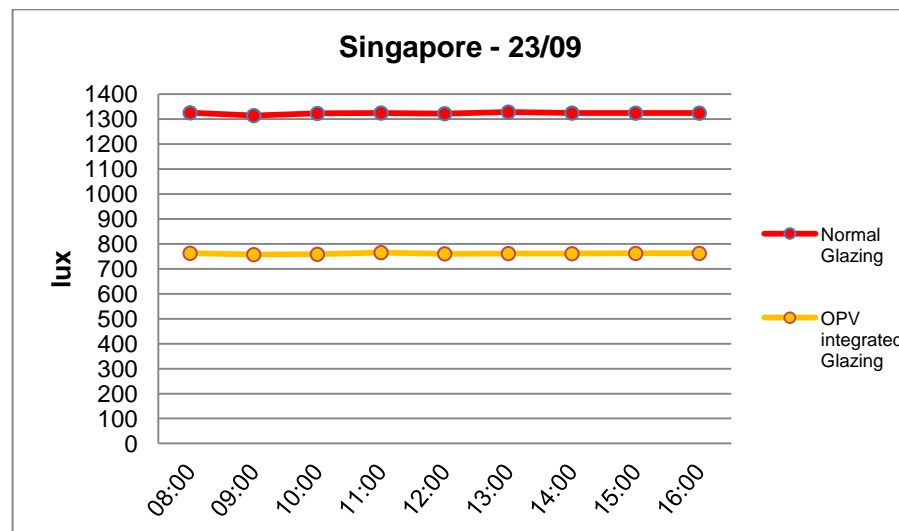


Figure 59 Average illuminance for model case without OPVs (above) and with OPVs (below).

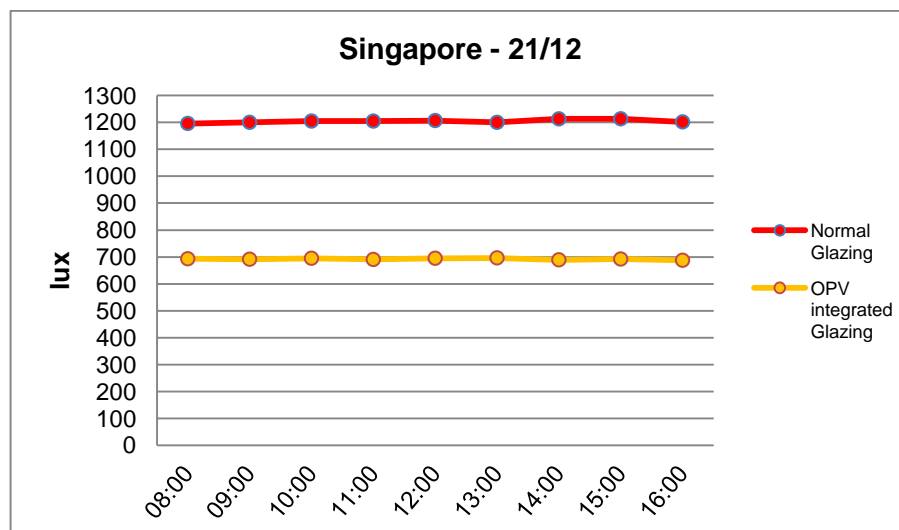


Figure 60 Average illuminance for model case without OPVs (above) and with OPVs (below).

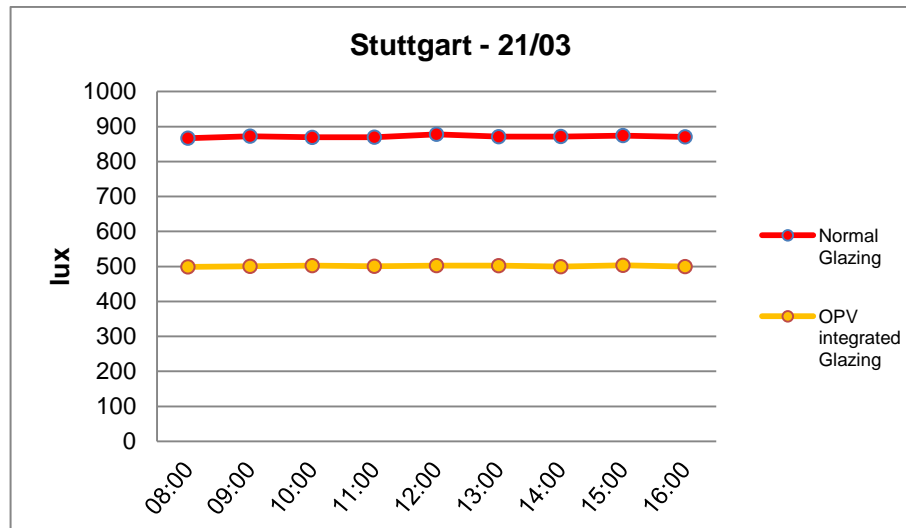


Figure 61 Average illuminance for model case without OPVs (above) and with OPVs (below).

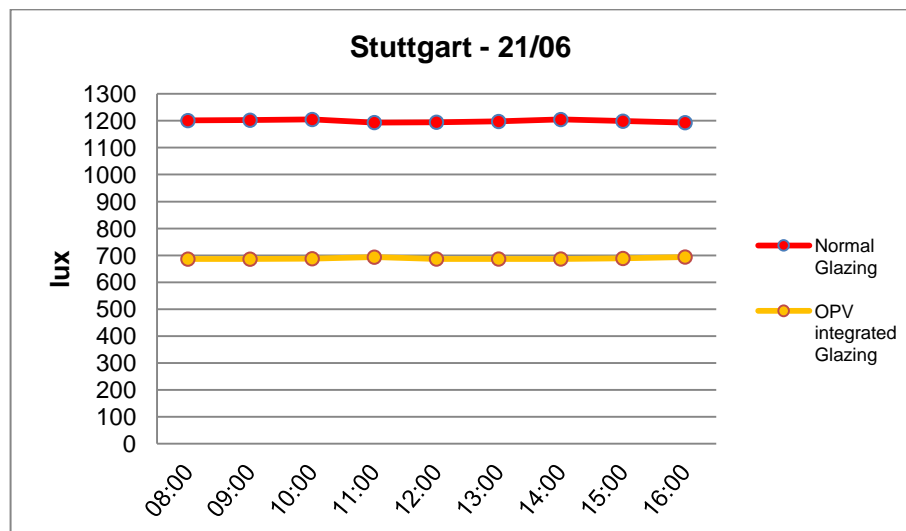


Figure 62 Average illuminance for model case without OPVs (above) and with OPVs (below).

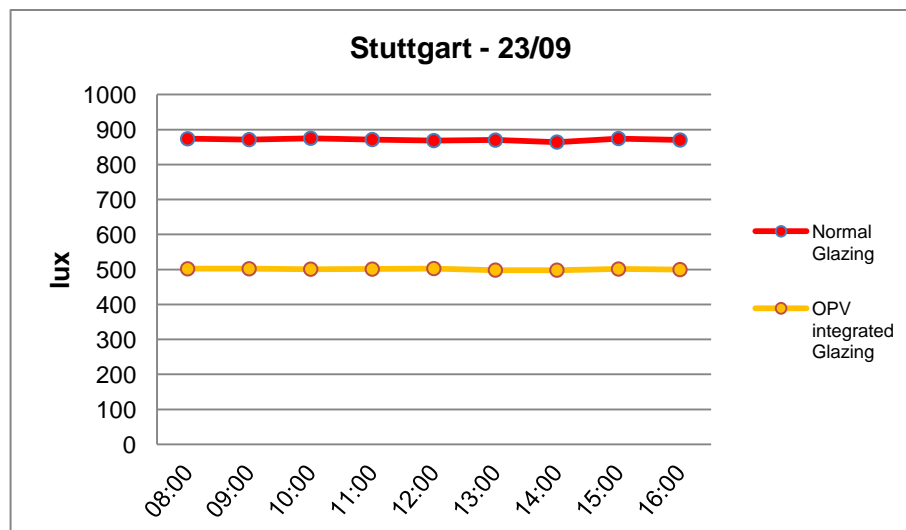


Figure 63 Average illuminance for model case without OPVs (above) and with OPVs (below).

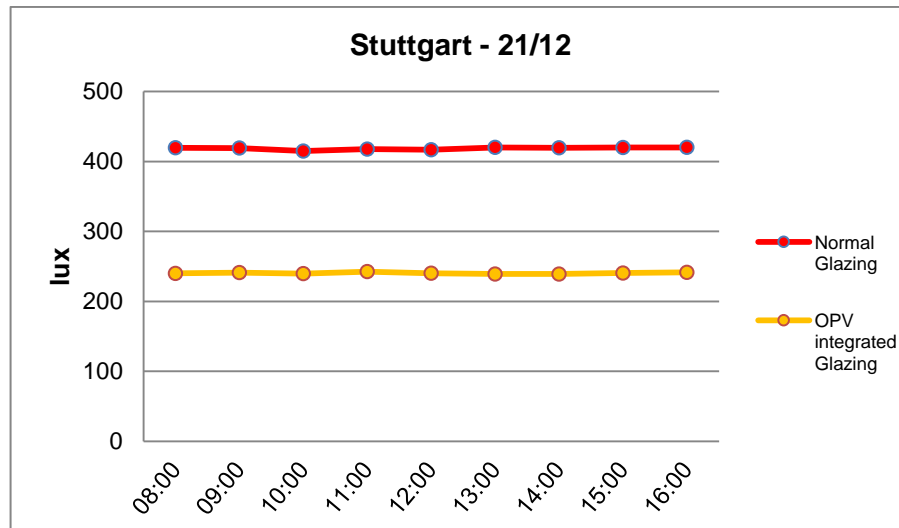


Figure 64 Average illuminance for model case without OPVs (above) and with OPVs (below).

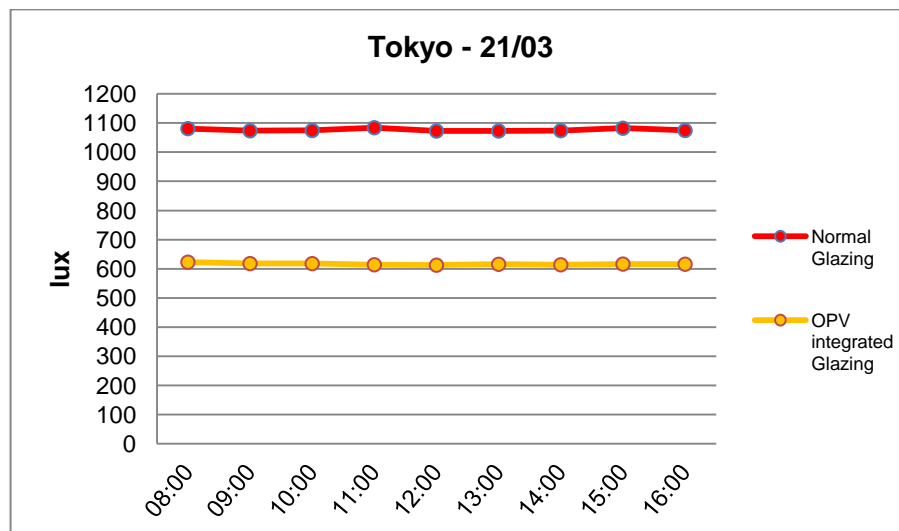


Figure 65 Average illuminance for model case without OPVs (above) and with OPVs (below).

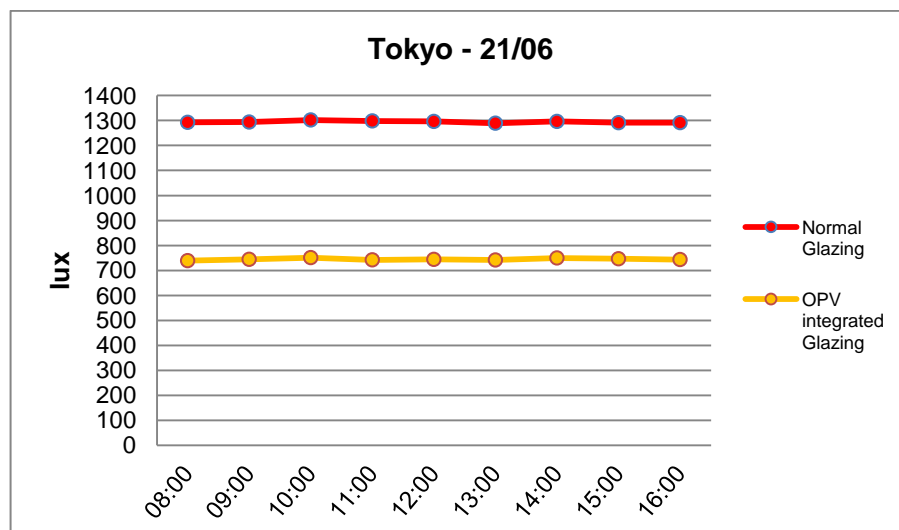


Figure 66 Average illuminance for model case without OPVs (above) and with OPVs (below).

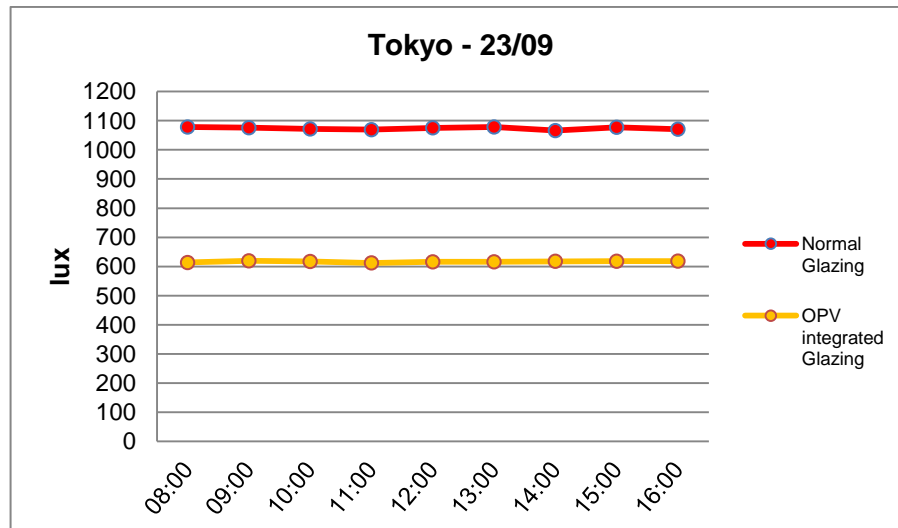


Figure 67 Average illuminance for model case without OPVs (above) and with OPVs (below).

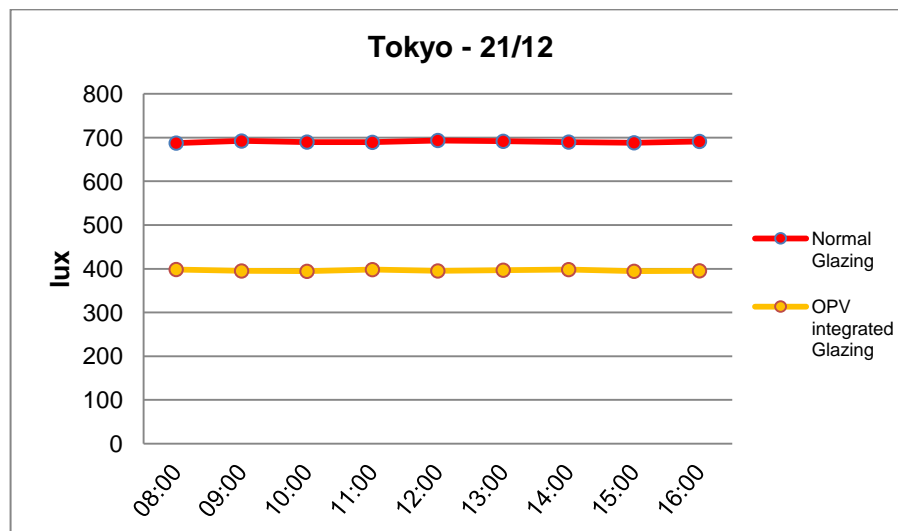


Figure 68 Average illuminance for model case without OPVs (above) and with OPVs (below).

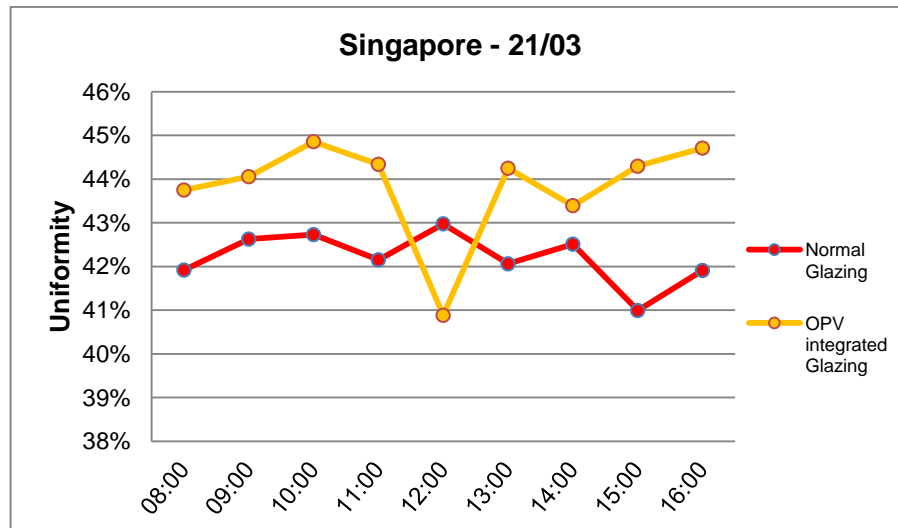


Figure 69 Average uniformity for Singapore model case with and without OPVs.

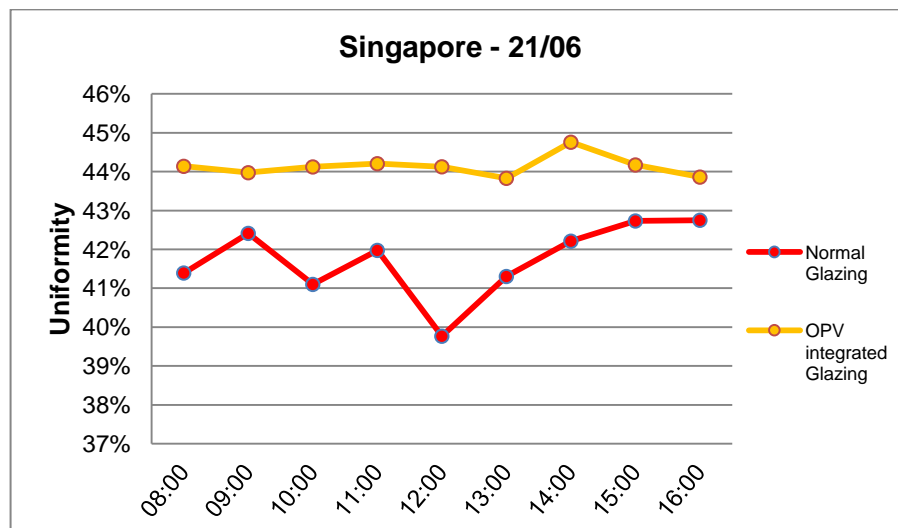


Figure 70 Average uniformity for Singapore model case with and without OPVs.

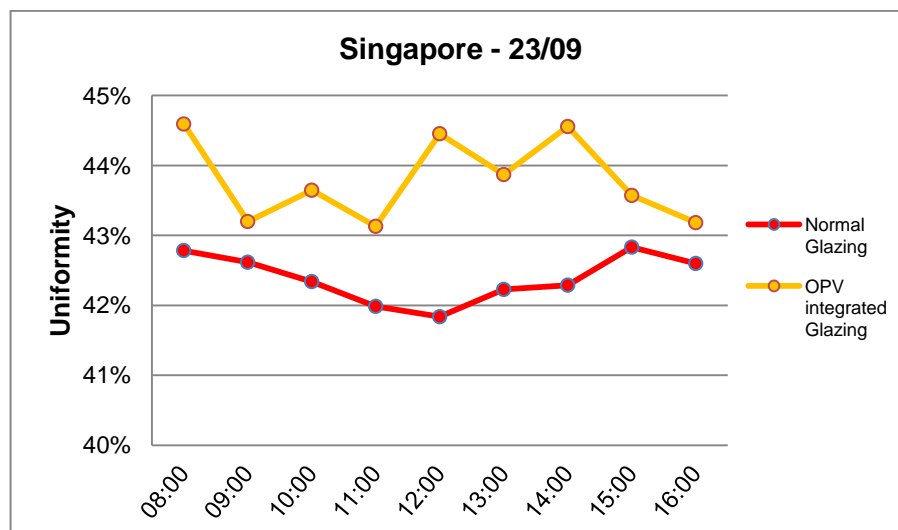


Figure 71 Average uniformity for Singapore model case with and without OPVs.

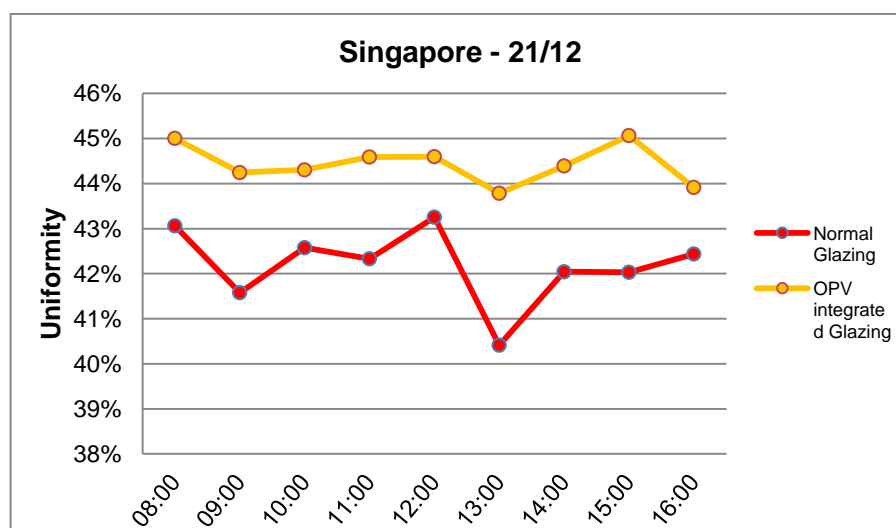


Figure 72 Average uniformity for Singapore model case with and without OPVs.

The results of uniformity do not differ very much from each other: the case of Singapore is here shown to understand the general behavior of the indicator. The other model cases can be found in the Appendix B in the Table part.

3.3.2 Daylight Autonomy

The DA is calculated starting from the illuminance values and defines the percentage of hours in which the daylight can satisfy the lighting requirements. It is presented in the following table: the different percentages are put beside to see their changing.

Standing to requirements (DIN 5035), the Daylight Autonomy for office buildings should be at least 70%. As most of the values obtained cannot satisfy it, the results lower than 50% have been considered unacceptable performance values. The results show that the worst performance belongs to the models in Stuttgart for the month of December. In particular the case with OPVs integrated has a percentage under 10%, meaning that the required illuminance is rarely reached: as shown below, the average illuminance for every hour through the whole month is much lower than 500 lux.

Table 15 Daylight Autonomy summary

Model Cases	DA without OPV [%]	DA with OPV [%]
Addis Ababa_March	100	66.56
Addis Ababa_June	100	66.56
Addis Ababa_September	100	66.56
Addis Ababa_December	83.63	58.44
San Francisco_March	83.23	52.58
San Francisco _June	100	66.56
San Francisco _September	83.75	52.5
San Francisco _December	57.69	20.79
Singapore_March	100	66.56
Singapore _June	99.94	66.54
Singapore _September	100	66.56
Singapore _December	99.34	65.97
Stuttgart_March	66.74	41.66
Stuttgart _June	99.51	65.68
Stuttgart _September	66.71	41.65
Stuttgart _December	25.18	8.33
Tokyo_March	83.3	56.63
Tokyo _June	100	66.66
Tokyo _September	83.3	56.42
Tokyo _December	61.28	24.97

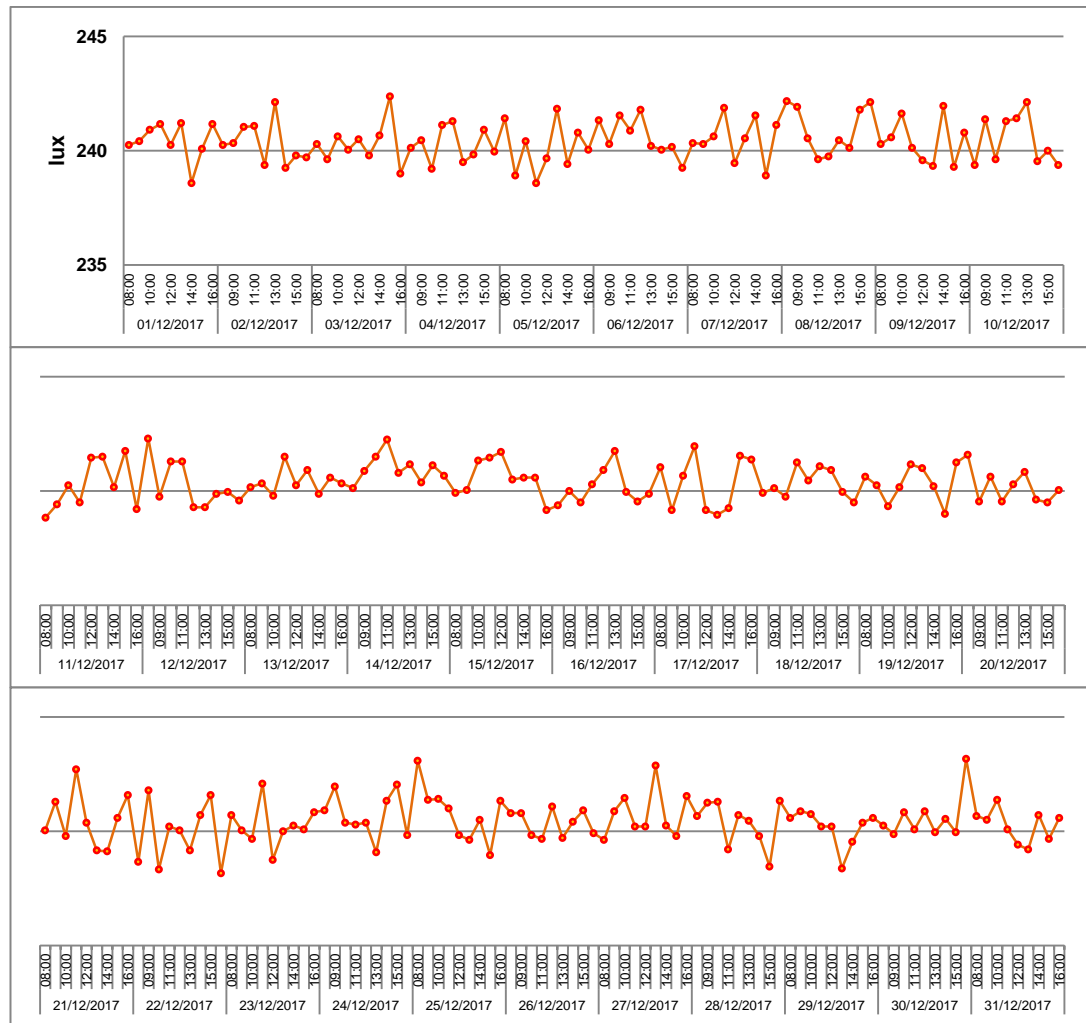


Figure 73 Average illuminance for the Stuttgart model with OPVs in December..

3.3.3 Daylight Glare

The daylight glare index calculation depends on different values, as the luminance of the source, the average background luminance, the angular size of the source as seen by the eye, the solid angle subtended by the source, modified for the effect of the position of the observer in relation to the source. Starting from this, the calculation of the indicator on the workplane height (0.8m) did not return significant values, meaning that the glare did not happen at that height. Not to consider all the standing and sitting position possibilities in the room, it has been mainly considered the luminance of the source for discovering the potential glare problems.

The high luminance values that can cause glare situation are below directly presented on the falsecolor scene-images. Standing to the requirements expressed

in the norm ISO 9241-302 and EN 12464-1, the indirect lighting should have the following values:

- average luminance on walls $> 30 \text{ cd/m}^2$;
- maximum luminance on walls $< 1000 \text{ cd/m}^2$;
- maximum luminance on ceiling $< 1500 \text{ cd/m}^2$;
- average luminance on ceiling $< 500 \text{ cd/m}^2$.

Regarding the working areas, the norms define as follows:

High luminance monitors	High luminance monitors $L > 200 \text{ cd/m}^2$	Medium luminance monitors $L < 200 \text{ cd/m}^2$
Type A (positive polarity and normal requirements with respect to colour detail properties of the displayed information – as, for example, in an office, educational establishment, etc.)	$\leq 3000 \text{ cd/m}^2$	$\leq 1500 \text{ cd/m}^2$
Type B (negative polarity and/or higher requirements with respect to colour detail properties of the displayed information – as, for example, for CAD work, inspection of colours, etc.)	$\leq 1500 \text{ cd/m}^2$	$\leq 1000 \text{ cd/m}^2$

Figure 74 High luminance monitors values up to norm EN12464-1.

From that, for the calculation, the taken reference threshold value for Luminance is 1500 cd/m^2 , equal to the maximum value for glare visual comfort for working positions in offices; the situations where the luminance oversteps this value can be considered as potential glare problems. It is here shown the example of Singapore on 21st of June: the luminance distribution is plotted in the falsecolor images, so the areas with luminance higher than 1500 cd/m^2 can be easily discovered.

Table 16 Computation of glare probability inside the room for scene 1. Example of Singapore on 21.06. Comparison between the different models.

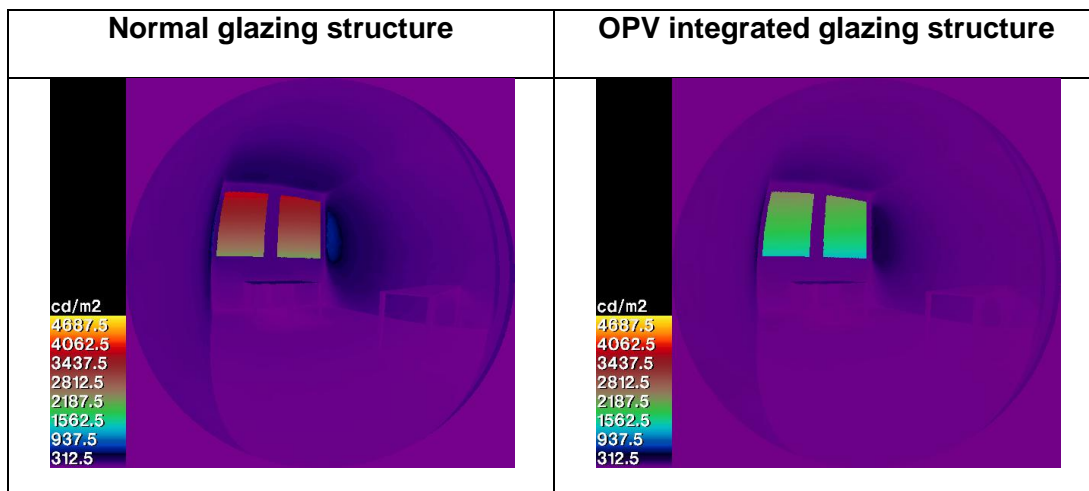


Table 17 Computation of glare probability inside the room for scene 2. Example of Singapore on 21.06. Comparison between the different models.

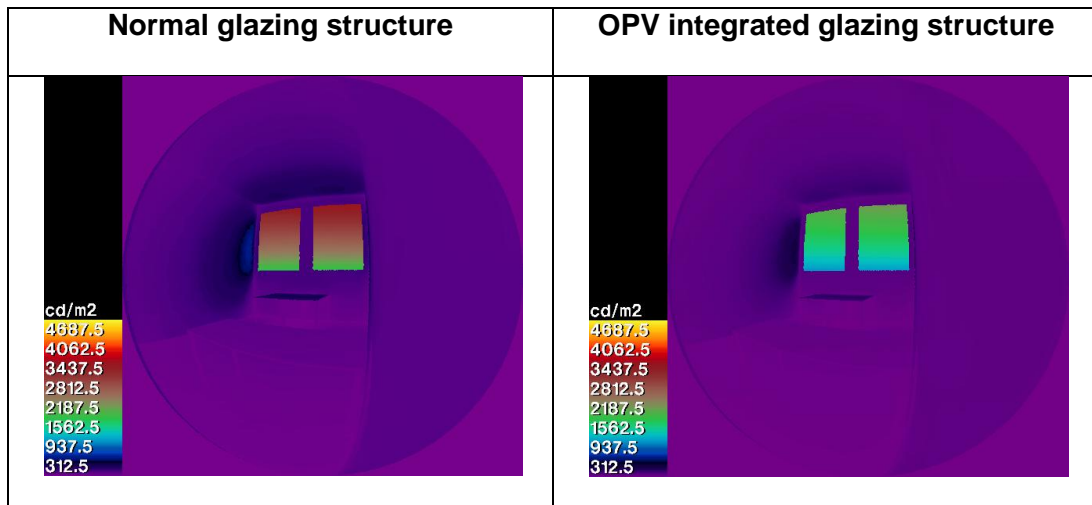
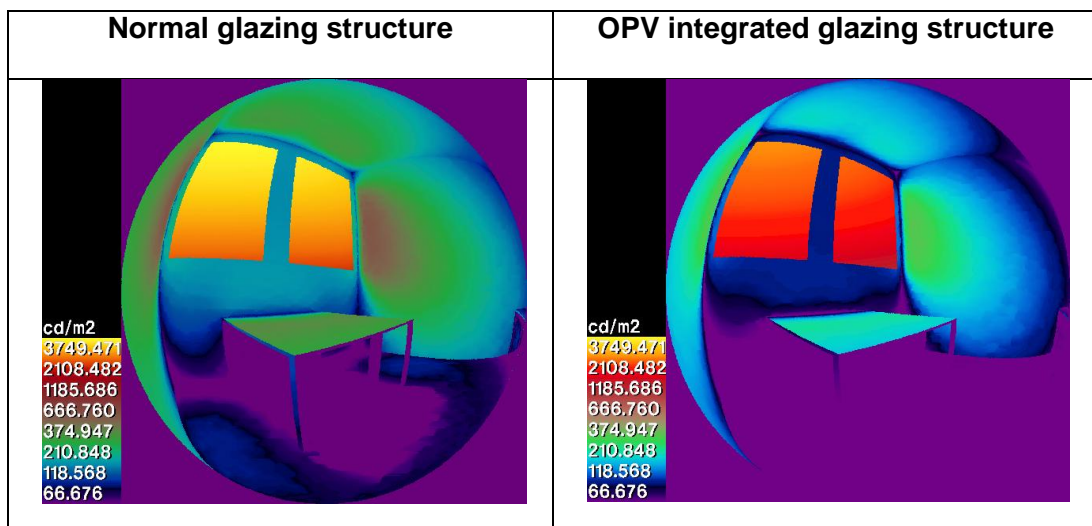


Table 18 Computation of glare probability inside the room for scene 3. Example of Singapore on 21.06. Comparison between the different models.

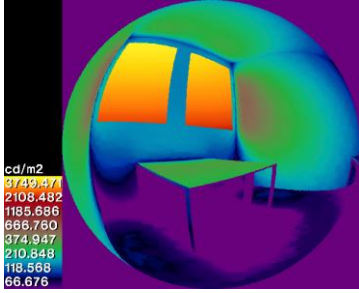
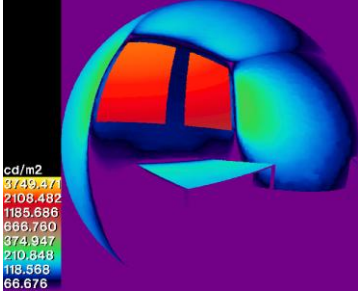
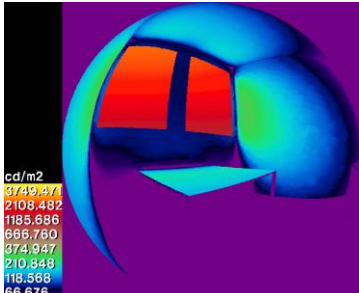
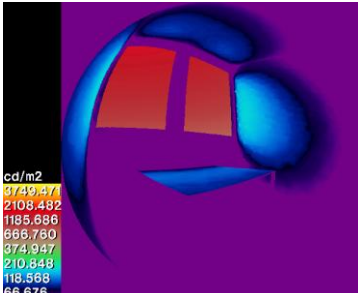
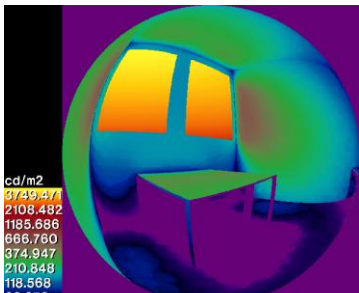
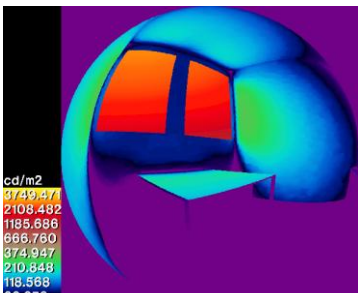
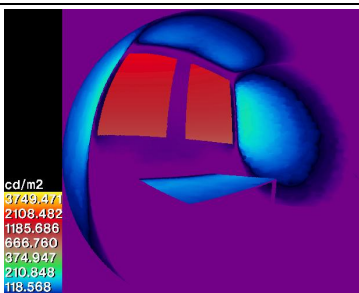
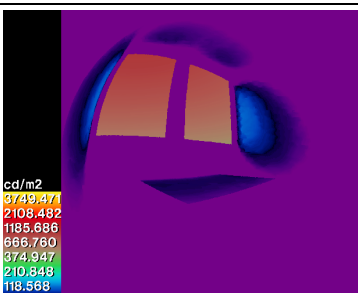
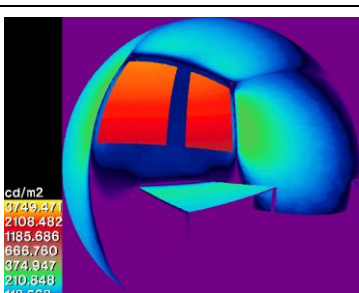
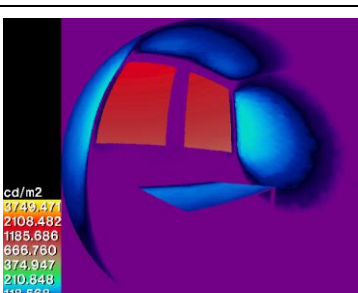


The luminance distribution, together with the UGR values has been evaluated for the most significant days and times of the year (refer to the Appendix for the other tables), as follows:

- Spring Equinox at 12:00;
- Summer Solstice at 12:00;
- Autumn Equinox at 12:00;
- Winter Solstice at 12:00.

This allows to have a general and qualitative description of daylight all over the year, as these are the most descriptive moments of the sun position and sunlight power.

Table 19 Luminance distribution on 21.12 for every model case.

	Scene 3	Scene 3 with OPVs
Addis Ababa		
San Francisco		
Singapore		
Stuttgart		
Tokyo		

In the table 19 above it is presented the luminance distribution and the problematic areas for the Winter Solstice at 12:00 for the city of Singapore. For this day, the third scene has been inspected, as it revealed to be the most valuable for its close position to the windows.

The UGR calculation for the only daylight did not return remarkable values. To have more valuable results, artificial lighting has been inserted as set in the sample office description: 4 parabolic louver and non-vented luminaires on the ceiling. The UGR is computed for the three different sitting positions. The view angles and the positions of the viewer are shown in the following figures.

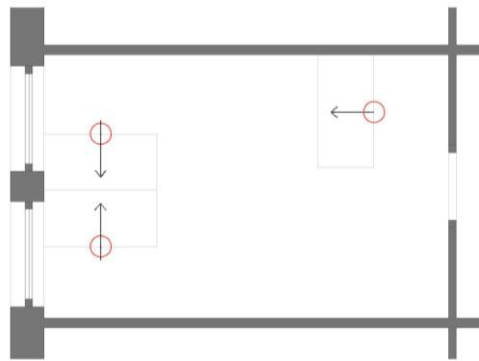


Figure 75 UGR calculation points positions and view direction. Three sitting eyes-height (1.2m).

The results do not show a very different behavior between the glazing systems: UGR values are almost the same in both the cases. The reference standard values for not disturbing UGR are below 22.

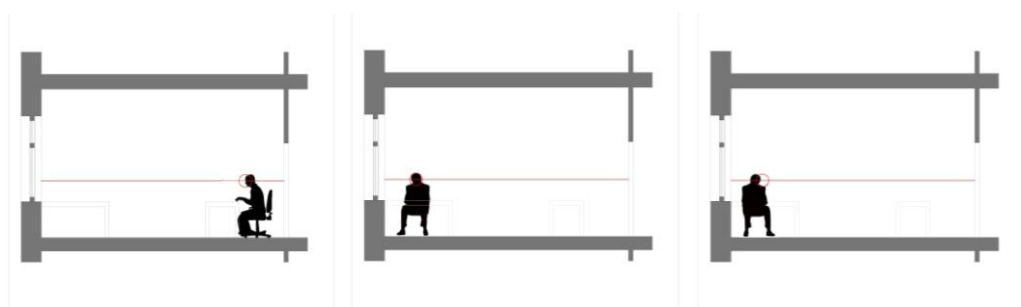


Figure 76 Sitting positions and height of UGR calculation points.

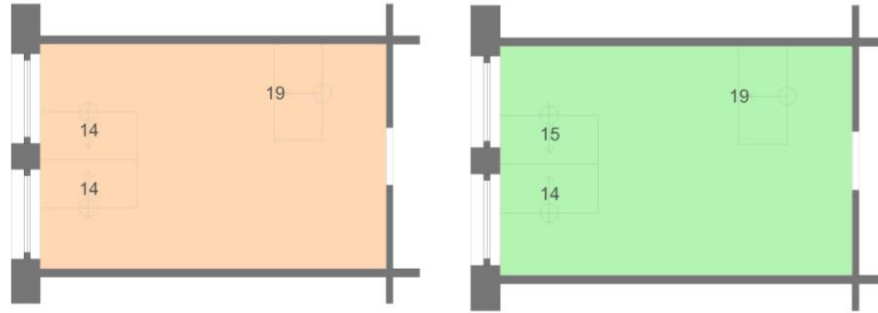


Figure 77 UGR results for the three sitting positions. Model without PV on the left, model with OPVs on the right.

3.3.4 Daylight Factor

The daylight factor has been computed both with Radiance software and manually. Two formulas have been used. The first is more general, referred to the geometry of the window and not related to day and time of the year. The output is a mean value:

$$DF_m [\%] = A_g / A_r \cdot \theta \tau_d M / (1 - \rho_m)^2. \quad (3)$$

The second one, instead, considers the average illuminance for each day of the months and an average outside illuminance, set to 10.000 lux:

$$DF [\%] = E_i / E_e \cdot 100. \quad (4)$$

Table 20 Daylight Factor (DF) computation.

	Model case without OPVs	Model case with OPVs
$A_g [m^2]$	5.32	5.32
$A_r [m^2]$	101.88	101.88
$\theta [^\circ]$	65	65
$\tau_d [\%]$	0.82	0.64
ρ_m	0.509	0.509
M	0.8	0.8
$DF_m [\%]$	1.65	1.29

The geometry based and illuminance based results are here compared to the ones obtained with Radiance. The computation is based on the daylight referred to the different skies corresponding to the different cities and seasons.

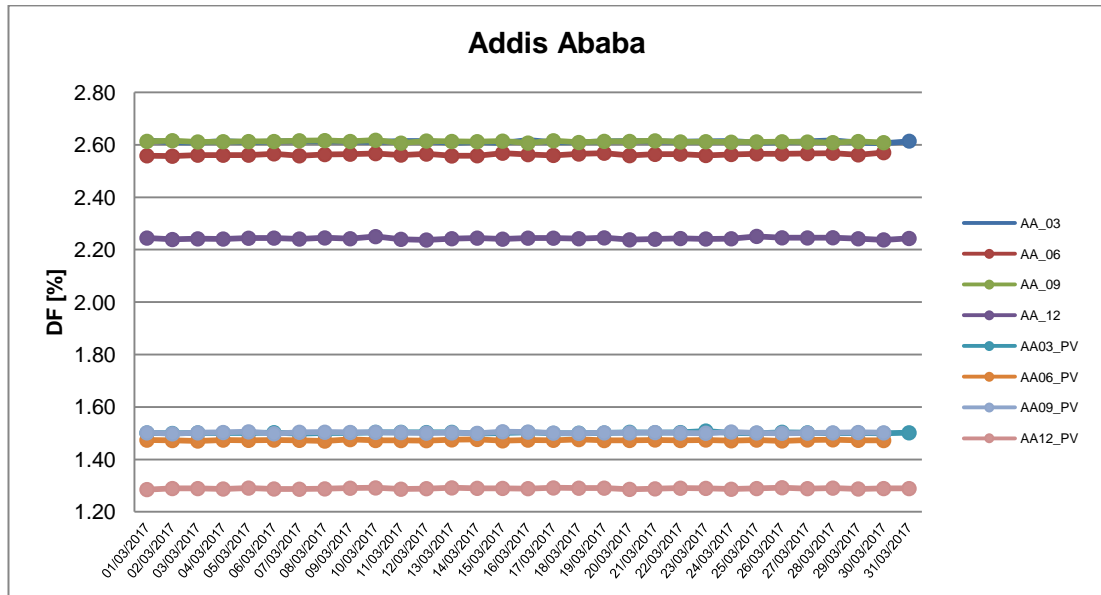


Figure 78 Daylight Factor month distribution for Addis Ababa. Model case without and with OPVs.

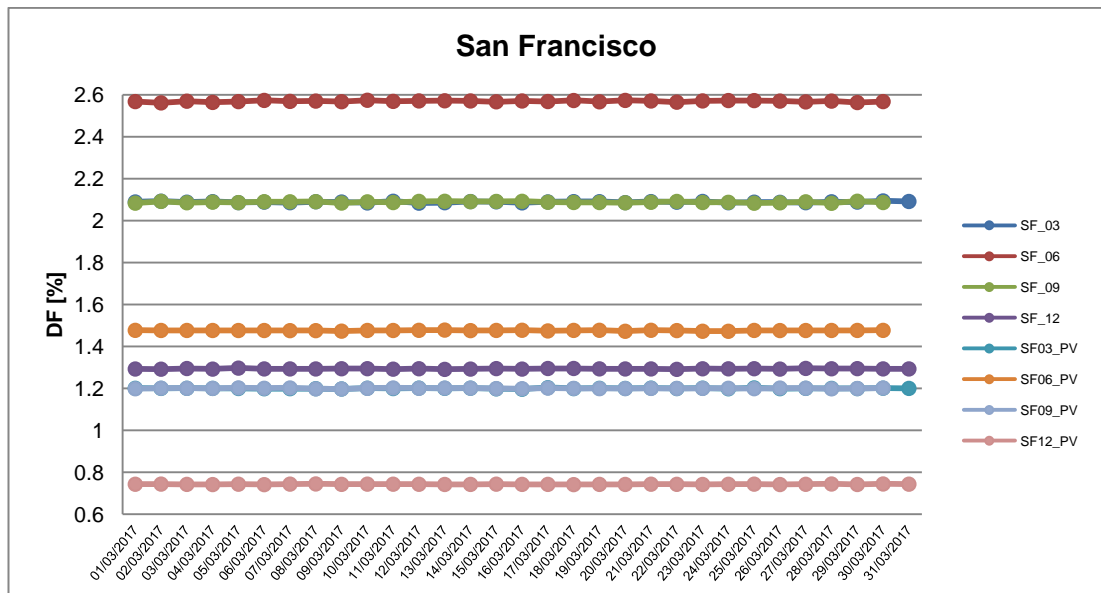


Figure 79 Daylight Factor month distribution for San Francisco. Model case without and with OPVs.

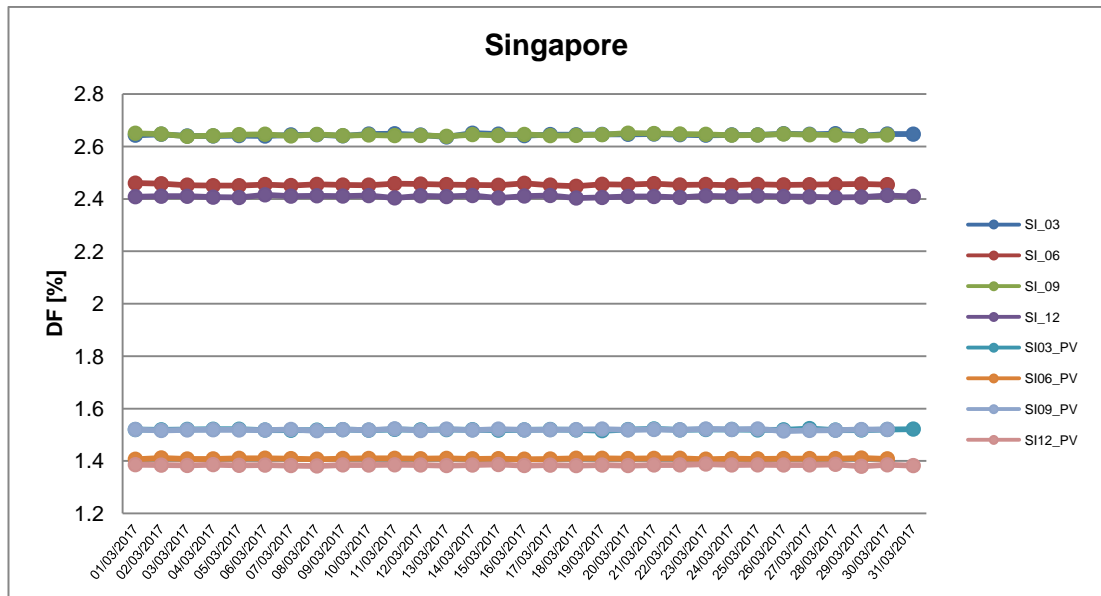


Figure 80 Daylight Factor month distribution for Singapore. Model case without and with OPVs.

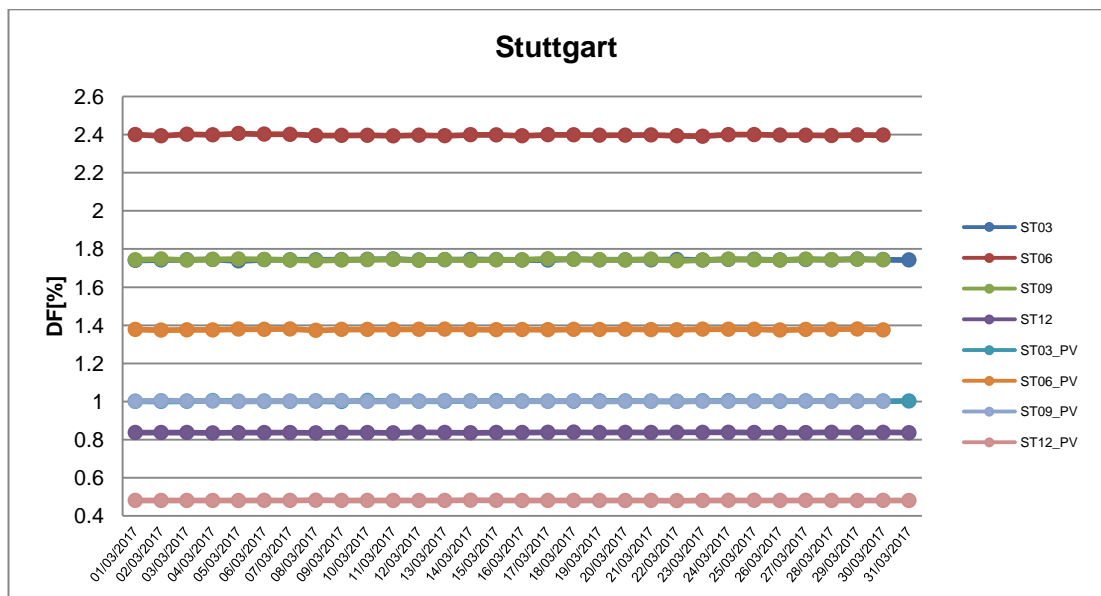


Figure 81 Daylight Factor month distribution for Stuttgart. Model case without and with OPVs.

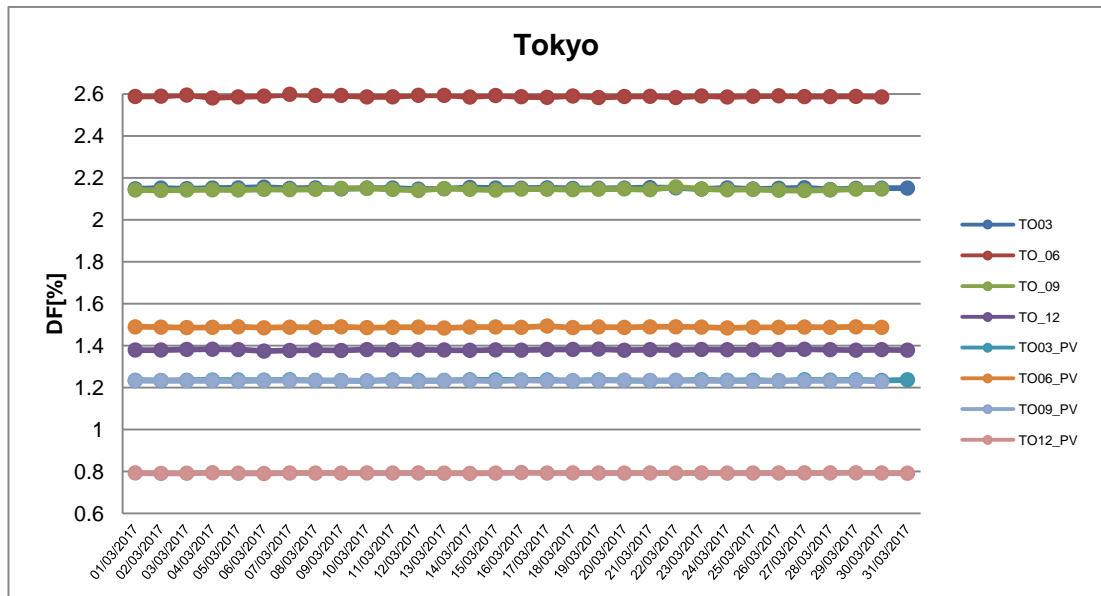


Figure 82 Daylight Factor month distribution for Tokyo. Model case without (grey) and with OPVs (green).

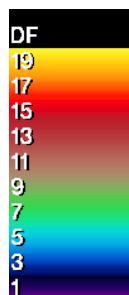
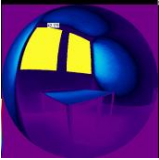
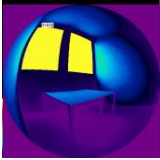
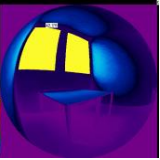
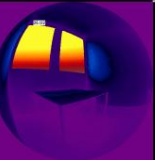
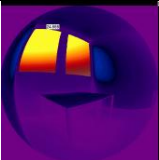
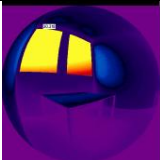
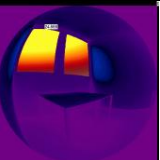
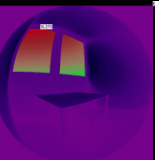
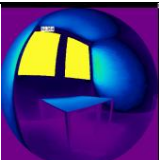
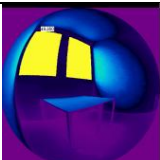
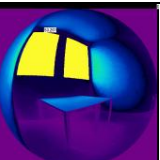
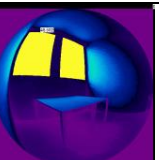
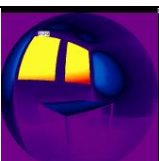
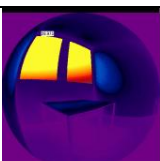
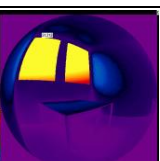
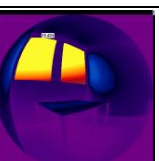
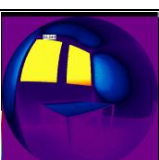

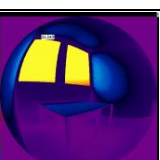
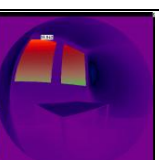
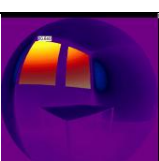
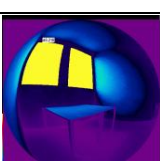
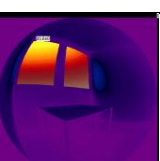
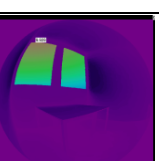
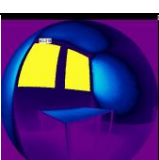


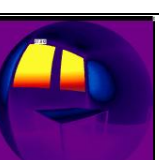
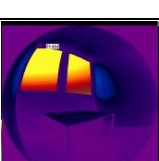
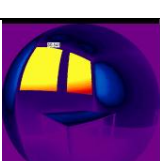
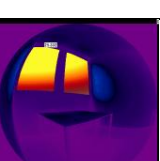
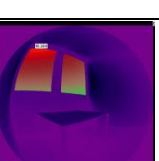


Table 21 Radiance DF computation for every model case.

Model Case		Spring Equinox 12:00	Summer Solstice 12:00	Autumn Equinox 12:00	Winter Solstice 12:00
Addis Ababa	Without OPVs				
	With OPVs				

San Francisco	Without OPVs				
	With OPVs				
Singapore	Without OPVs				
	With OPVs				
Stuttgart	Without OPVs				
	With OPVs				
Tokyo	Without OPVs				
	With OPVs				

In the case of models without OPVs, the mean value resulted from the manual calculation is around 2%, which means that according to standards, additional artificial lighting is necessary. The Radiance falsecolor images confirm that the DF is pretty low inside the office room, especially for Stuttgart in December. Although that, most of the other cities' situations over the year seem to reach the 2%, as it can be seen by the two last calculations.

In the other cases, the mean value resulted is lower than the one for the previous models. The images confirm that the integration of OPVs decreases the values of DF. The highest results corresponding to the windows are also lower than the other model case: confirmed also by the manual calculations, the values on the workplane seem to be around 1.5%, so it should be necessary an additional artificial lighting.

3.3.5 Irradiance

The irradiance is defined as the solar incident power on the surfaces of the model cases studied. It is defined the incident power, depending on the latitudes of the different cities, and the total sunlight hours, meant as the daily hours in which it is possible to have incident sunlight power on the windows.

The calculation is empirical, meaning that the data collected are referred to the general sunlight behavior according to the different latitudes considered. The sunlight irradiance is not specifically calculated taking into consideration the different weather conditions, the building properties, the shading of the surroundings. Although that, the specification of the sunlight power and the sunlight daily hours are necessary to understand the amount of light that is available on the surface of the windows, its variability during the day and its duration.

Here below the results are presented. The main differences stand in the availability of sunlight hours, and in the irradiance through the year, which most of times remains quite stable for the middle seasons and decreases in correspondence of winter times.

Table 22 Addis Ababa irradiance evaluation.

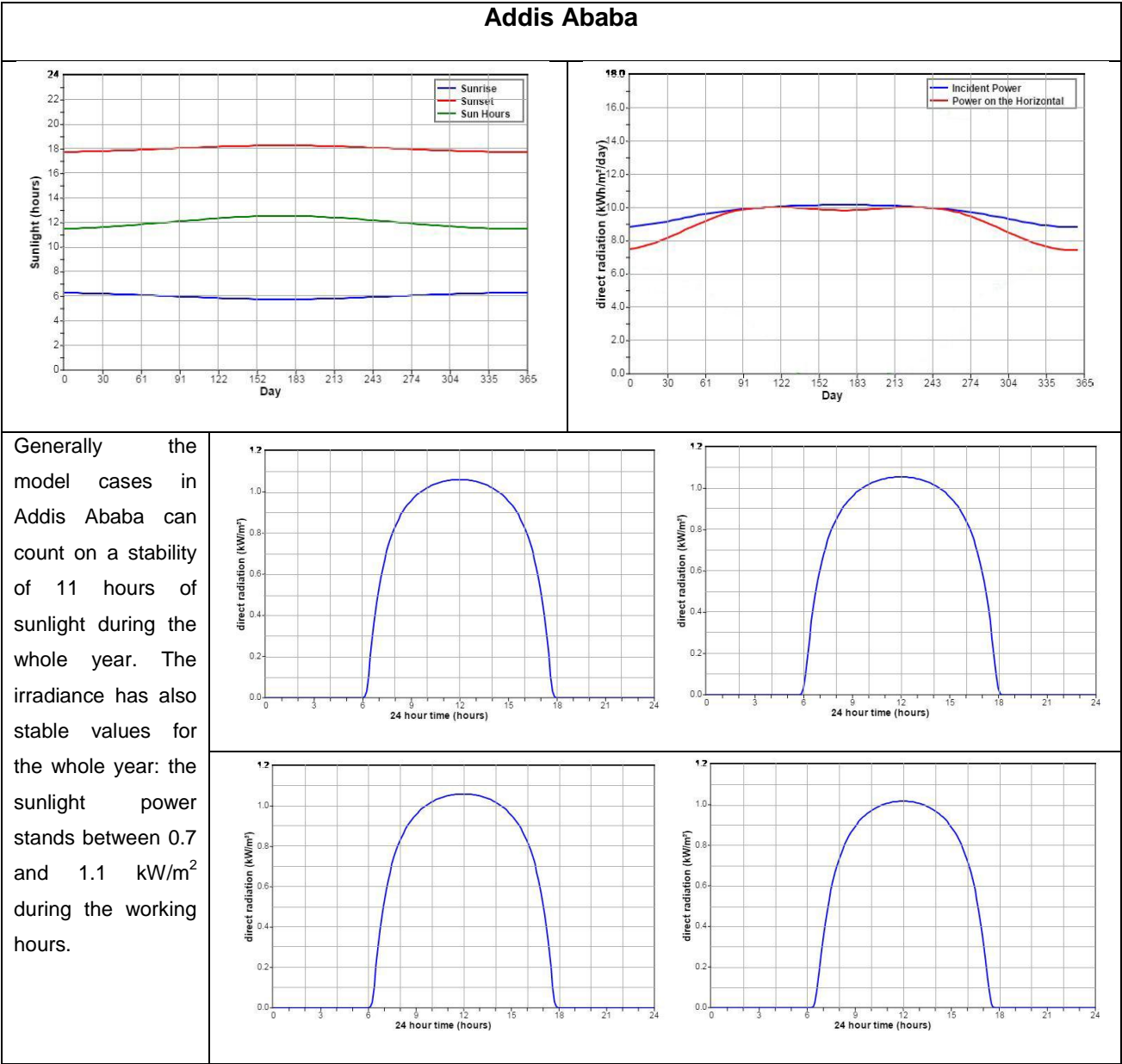


Table 23 San Francisco irradiance evaluation.

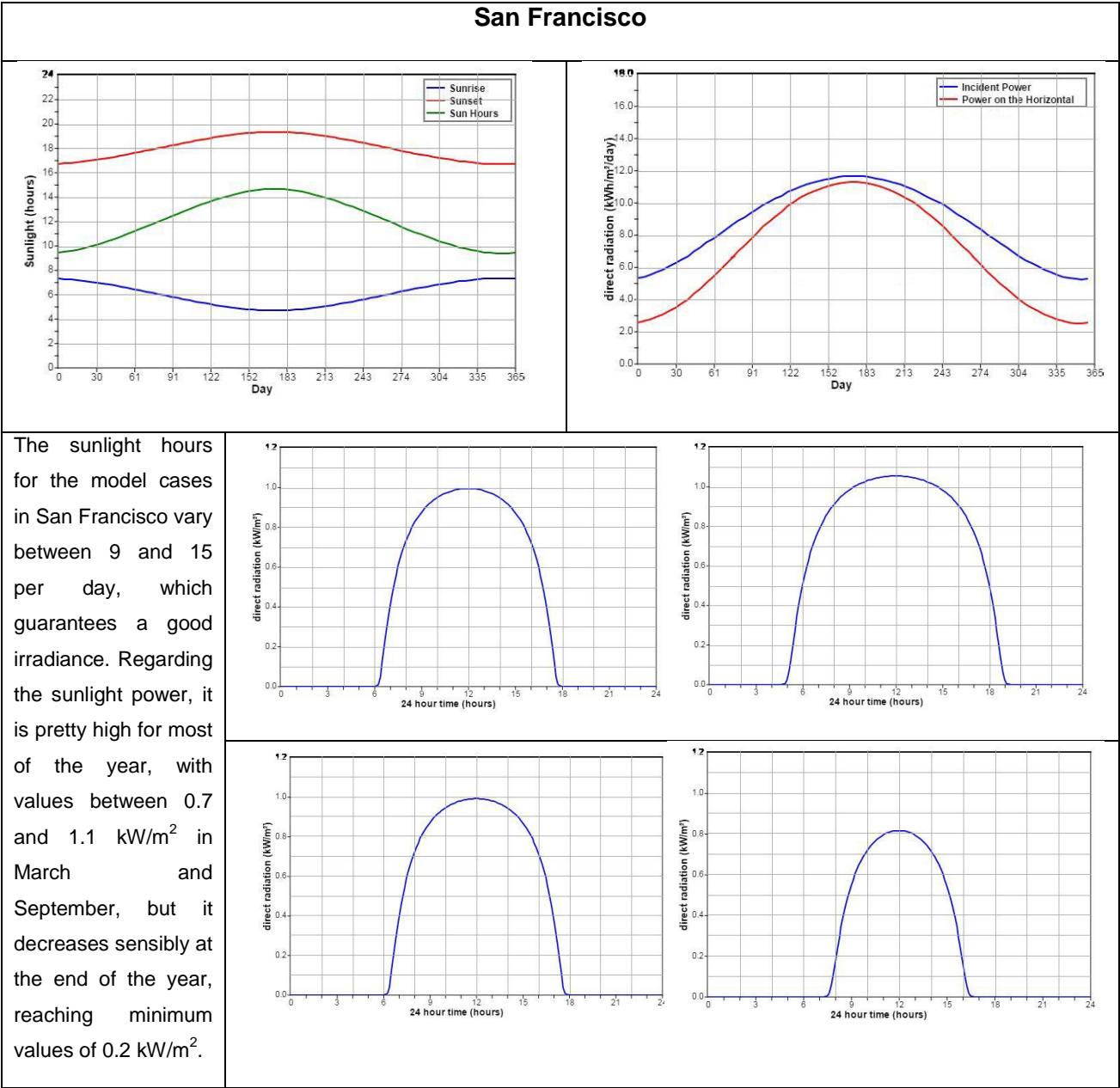


Table 24 Singapore irradiance evaluation.

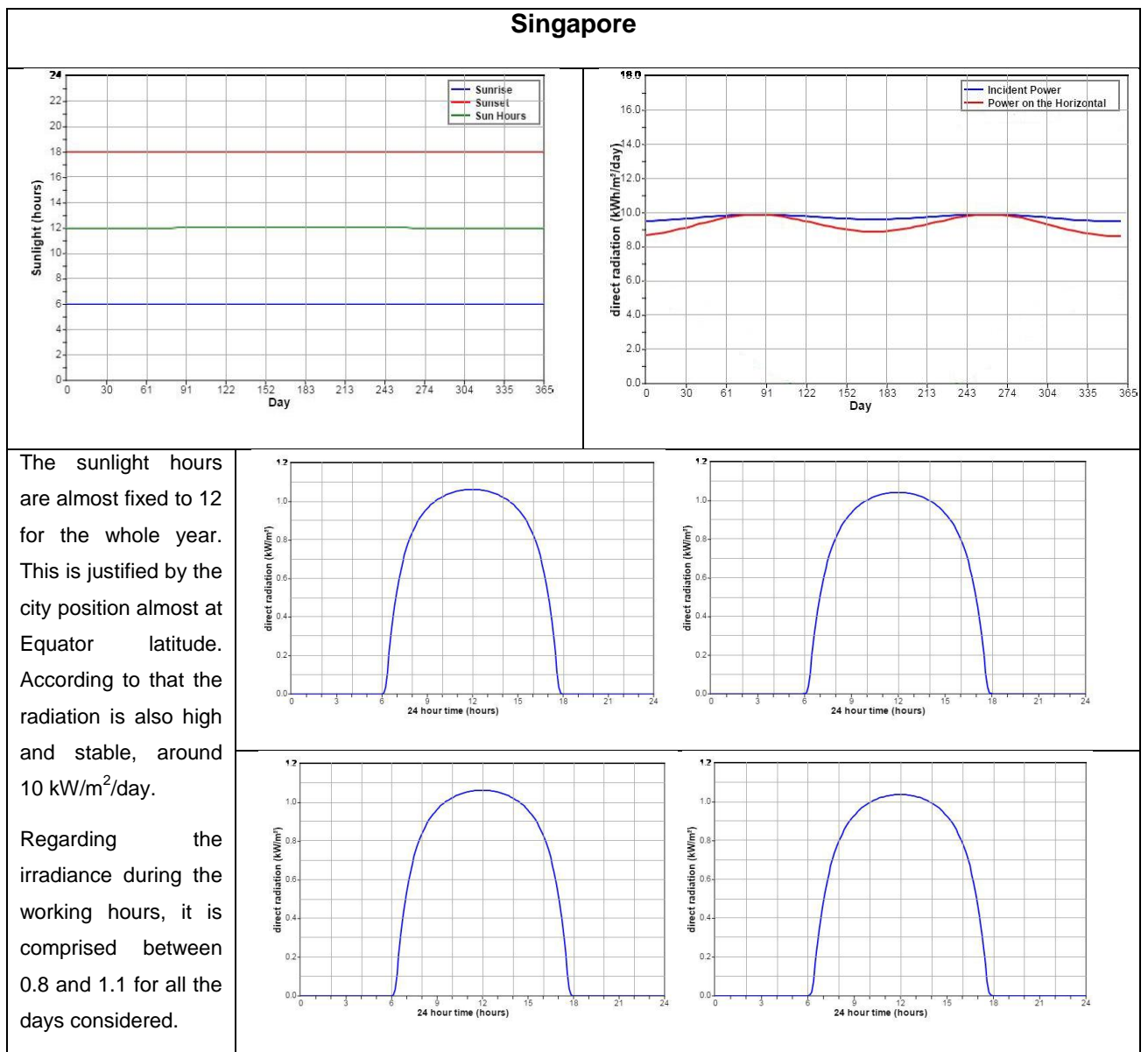


Table 25 Stuttgart irradiance evaluation.

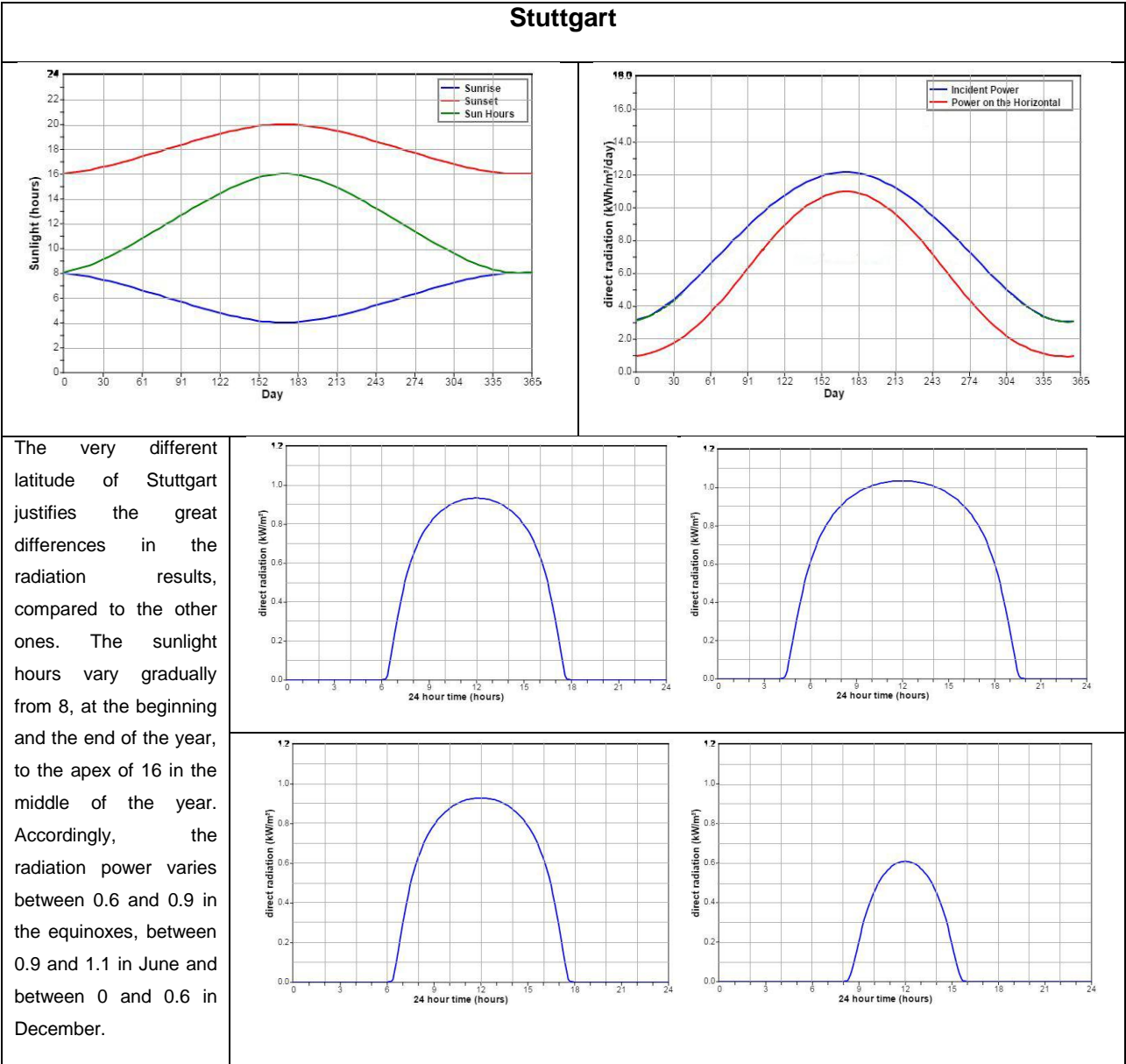
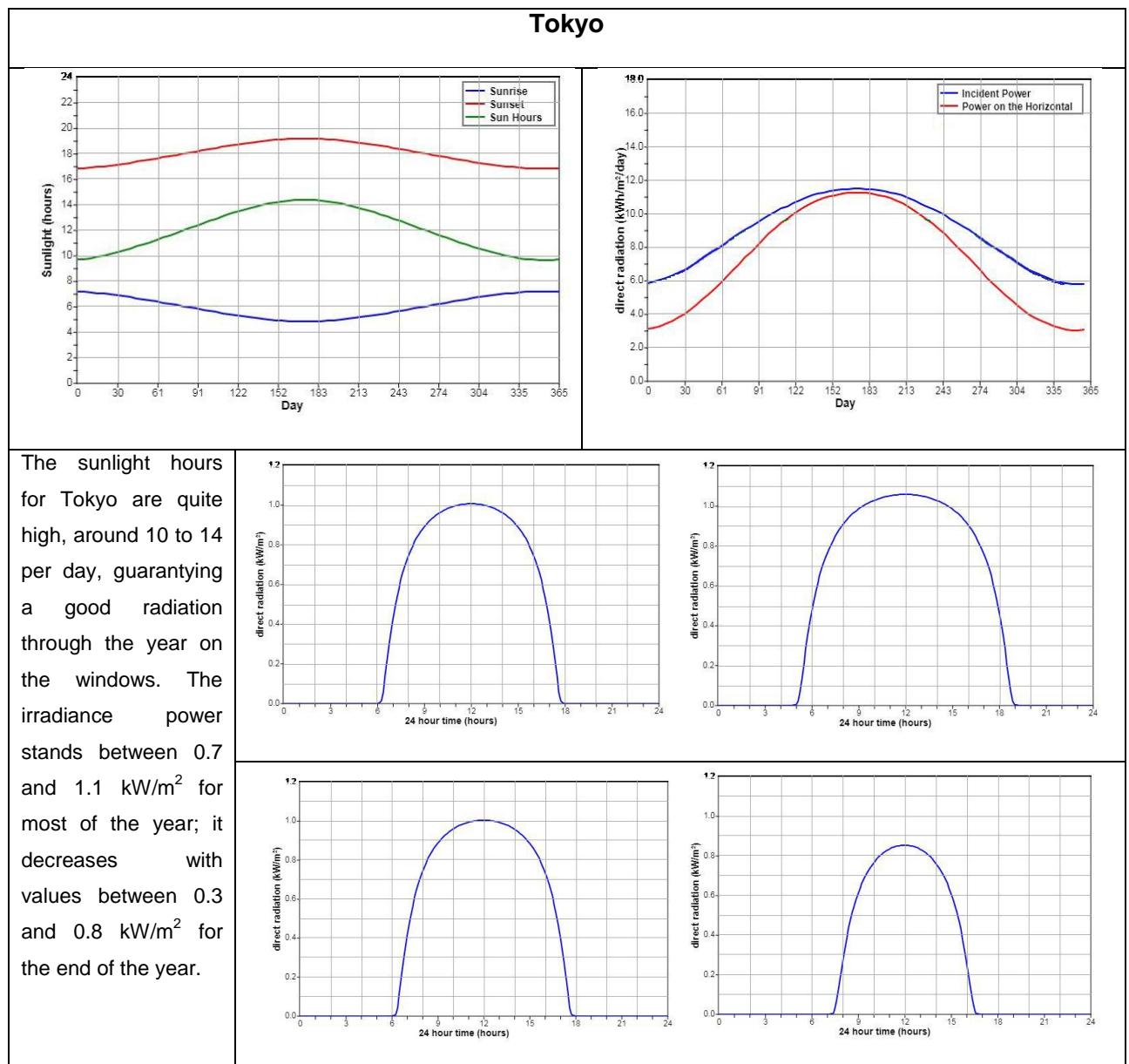


Table 26 Tokyo irradiance evaluation.



3.3.6 Color Spectrum

Defining the properties of the light inside a building requires the specification of its color spectrum. In the case of artificial lighting, it is known that the calculation would report light conditions which should try to imitate the daylight but would not be totally the same. In the case of the daylight inside a room, the evaluation starts from the analysis of the glazing structure and the other window properties to the reflection properties of the covering materials.

The daylight inside the room should not be too different from the outside conditions if it is considered an overcast sky: this is the case, in fact, when no sunlight is directly coming into the room and the shadows are reduced to the minimum.

Radiance is able to calculate the color spectrum of the artificial lighting inside a room or building by acquiring color data, spectral transmission data and using them to return rgb values of the light inside. The steps are the following:

- acquisition of color data;
- CIE Yxy to Radiance rgb via xyz_rgb.cal;
- creation of mycut.cal file;
- generation of rgb color file (ies2rad);
- acquisition of spectral data;
- conversion of spectral data to radiance rgb;
- creation of illuminants' spectra by mgfilt;
- combination of illuminants and gel spectra;
- conversion to CIE Yxy using mgfilt;
- conversion to rgb with rcalc and mycut.cal.

The process is intended to convert illuminants, meant as sky or artificial light source data, into rgb coordinates to understand the color spectrum of the light inside.

In the case of daylight, the calculation does not return values too different from the daylight outside. As it is described in the picture below, the outside daylight properties are known.

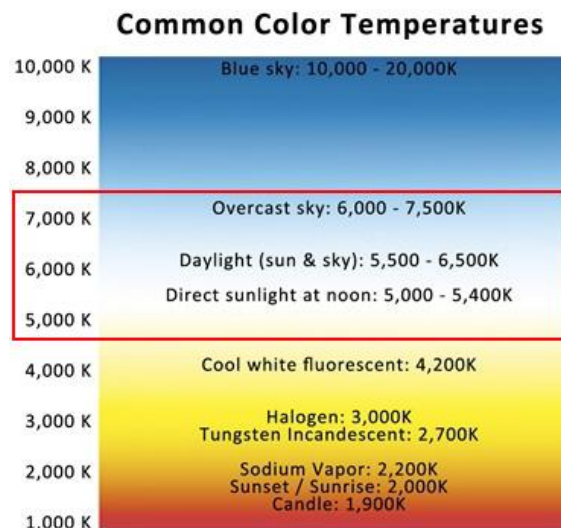


Figure 83 Color temperatures for most used lamps and daylight conditions.

For daylight, in the cases here presented, it can be defined the following properties:

- Color Temperature: 6500 K;
- Color Rendering Index: 100.

The properties for the inside daylight, as mentioned before, has to be defined through the analysis of the glazing structure. The double glazing structures, without and with OPVs integration, used for the calculation are here described. The dimensions and the glazing properties are taken into the Glass Configurator, offered by AGC glass, to see the difference in the CRI. The integration of organic cells is made through the definition of their color and transparency, setting a colored-glass pane with the chosen light transmission.

LIGHT		ENERGY		LIGHT PROPERTIES (EN 410)		EN 410
Transmission	89	Solar factor	76	Light Transmission - τ_v (%)		89
Reflection	9	Reflection	20	Light Reflection - ρ_v (%)		9
				Internal light reflection - ρ_{vi} (%)		9
				Colour Rendering - RD65 - Ra (%)		99

LIGHT		ENERGY		LIGHT PROPERTIES (EN 410)		EN 410
Transmission	46	Solar factor	51	Light Transmission - τ_v (%)		46
Reflection	8	Reflection	7	Light Reflection - ρ_v (%)		8
				Internal light reflection - ρ_{vi} (%)		12
				Colour Rendering - RD65 - Ra (%)		93

Figure 84 Glazing structure lighting properties. Double glazing structure (above). Double glazing structure with OPVs (below).

Although the calculation is not precise and not including spectral data or wavelengths transmission analysis, it can be considered a starting point to understand the performance of the organic cells, according to their color.

Apparently the integration of a thin photovoltaic layer does not influence the color rendering index of the light that is transmitted inside the room. However, the chance to use different colors for the organic photovoltaic cells may influence the CRI here obtained. The performance in those cases can be compared to the use of a colored lamp. The colors available for OPVs on market include shades of blue, green and grey, all adaptable to the desired transparency.



Figure 85 Color shades for OPVs produced by Heliatek.

4 DISCUSSION

The results of the simulations give back a list of values for each performance indicator. The detailed description of the behavior of the sample building could express the performance under every aspect. The thermal simulation refers to the whole building, so the results may be applicable to a generic building. The importance of that analysis stands principally in the comparison between the performance of silicon and organic photovoltaic cells. The values about the heating and cooling demands are in function of the understanding on how much can the photovoltaic support the energetic consumption of the building.

A general overview about the energy production annual results tells that the performance of OPVs is better than the aSi. According to the efficiency difference, it is visible that there is no case where organic cells perform worse than the silicon ones; moreover, although the few percentage points of difference, a lot of aSi results appear to be half of the OPVs. So, in the end, the OPVs can assure a better performance in energy collection, providing the same transparency as aSi.

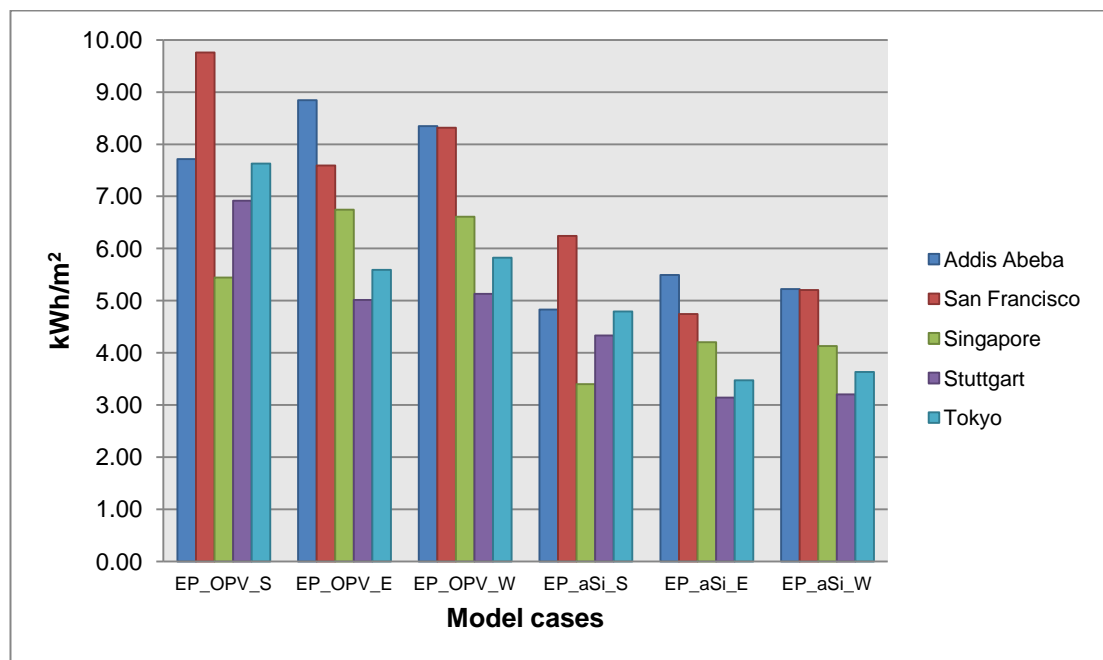


Figure 86 Annual energy production for different models.

Standing at the results of the energy production, it seems that for both the technologies the best orientations are South and East, while the worst is to West; there are just two cases where West oriented buildings provided more energy than East oriented, in Tokyo and San Francisco.

Regarding the month production of energy, the amount of power produced by the photovoltaic systems is well distributed through the year. For each model for every city there are not months of very low energy production. This is a positive value, because it is allowed the use of these thin film cells also for months with lower sunlight availability.

Once the energy produced is compared to the total demand of the building the general result is not promising as the single performance indicators seemed. It is to say that the chosen building have some properties that influence negatively the general consumptions: it is pretty big and the systems are not set in their best performance possibilities. For example, the HVAC system is a basic one, with no Economizer settings, and there is no natural ventilation possibility. This fact, for sure, has a strong influence on the heating and cooling systems, which have to work for every hour of the day and night.

Visible results are there for the model cases in Addis Ababa and San Francisco, where the photovoltaic performance is able to decrease, even if partially, the energetic consumptions. For the other models, the building systems require too much energy to see the influence of PVs (in particular the cooling demand for Singapore models and the heating demand for Stuttgart are very considerable and the photovoltaic performance is barely visible). These aspects lead to the consideration that an improved and a more sensible PV performance belongs to smaller and smarter buildings. Although that, it is remarkable that the OPVs behavior is confirmed to overstep the aSi one.

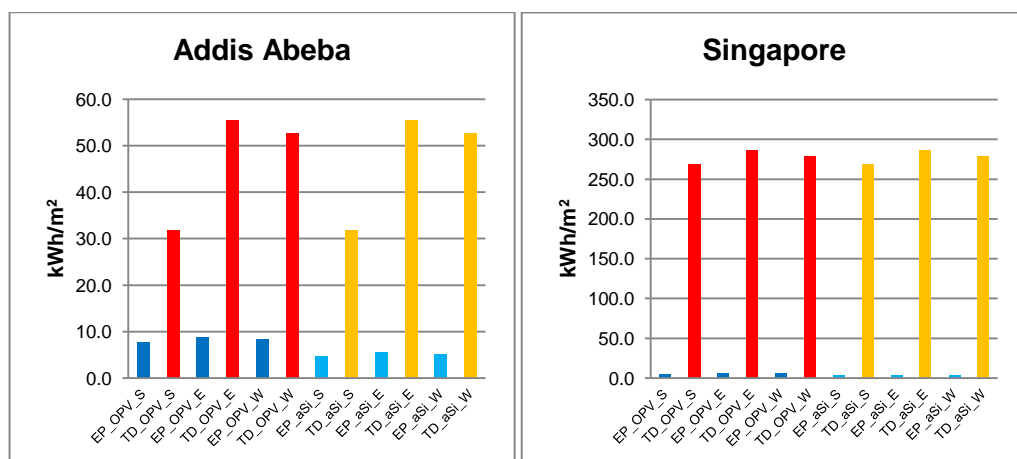


Figure 87 Total demand and energy production comparison. Good performance for model cases in Addis Ababa. Insufficient performance for model cases in Singapore.

The expectations for the OPVs performance are satisfied. The general behavior, as just said, is not the expected one but it was known and well proved that for consistent buildings the crystalline modules are desired to get enough power for facing the energetic consumption that the dimensions required. This analysis confirmed that but additionally told that the organic cells performance is valuable and competing: it does not required special conditions, as it is proved to work well for every orientations and climate conditions. The need of balancing the integration of these thin film layers with a good ventilation system is required in order to get an improved performance and this could be a good next step for this kind of analysis.

The thermal simulation was needed to support the visual analysis of the inside conditions. The comfort provided by the daylight inside has to be preserved in order for the technology of OPVs to be competitive and overcome the limits of the crystalline modules in the photovoltaic market.

The major evaluation regarded the illuminance values and the reaching of the visual comfort requirements for offices. The many graphs plotted show very precisely the behavior of incoming daylight in one single office room under different sky and sun conditions for various moments of the year. The illuminance values are accompanied by their uniformity description. In order to be valuable illuminance should not just reached the standard values but needs to be uniformly distributed into the room. The results show that uniformity has rarely values below 40%: this means that for every condition set, almost half of the room have a good light distribution. This is not a great achievement because a more balanced distribution would be desired to have a good natural lighting. The reasons of this behavior are related to the big windows compared to the small room: there would be necessary an analysis of an entire floor of offices to see the real distribution of the light. Despite this, most of the uniformity percentages of OPV models are higher than the other models. It seems so that the PV layer integrated while decreases the illuminance, it can improve the uniformity.

Regarding the illuminance results, they are very promising: acceptable values are reached most of the time. The requirement of 500 lux is satisfied nearly in every model case. The reasons of having sometimes results of $E < 500$ lux regard, once again, the geometry of the room, which is not optimal for a good illuminance distribution: the lower values are found in the middle of the room, where less direct and surfaces reflected light comes. Although that, a notable recurrence of illuminance low values regards the time of the year: it is visible that model cases with OPVs integrated in the month of December difficulty reach the requirements.

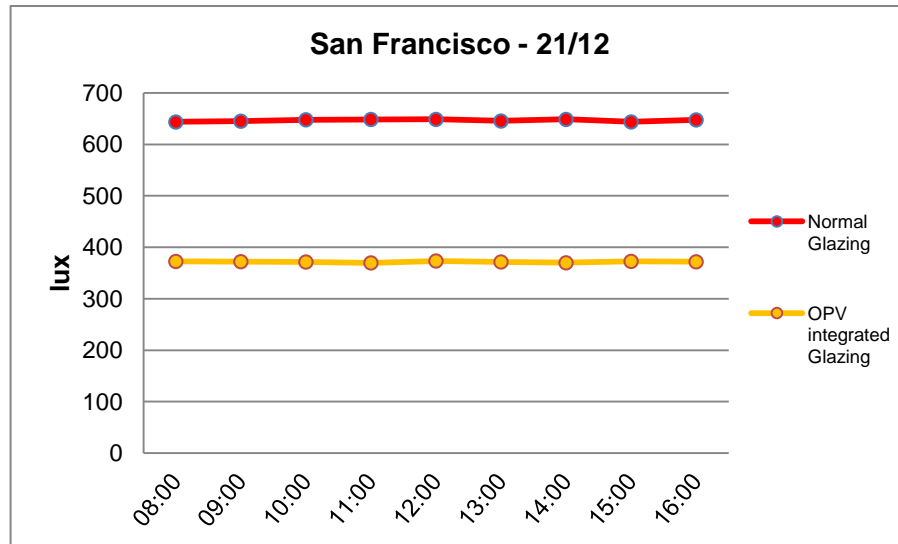


Figure 88 Model with OPVs in San Francisco. December 21st illuminance distribution.

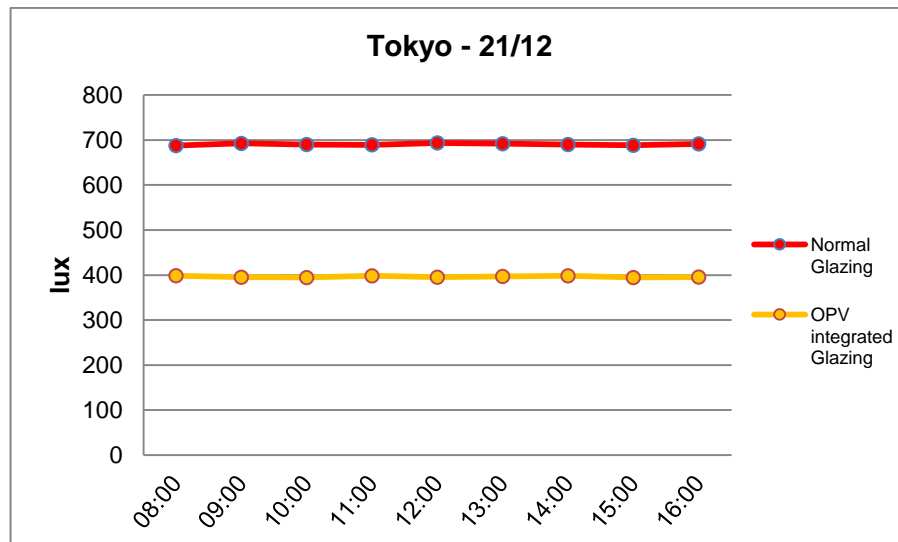


Figure 89 Model with OPVs in Tokyo. December 21st illuminance distribution.

These two graphs show the illuminance behavior with its average values for 21st of December. For both San Francisco and Tokyo, the E_{av} values are acceptable.

The case of Stuttgart is very different from the others: here the values are low but not as in the previous cases. In the case of PV integration, the minimum values do not go over 100 lux and the average ones do not go over 240 lux. These values are below half of the required illuminance, meaning that there is the need of a fixed artificial lighting system and not only for the month of December. In fact, also the other months show low illuminances, revealing that the integration of OPVs for the sky conditions of Stuttgart does not have a total positive response.

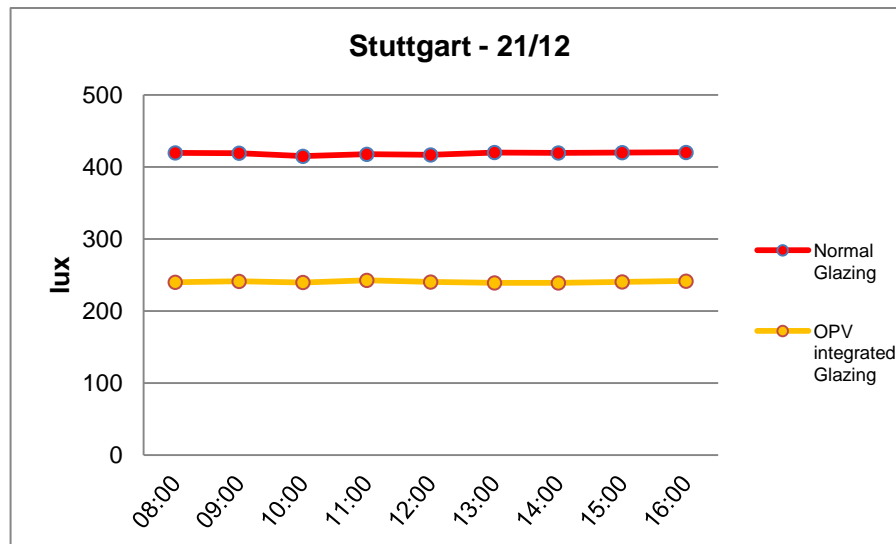


Figure 90 Model with OPVs in Stuttgart. December 21st illuminance distribution.

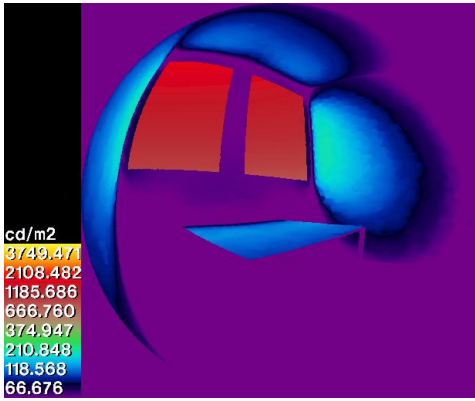
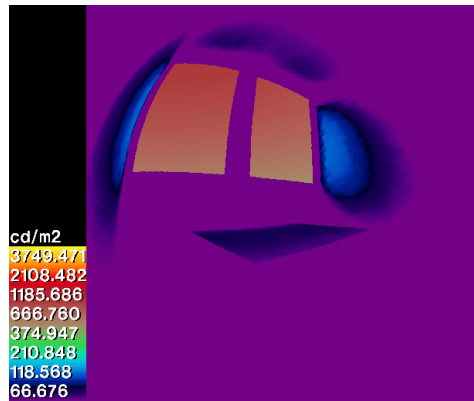
Generally it is visible that OPV models have E results lower than no OPV models. Of course, part of the incident light is absorbed by the photovoltaic cells for the energy production and consequentially, the glass transmits differently than a normal double glazing structure.

All considered, the average illuminance is really promising, leading to the consideration that for cities with higher sun conditions and warmer climates, like Addis Ababa and Singapore, the organic photovoltaic layer can perform very well adding a good function of shading.

The daylight autonomy is the reflection of the considerations above. Model cases with OPVs rarely reach the 70% required but they overstep the 50%. It may be considered that the 20% of difference is reached with an artificial lighting able to work thanks to the energy collected by the photovoltaic system. In this way, the daylight lost in the visual is recovered as energy for artificial light, without additional consumptions that weight on the grid energy.

The computation of potential glare problems through the luminance distribution analysis supports the good OPVs performance explained until now. The luminance values tells that in correspondence to the working areas close to the windows glare can happen, but it is also visible that for the model cases with PV integrated luminance decreases in every situation, having, in some cases, situation with very low values and so little potential glare. Contrary, normal glazing structure has always high luminance on windows and so high glare probability for every situation.

Table 27 Stuttgart glare probability evaluation on 21st December. Better performance of OPVs glazing structure, with lower glare probability.

Normal glazing structure	OPV integrated glazing structure
 <p>cd/m²</p> <p>3749.471 2108.482 1185.686 666.760 374.947 210.848 118.568 66.676</p>	 <p>cd/m²</p> <p>3749.471 2108.482 1185.686 666.760 374.947 210.848 118.568 66.676</p>

In the case of glare evaluation the models in Stuttgart perform at best. The glare probability is very low and for the case of December low luminance tells that there can be almost no glare problem inside the room.

The computation of the last performance indicators, that is needed to define the inside lighting, does not change the prospect outlined. In fact, the results follow the structure of all the other performance indicators: OPVs model cases show lower values than the normal glazing structure models. Although that, the difference is not great enough to define it a negative performance. The values are very close, so the little difference is “expendable” for having the PV integration.

The tiny difference between the behavior of glazing structure with PV and the normal glazing structure in each of the performance indicators analyzed leads to the claim that the OPV integration does not have a negative effect on visual comfort. It is true that the evaluation has been done for working hours and that the first and last hours sometimes have values close to the limit of unacceptability, so maybe a whole day simulation would give a different response. Although that, the system evaluated is well working and so it is suitable for offices.

Combining the responses of the two simulations, it is possible to say that the integration of OPVs is performing very well for smart office buildings. The visual comfort requirements inside can be satisfied for a wide range of conditions of time and place situations, allowing to have an amount of collected electric energy that helps to cover a part of the total energy demand.

Standing at the 'state of the art' the need of developing the technology both theoretically and practically is required; adding the confirmation about OPVs potential that this work gives, it is now essential. This research and simulation only prove simple facts that a further and more complete evaluation on real buildings can potentiate.

The main limit of this work stands in the 'virtuality' of the model simulated. It is well known that the real experience of existing buildings would be different. The background did not help very much in this way: the development of the technology and its installation is unfortunately bound to the high costs. However this analysis shows that the risk can pay back positively. A further research may include and develop the following aspects:

- improvement of basic building systems settings;
- analysis of different building designs;
- evaluation of different OPVs design's possibilities (different substrates);
- analysis of an integration of OPVs on all the windows;
- evaluation of visual comfort of wider office spaces;
- evaluation of visual comfort on different floor level.

The influence and the attraction for this technology as well as the expectations are very high. The OPVs integration in buildings has valuable results, which can compete in the present market and win in the future one. The background research already underlined the better performance of OPVs in hot climates. It is an additional value that this technology carries: the quick and possibly low cost process of production and installation facilities can have a strong ecological and social impact and positive twist for those countries in need of electrical energy, sustainable buildings and improved life conditions.

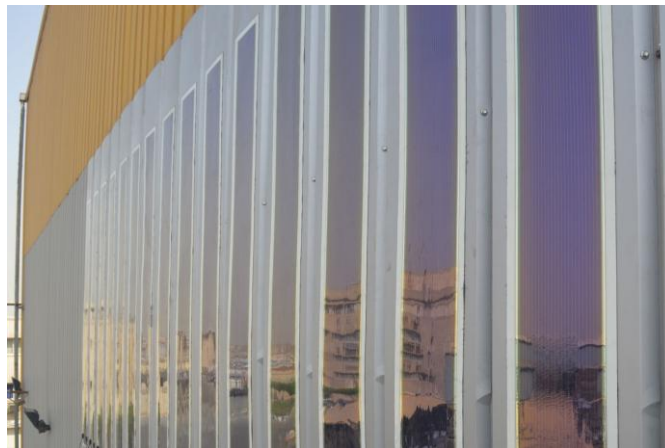


Figure 91 Project of OPVs integration on steel and concrete in a new building in Egypt

5 CONCLUSION

This work aims to show a clear and simplified prospect of the behavior of organic photovoltaic cells integrated in windows. The necessity of developing this research comes from the wide literature about photovoltaic technologies, developments and improvements of OPV efficiency, advantages and disadvantages of possible integration in buildings. All that reveals that the real experiment of a study which could concretely show the effect of this integration was necessary to make a point into the very wide ocean of scientific research about OPVs. This research only underlines some already known theoretical points but accompanies with that a practical example and relative results that the technology can offer.

The thermal and visual simulations are conducted with simple tool on a very simple building. This simplicity helps to understand in a very clear way how the OPVs perform on a building, without the mathematical process of light conversion which is well known and documented.

The importance of keeping developing the technology needs now to be accompanied by a practical process of installation of these cells on buildings. This is necessary for the progress of the photovoltaic markets according to the emerging necessity of sustainability, ecology for our climate but also of new designs that can provide a good aesthetic together with the best performances.

The performance of OPVs has been evaluated through the computation of the main indicators that define the thermal and visual comfort. The analysis reveals that OPVs can guarantee a good performance in respect to the comfort requirements. Starting from here, the further research should include more complicated and advanced building models and more realistic conditions, as the visual simulation took into consideration only the conditions of overcast skies.

This work would like to be an incentive for companies and for the scientific community to develop analysis and literature about the practical installation on OPVs in buildings as already is for other photovoltaic technologies. A prolific literature of concrete examples of organic cells integration leads to the spread of the knowledge about it and so to new possibilities for investments and new installations.

6 INDEX

6.1 List of Figures

Figure 1 BIPV elements summary.

Figure 2 Panels orientation influence on electrical consumptions: electrical consumption for air conditioning, for lighting and total electrical energy output. Example of a building in Hong Kong.

Figure 3 Cells utilization's distribution and efficiency differences of photovoltaic technologies.

Figure 4 Diffusion of PV integration methods divided by elements of the building.

Figure 5 Example of a BIPVT module's structure.

Figure 6 PV Integration mode on facades and windows (a). Three different positions cases. Heat behavior in the case of a window integration (b).

Figure 7 Comparison of the efficiency and transparency of aSi semitransparent solar modules (2014).

Figure 8 Mono and Poly crystalline cells design's differences.

Figure 9 Comparison between main silicon PV structures. Products of Ausind..

Figure 10 Integration of DSC. Example of SwissTech Convention Centre in Switzerland.

Figure 11 PV Manufacturers Rankings Comparison up to July 2016 by First Solar.

Figure 12 Donor and Acceptor working structure. Position into the cell (a). Donor-Acceptor junction (b). Mathematical explanation of the working method of the junction (c). HOMO and LUMO interface (d).

Figure 13 Flat heterojunction structure.

Figure 14 Bulk heterojunction structure.

Figure 15 Common donor and acceptor materials for OPVs.

Figure 16 Transparency properties of main diffuse OPVs materials.

Figure 17 OPVs efficiency and transparency comparison. Heliatek products in 2016.

Figure 18 Main production techniques for OPVs.

Figure 19 Architecture of an OPV cell. Normal structure and Inverse structure.

Figure 20 Cells distribution on a substrate.

Figure 21 Cell structure mounted layer by layer.

Figure 22 General plan of the sample building

Figure 23 Plan and Section of the sample office room

Figure 24 Prospects from outside and from inside of the room

- Figure 25 Constructive structures. Floor to ground. External wall. Partition wall
- Figure 26 Constructive structures. Flat roof. Partition slab.
- Figure 27 Models' orientation. To South on the left; to East and West on the right.
- Figure 28 Thermal zones distribution
- Figure 29 Energy Plus final elements' list for the simulation.
- Figure 30 Scene-images for the simulation. Scene 1, Scene 2, Scene 3
- Figure 31 Radiance Plugin for SketchUp. Settings for building export into Radiance.
- Figure 32 Distribution of calculation points at workplane height (0.8 m)
- Figure 33 Annual Heating Demand summary (HD: heating demand; NS: north-south orientation; EW: east-west orientation; OPV: organic photovoltaics; aSi: amorphous silicon photovoltaics.)
- Figure 34 Annual heating demand for Stuttgart model cases.
- Figure 35 Annual heating demand for Tokyo model cases.
- Figure 36 Annual Cooling Demand summary (CD: cooling demand; NS: north-south orientation; EW: east-west orientation; OPV: organic photovoltaics; aSi: amorphous silicon photovoltaics)
- Figure 37 Annual cooling demand for Addis Ababa model cases.
- Figure 38 Annual cooling demand for San Francisco model cases.
- Figure 39 Annual cooling demand for Singapore model cases.
- Figure 40 Annual cooling demand for Stuttgart model cases.
- Figure 41 Annual cooling demand for Tokyo model cases.
- Figure 42 Annual Energy Production per floor area by PVs summary (EP: energy production; NS: north-south orientation; EW: east-west orientation; OPV: organic photovoltaics; aSi: amorphous silicon photovoltaics).
- Figure 43 Annual energy production for Addis Ababa model cases.
- Figure 44 Annual energy production for San Francisco model cases.
- Figure 45 Annual energy production for Singapore model cases.
- Figure 46 Annual energy production for Stuttgart model cases.
- Figure 47 Annual energy production for Tokyo model cases.
- Figure 48 Total energetic demand for each building case compared to PV energy production. Blue and red columns: building cases with OPVs. Orange and light blue columns: building cases with aSi.
- Figure 49 Average illuminance for model case without OPVs (above) and with OPVs (below).
- Figure 50 Average illuminance for model case without OPVs (above) and with OPVs (below).

Figure 51 Average illuminance for model case without OPVs (above) and with OPVs (below).

Figure 52 Average illuminance for model case without OPVs (above) and with OPVs (below).

Figure 53 Average illuminance for model case without OPVs (above) and with OPVs (below).

Figure 54 Average illuminance for model case without OPVs (above) and with OPVs (below).

Figure 55 Average illuminance for model case without OPVs (above) and with OPVs (below).

Figure 56 Average illuminance for model case without OPVs (above) and with OPVs (below).

Figure 57 Average illuminance for model case without OPVs (above) and with OPVs (below).

Figure 58 Average illuminance for model case without OPVs (above) and with OPVs (below).

Figure 59 Average illuminance for model case without OPVs (above) and with OPVs (below).

Figure 60 Average illuminance for model case without OPVs (above) and with OPVs (below).

Figure 61 Average illuminance for model case without OPVs (above) and with OPVs (below).

Figure 62 Average illuminance for model case without OPVs (above) and with OPVs (below).

Figure 63 Average illuminance for model case without OPVs (above) and with OPVs (below).

Figure 64 Average illuminance for model case without OPVs (above) and with OPVs (below).

Figure 65 Average illuminance for model case without OPVs (above) and with OPVs (below).

Figure 66 Average illuminance for model case without OPVs (above) and with OPVs (below).

Figure 67 Average illuminance for model case without OPVs (above) and with OPVs (below).

Figure 68 Average illuminance for model case without OPVs (above) and with OPVs (below).

- Figure 69 Average uniformity for Singapore model case with and without OPVs.
- Figure 70 Average uniformity for Singapore model case with and without OPVs.
- Figure 71 Average uniformity for Singapore model case with and without OPVs.
- Figure 72 Average uniformity for Singapore model case with and without OPVs.
- Figure 73 Average illuminance for the Stuttgart model with OPVs in December..
- Figure 74 High luminance monitors values up to norm EN12464-1.
- Figure 75 UGR calculation points positions and view direction. Three sitting eyes-height (1.2m).
- Figure 78 Sitting positions and height of UGR calculation points.
- Figure 79 UGR results for the three sitting positions. Model without PV on the left, model with OPVs on the right.
- Figure 80 Daylight Factor month distribution for Addis Ababa. Model case without and with OPVs.
- Figure 81 Daylight Factor month distribution for San Francisco. Model case without and with OPVs.
- Figure 82 Daylight Factor month distribution for Singapore. Model case without and with OPVs.
- Figure 83 Daylight Factor month distribution for Stuttgart. Model case without and with OPVs.
- Figure 84 Daylight Factor month distribution for Tokyo. Model case without (grey) and with OPVs (green).
- Figure 85 Color temperatures for most used lamps and daylight conditions.
- Figure 86 Glazing structure lighting properties. Double glazing structure (above). Double glazing structure with OPVs (below).
- Figure 87 Color shades for OPVs produced by Heliatek.
- Figure 88 Annual energy production for different models.
- Figure 89 Total demand and energy production comparison. Good performance for model cases in Addis Ababa. Insufficient performance for model cases in Singapore.
- Figure 90 Model with OPVs in San Francisco. December 21st illuminance distribution.
- Figure 91 Model with OPVs in Tokyo. December 21st illuminance distribution.
- Figure 92 Model with OPVs in Stuttgart. December 21st illuminance distribution.
- Figure 93 Project of OPVs integration on steel and concrete in a new building in Egypt
- Figure 94 Average illuminance values for Addis Ababa. Respectively, E_{av} in March without (red lines) and with (orange lines) OPVs; E_{av} in June without and with OPVs.

Figure 95 Average illuminance values for Addis Ababa. Respectively, E_{av} in September without (red lines) and with (orange lines) OPVs; E_{av} in December without and with OPVs.

Figure 96 Average illuminance for San Francisco. Respectively, E_{av} in March without (red lines) and with (orange lines) OPVs; E_{av} in June without and with OPVs.

Figure 97 Average illuminance for San Francisco. Respectively, E_{av} in September without (red lines) and with (orange lines) OPVs; E_{av} in December without and with OPVs.

Figure 98 Average illuminance for Singapore. Respectively, E_{av} in March without (red lines) and with (orange lines) OPVs; E_{av} in June without and with OPVs.

Figure 99 Average illuminance for Singapore. Respectively, E_{av} in September without (red lines) and with (orange lines) OPVs; E_{av} in December without and with OPVs.

Figure 100 Average illuminance for Stuttgart. Respectively, E_{av} in March without (red lines) and with (orange lines) OPVs; E_{av} in June without and with OPVs.

Figure 101 Average illuminance for Stuttgart. Respectively, E_{av} in September without (red lines) and with (orange lines) OPVs; E_{av} in December without and with OPVs.

Figure 102 Average illuminance for Tokyo. Respectively, E_{av} in March without (red lines) and with (orange lines) OPVs; E_{av} in June without and with OPVs.

Figura 103 Average illuminance for Tokyo. Respectively, E_{av} in September without (red lines) and with (orange lines) OPVs; E_{av} in December without and with OPVs.

Figure 104 Average illuminance distribution in Addis Ababa for models cases without and with OPVS.

Figure 105 Average illuminance distribution in San Francisco for models cases without and with OPVS.

Figure 106 Average illuminance distribution in Stuttgart for models cases without and with OPVS.

Figura 107 Average illuminance distribution in Tokyo for models cases without and with OPVS.

6.2 List of Tables

Table 1 Building materials' properties.

Table 2 Normal double glazing structure's properties.

Table 3 Constructive elements' properties.

Table 4 Photovoltaic cells' properties.

Table 5	Energy Plus settings. Building position and simulation period.
Table 6	Model cases for thermal simulation.
Table 7	Radiance settings. Sky settings for each city.
Table 8	Radiance settings. Covering materials' properties.
Table 9	Model cases for visual simulation.
Table 10	Annual Heating Demand summary.
Table 11	Annual Cooling Demand summary.
Table 12	Month Electric Demand summary.
Table 13	Annual Energy Production summary.
Table 14	Annual total demand and energy production comparison. (EP: energy production; TD: total demand; NS: north-south orientation; EW: east-west orientation; OPV: organic photovoltaics; aSi: amorphous silicon photovoltaics).
Table 15	Daylight Autonomy summary
Table 16	Computation of glare probability inside the room for scene 1. Example of Singapore on 21.06. Comparison between the different models.
Table 17	Computation of glare probability inside the room for scene 2. Example of Singapore on 21.06. Comparison between the different models.
Table 18	Computation of glare probability inside the room for scene 3. Example of Singapore on 21.06. Comparison between the different models.
Table 19	Luminance distribution on 21.12 for every model case.
Table 20	Daylight Factor (DF) computation.
Table 21	Radiance DF computation for every model case.
Table 22	Addis Ababa irradiance evaluation.
Table 23	San Francisco irradiance evaluation.
Table 24	Singapore irradiance evaluation.
Table 25	Stuttgart irradiance evaluation.
Table 26	Tokyo irradiance evaluation.
Table 27	Stuttgart glare probability evaluation on 21 st December. Better performance of OPVs glazing structure, with lower glare probability.
Table 28	Energy Plus settings. Ground properties
Table 29	Energy Plus settings. Schedule Type Limits
Table 30	Energy Plus settings. Schedules compact definition
Table 31	Luminance distribution on 21.03 for every model case.
Table 32	Luminance distribution on 21.06 for every model case.
Table 33	Luminance distribution on 23.09 for every model case.

6.3 List of Equations

- (1) Equation for the calculation of photovoltaic internal quantum efficiency
- (2) Equation for the calculation of photovoltaic power conversion efficiency
- (3) Equation for the calculation of Daylight Factor with geometry
- (4) Equation for the calculation of Daylight Factor with illuminance

7 LITERATURE

- Agrawal, B., & Tiwari, G. N. (2011). *Building Integrated Photovoltaic Thermal Systems: for sustainable developments*: RSC Publishing.
- Baljit, S., Chan, H.-Y., & Sopian, K. (2016). Review of building integrated applications of photovoltaic and solar thermal systems. In *Journal of Cleaner Production*, (137), 677–689. doi:10.1016/j.jclepro.2016.07.150
- Cao, M. (2015). *Future growth of organic solar cells in the building integrated photovoltaic market*. San Diego State University, San Diego.
- Cerón, I., Caamaño-Martín, E., & Neila, F. J. (2013). 'State-of-the-art' of building integrated photovoltaic products. In *Renewable Energy*, (58), 127–133. doi:10.1016/j.renene.2013.02.013
- Chae, Y. T., Kim, J., Park, H., & Shin, B. (2014). Building energy performance evaluation of building integrated photovoltaic (BIPV) window with semi-transparent solar cells. *Applied Energy*, (129), 217–227. Retrieved from <http://dx.doi.org/10.1016/j.apenergy.2014.04.106>
- Connelly, K., Wu, Y., Chen, J., & Lei, Y. (2016). Design and development of a reflective membrane for a novel Building Integrated Concentrating Photovoltaic (BICPV) 'Smart Window' system. In *Applied Energy*, (182), 331–339. doi:10.1016/j.apenergy.2016.07.125
- Gupta, S., Medwal, R., Limbu, T. B., Katiyar, R. K., Pavunny, S. P., Tomar, M., ...Katiyar, R. S. (2015). Graphene/semiconductor silicon modified BiFeO₃/indium tin oxide ferroelectric photovoltaic device for transparent self-powered windows. In *Applied Physics Letters*, (107). doi:10.1063/1.4928541
- Laura Maturi, Roberto Lollini, David Moser, & Wolfram Sparber. (2015). Experimental investigation of a low cost passive strategy to improve the performance of Building Integrated Photovoltaic systems. In *Solar Energy*, (111), 288–296. <http://dx.doi.org/10.1016/j.solener.2014.11.001>
- Merck & Co Inc, Ticker: MRK, NAICS: 325411, & DUNS: 00-131-7064 (2016, April 21). *CPI, Merck and Polysolar to develop building integrated photovoltaic windows*. In *Trade Journal*. <https://search.proquest.com/docview/1798302584?accountid=39579>
- Paul, D., Mandal, S. N., Mukherjee, D., & Bhadra Chaudhuri, S. R. (2010). Optimization of significant insolation distribution parameters – A new approach towards BIPV system design. In *Renewable Energy*, (35), 2182–2191. doi:10.1016/j.renene.2010.02.026
- Rajoria, C. S., Agrawal, S., Chandra, S., Tiwari, G., & Chauhan, D. (2016). A Novel investigation of building integrated photovoltaic thermal (BiPVT) system: A comparative study. In *Solar Energy*, (131), 107–118. <http://dx.doi.org/10.1016/j.solener.2016.02.037>
- Sick, F., & Erge, T. *Photovoltaics in buildings: A design handbook for architects and engineers*. London: BSI British Standards.
- Tiwari, G. N., Saini, H., Tiwari, A., Deo, A., Gupta, N., & Saini, P. S. (2016). Periodic theory of building integrated photovoltaic thermal (BiPVT) system. In *Solar Energy*, (125), 373–380. doi:10.1016/j.solener.2015.12.028
- Wu, Y., Connelly, K., Liu, Y., Gu, X., Gao, Y., & Chen, G. Z. (2016). Smart solar concentrators for building integrated photovoltaic façades. In *Solar Energy*, (133), 111–118. doi:10.1016/j.solener.2016.03.046

- Yang, T., & Athienitis, A. K. (2016). *A review of research and developments of building-integrated photovoltaic/thermal (BIPV/T) systems*. In *Renewable and Sustainable Energy Reviews*, (66), 886–912. doi:10.1016/j.rser.2016.07.011
- Yoon, J.-H., Song, J., & Lee, S.-J. (2011). *Practical application of building integrated photovoltaic (BIPV) system using transparent amorphous silicon thin-film PV module*. In *Solar Energy*, (85), 723–733. doi:10.1016/j.solener.2010.12.026
- Yoon, S., Tak, S., Kim, J., Jun, Y., Kang, K., & Park, J. (2011). *Application of transparent dye-sensitized solar cells to building integrated photovoltaic systems*. In *Building and Environment*, (46), 1899–1904. doi:10.1016/j.buildenv.2011.03.010
- Z. Ding, V. Stoichkov, M. Horie, E. Brousseau, & J. Kettle. (2016). *Spray coated silver nanowires as transparent electrodes in OPVs for Building Integrated Photovoltaics applications*. In *Solar Energy Materials & Solar Cells*, (157), 305–311. <http://dx.doi.org/10.1016/j.solmat.2016.05.053>
- Zhang, W., Lu, L., Peng, J., & Song, A. (2016). *Comparison of the overall energy performance of semi-transparent photovoltaic windows and common energy-efficient windows in Hong Kong*. In *Energy and Buildings*, (128), 511–518. <http://dx.doi.org/10.1016/j.enbuild.2016.07.016>
- Bauer, G. H. (2015). *Photovoltaic solar energy conversion*: Springer Verlag Berlin Heidelberg.
- Brabec, C., Dyakinov, V., & Scherf, V. (2008). *Organic Photovoltaics: materials, device physics and manufacturing technologies*: Wiley-VCH Verlag.
- Cao, W., & Xue, J. (2014). *Recent progress in organic photovoltaics: Device architecture and optical design*. In *Energy & Environmental Science*, (7), 2123–2144. doi:10.1039/c4ee00260a
- Chen, K.-S., Salinas, J.-F., Yip, H.-L., Huo, L., Hou, J., & Jen, A. K.-Y. (2012). *Semi-transparent polymer solar cells with 6% PCE, 25% average visible transmittance and a color rendering index close to 100 for power generating window applications*. In *Energy & Environmental Science*, (5), 9551–9557. doi:10.1039/c2ee22623e
- Chong, K.-K., Khlyabich, P. P., Hong, K.-J., Reyes-Martinez, M., Rand, B. P., & Loo, Y.-L. (2016). *Comprehensive method for analyzing the power conversion efficiency of organic solar cells under different spectral irradiances considering both photonic and electrical characteristics*. In *Applied Energy*, (180), 516–523. doi:10.1016/j.apenergy.2016.08.002
- Chuo, Y., Omrane, B., Landrock, C., Aristizabal, J., Hohertz, D., Grayli, S. V., & Kaminska, B. (2011). *Powering the future: organic solar cells with polymer energy storage*. In *IEEE Design & test of Computers*, 33–40.
- Conibeer, G. J., & Willoughby, A. (2014). *Solar cell materials: developing technologies*: Wiley.
- Häberlin, H. (2012). *Photovoltaics- System design and practise*: Electrosuisse Verlag.
- Jin, J. W., Jung, S., Bonnassieux, Y., Horowitz, G., Stamateri, A., Kapnopoulos, C., Logothetidis, S. (2016). *Universal Compact Model for Organic Solar Cell*. In *IEEE Transactions on Electron Devices*, 63(10), 4053–4059. doi:10.1109/TED.2016.2598793
- Kafafi, Z. H., Lane, P. A., & Samuel, I. D. W. (Eds.) 2016. *SPIE Organics + Electrons. SPIE Proceedings: Vol. 9942*: SPIE.
- Kaltenbrunner, M., White, M. S., Glowacki, E. D., Sekitani, T., Someya, T., Sariciftci, N. S., & Bauer, S. (2012). *Ultrathin and lightweight organic solar cells with high flexibility*. In *Nature communications*, (3), 770. doi:10.1038/ncomms1772

- Krebs, F. C., & Jørgensen, M. (2013). *Polymer and organic solar cells viewed as thin film technologies: What it will take for them to become a success outside academia*. In *Solar Energy Materials and Solar Cells*, (119), 73–76. doi:10.1016/j.solmat.2013.05.032
- Krebs, F. C., Tromholt, T., & Jørgensen, M. (2010). *Upscaling of polymer solar cell fabrication using full roll-to-roll processing*. In *Nanoscale*, (2), 873–886. doi:10.1039/b9nr00430k
- Lecover, R., Williams, N., Markovic, N., Reich, D. H., Naiman, D. Q., & Katz, H. E. (2012). *Next-generation polymer solar cell materials: designed control of interfacial variables*. In *ACS nano*, 6(4), 2865–2870. doi:10.1021/nn301140w
- McEvoy, A., Markvart, T., & Castaner, L. (2013). *Solar cells-materials, manufacture and operation*: Elsevier.
- Mertens, K. (2015). *Photovoltaik-Lehrbuch zu Grundlagen, Technologie und Praxis*: Hanser.
- Mohanty, P., Muneer, T., & Kohle, M. (2016). *Solar photovoltaic system applications: A guidebook for Off-grid electrification*: Springer International Publishing Switzerland.
- Park, Y., Berger, J., Will, P.-A., Soldera, M., Glatz, B., Müller-Meskamp, L., Leo, K. (2016). *Light trapping for flexible organic photovoltaics*. In Z. H. Kafafi, P. A. Lane, & I. D. W. Samuel (Eds.): *Vol. 9942. SPIE Proceedings, SPIE Organics + Electrons* (p. 994211). SPIE.
- Park, Y., Bormann, L., Müller-Meskamp, L., Vandewal, K., & Leo, K. (2016). *Efficient flexible organic photovoltaics using silver nanowires and polymer based transparent electrodes*. In *Organic Electronics*, (36), 68–72. doi:10.1016/j.orgel.2016.05.032
- Park, Y., Nehm, F., Muller-Meskamp, L., Vandewal, K., & Leo, K. (2016). *Optical display film as flexible and light trapping substrate for organic photovoltaics*. In *Optics express*, 24(10). doi:10.1364/OE.24.00A974
- Rahimi, R., Roberts, A., Narang, V., & Korakakis, D. (2013). *Investigate the role of the active layers' structures and morphology in the performance of the organic solar cell devices*. In *Applied Physics Letters*, (102). doi:10.1063/1.4793201
- Randy, B. P., & Richter, H. (Eds.). (2014). *Organic Solar Cells: Fundamentals, Devices and Upscaling*. USA: Pan Stanford Publishing.
- Scharber, M. C., Mühlbacher, D., Koppe, M., Denk, P., Waldauf, C., Heeger, A. J., & Brabec, C. J. (2006). *Design Rules for Donors in Bulk-Heterojunction Solar Cells—Towards 10 % Energy-Conversion Efficiency*. In *Advanced Materials*, (18), 789–794. doi:10.1002/adma.200501717
- Schmidt-Mende, L., & Weickert, J. (2016). *Organic and hybrid solar cells: An introduction*: Walter de Gruyter GmbH, Berlin/Boston.
- Tress, W. (2014). *Organic solar cells: Theory, Experiment and Device simulation*: Springer International Publishing Switzerland.
- van Franeker, J. J., Turbiez, M., Li, W., Wienk, M. M., & Janssen, R. A. J. (2015). *A real-time study of the benefits of co-solvents in polymer solar cell processing*. In *Nature communications*. doi:10.1038/ncomms7229
- Yan, F., Noble, J., Peltola, J., Wicks, S., & Balasubramanian, S. (2013). *Semitransparent OPV modules pass environmental chamber test requirements*. In *Solar Energy Materials and Solar Cells*, (114), 214–218. doi:10.1016/j.solmat.2012.09.031
- Bellia, L., Marino, C., Minichiello, F., & Pedace, A. (2014). *An Overview on Solar Shading Systems for Buildings*. In *Energy Procedia*, (62), 309–317. doi:10.1016/j.egypro.2014.12.392

- David, M., Donn, M., Garde, F., & Lenoir, A. (2011). *Assessment of the thermal and visual efficiency of solar shades*. In *Building and Environment*, (46), 1489–1496. doi:10.1016/j.buildenv.2011.01.022
- Gaur, A., & Tiwari, G. N. (2013). *Performance of Photovoltaic Modules of Different Solar Cells*. In *Journal of Solar Energy*, (6), 1–13. doi:10.1155/2013/734581
- Li, L., Qu, M., & Peng, S. (2016). *Performance evaluation of building integrated solar thermal shading system: Building energy consumption and daylight provision*. In *Energy and Buildings*, (113), 189–201. doi:10.1016/j.enbuild.2015.12.040
- Mandalaki, M., Tsoutsos, T., & Papamanolis, N. (2014). *Integrated PV in shading systems for Mediterranean countries: Balance between energy production and visual comfort*. In *Energy and Buildings*, (77), 445–456. doi:10.1016/j.enbuild.2014.03.046
- Rachchh, R., Kumar, M., & Tripathi, B. (2016). *Solar photovoltaic system design optimization by shading analysis to maximize energy generation from limited urban area*. In *Energy Conversion and Management*, (115), 244–252. doi:10.1016/j.enconman.2016.02.059
- Saranti, A., Tsoutsos, T., & Mandalaki, M. (2015). *Sustainable energy planning. Design shading devices with integrated photovoltaic systems for residential housing units*. In *Procedia Engineering*, (123), 479–487. doi:10.1016/j.proeng.2015.10.099
- Sun, L., Lu, L., & Yang, H. (2012). *Optimum design of shading-type building-integrated photovoltaic claddings with different surface azimuth angles*. In *Applied Energy*, (90), 233–240. doi:10.1016/j.apenergy.2011.01.062
- SHC task 27 (March 2006).
- ÖNORM B 8110-7 (2015, March 15).
- EN ISO 12464-1.
- ISO 9241-302.
- Abylev, G.M., Kosrev, I., Kukin, V., Semerukhin, M.Y., Shvarts, M.Z., Ternkov, E.I., Zhilina, D.V. (2014). *Semitransparent solar modules based on amorphous and microcrystalline silicon*. In *Journal of Physics*, 572. doi:10.1088/1742-6596/572/1/012049
- Adam, G., Munkhbat, B., Denk, P., Ulbricht, C., Hrelescu, C., & Scharber, M. (2016). *Different Device Architectures for Bulk-Heterojunction Solar Cells*. In *Frontiers in Materials*, (39). doi:10.3389/fmats.2016.00039
- Bolashikov, Z. D., Mustakallio, P., Kolencikova, S., Kostov, K., Melikov, A. K., & Kosonen, R. *Thermal comfort in simulated office environment with four convective and radiant cooling systems-clima2013*. Technical University of Denmark.
- Goetzberger, A., Hebling, C., & Schock, H.-W. (2003). *Photovoltaic materials, history, status and outlook*. In *Material Science and Engineering*, (40), 1–46.
- Johnsen, K., Dubois, M., & Grau, K. (2006). *Assessment of daylight quality in simple rooms: Impact of three window configurations on daylight conditions, Phase 2* (1st ed.). Hørsholm: Sbi.
- Miles, R. W. (2006). *Photovoltaic solar cells: Choice of materials and production methods*. In *Vacuum*, (80), 1090–1097. doi:10.1016/j.vacuum.2006.01.006
- Nielsen, T. R., Rosenfeld, J., & Svendsen, S. *A simple energy rating for solar shading devices*. Danmarks Tekniske Universitet.
- Ochoa, C. E., Aries, M. B., van Loenen, E. J., & Hensen, J. (2012). *Considerations on design optimization criteria for windows providing low energy consumption*

and high visual comfort. In *Applied Energy*, (95), 238–245.
doi:10.1016/j.apenergy.2012.02.042

Platzer, W., Simmler, H., & Bryn, I. Energy performance of facades and buildings-IEA as support for the European directive.

Van Dijk, D. *Thermal and solar modelling and characterization: the role of IEA SHC Task 27.*

8 APPENDIX

A. Thermal Simulation tables

Table 28 Energy Plus settings. Ground properties

Name	GroundTemperature: UndisturbedFiniteDifference
Soil Thermal Conductivity	1.5 W/mK
Soil Density	2800 kg/m ³
Soil Specific Heat	850 J/kgK
Soil Moisture Content Volume Fraction	30%
Soil Moisture Content Volume Fraction at Saturation	50%
Evapotranspiration Ground Cover Parameter	0.4
	Ground Domain:Slab
Ground Domain Depth	10
Aspect Ratio	1
Perimeter Offset	5
Soil Thermal Conductivity	1.5 W/mK
Soil Density	2800 kg/m ³
Soil Specific Heat	850 J/kgK
Soil Moisture Content Volume Fraction	30%
Soil Moisture Content Volume Fraction at Saturation	50%
Undisturbed Ground Temperature Model Type	Site:GroundTemperature Undisturbed:FiniteDifference

Undisturbed Ground Temperature Model Name	GroundTemperature:Undisturbed FiniteDifference
Evapotranspiration Ground Cover Parameter	0.4
Slab Boundary Condition Model Name	Ground Domain:Slab
Slab Location	OnGrade

Table 29 Energy Plus settings. Schedule Type Limits

Name	On/Off	Fraction	Activity
Lower Limit Value	0	0	0
Upper Limit Value	1	1	115
Numeric Type	Discrete	Continuous	Discrete

Table 30 Energy Plus settings. Schedules compact definition

Schedule Compact Office HVAC									
On/Off									
Through: 12/31									
For Weekdays	Until 06:00 0		Until 22:00 1		Until 24:00 0				
For Saturdays	Until 06:00 0		Until 18:00 1		Until 24:00 0				
For Sundays	Until 24:00 0								
Schedule Compact Office Lighting									
Fraction									
Through: 12/31									
For Weekdays	Until 05:00 0.05	Until 07:00 0.1	Until 08:00 0.3	Until 17:00 0.9	Until 18:00 0.5	Until 20:00 0.3	Until 22:00 0.2	Until 23:00 0.1	Until 24:00 0.05
For	Until 06:00	Until 08:00	Until 12:00	Until 17:00	Until 24:00				

<i>Saturdays</i>	0.05	0.1	0.3	0.15	0.05				
<i>For Sundays</i>	Until 24:00 0.05								
Schedule Compact Office Occupancy									
Fraction Through: 12/31									
<i>For Weekdays</i>	Until 06:00 0	Until 07:00 0.1	Until 08:00 0.2	Until 12:00 0.95	Until 13:00 0.5	Until 17:00 0.95	Until 18:00 0.3	Until 22:00 0.1	Until 24:00 0.05
<i>For Saturdays</i>	Until 06:00 0	Until 08:00 0.1	Until 12:00 0.3	Until 17:00 0.1	Until 19:00 0.05	Until 24:00 0			
<i>For Sundays</i>	Until 06:00 0	Until 18:00 0.05	Until 24:00 0						
Schedule Compact Office Equipment									
Fraction Through: 12/31									
<i>For Weekdays</i>	Until 05:00 0.05	Until 07:00 0.1	Until 08:00 0.3	Until 17:00 0.9	Until 18:00 0.5	Until 20:00 0.3	Until 22:00 0.2	Until 23:00 0.1	Until 24:00 0.05
<i>For Saturdays</i>	Until 06:00 0.05	Until 08:00 0.1	Until 12:00 0.3	Until 17:00 0.15	Until 24:00 0.05				
<i>For Sundays</i>	Until 24:00 0.05								

Schedule Compact Activity Level		Schedule Compact Infiltration		Schedule Compact Inverter	
Activity 115 Through: 12/31		Fraction Through: 12/31		Fraction Through: 12/31	
<i>For Alldays</i>	Until 24:00 115	<i>For Alldays</i>	Until 24:00 1	<i>For Alldays</i>	Until 24:00 1

B. Visual Simulation tables and graphs

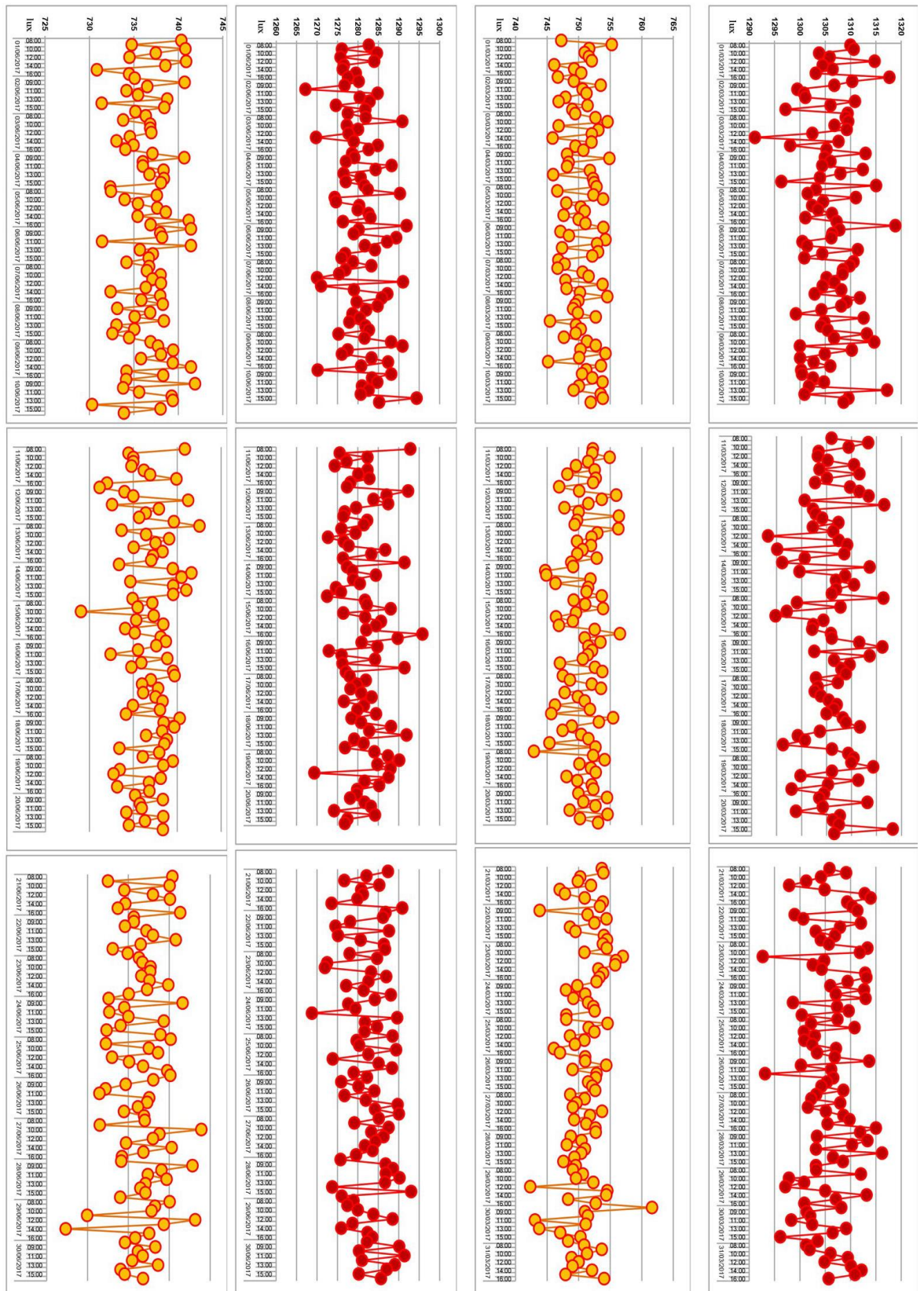


Figure 92 Average illuminance values for Addis Ababa. Respectively, E_{av} in March without (red lines) and with (orange lines) OPVs; E_{av} in June without and with OPVs.

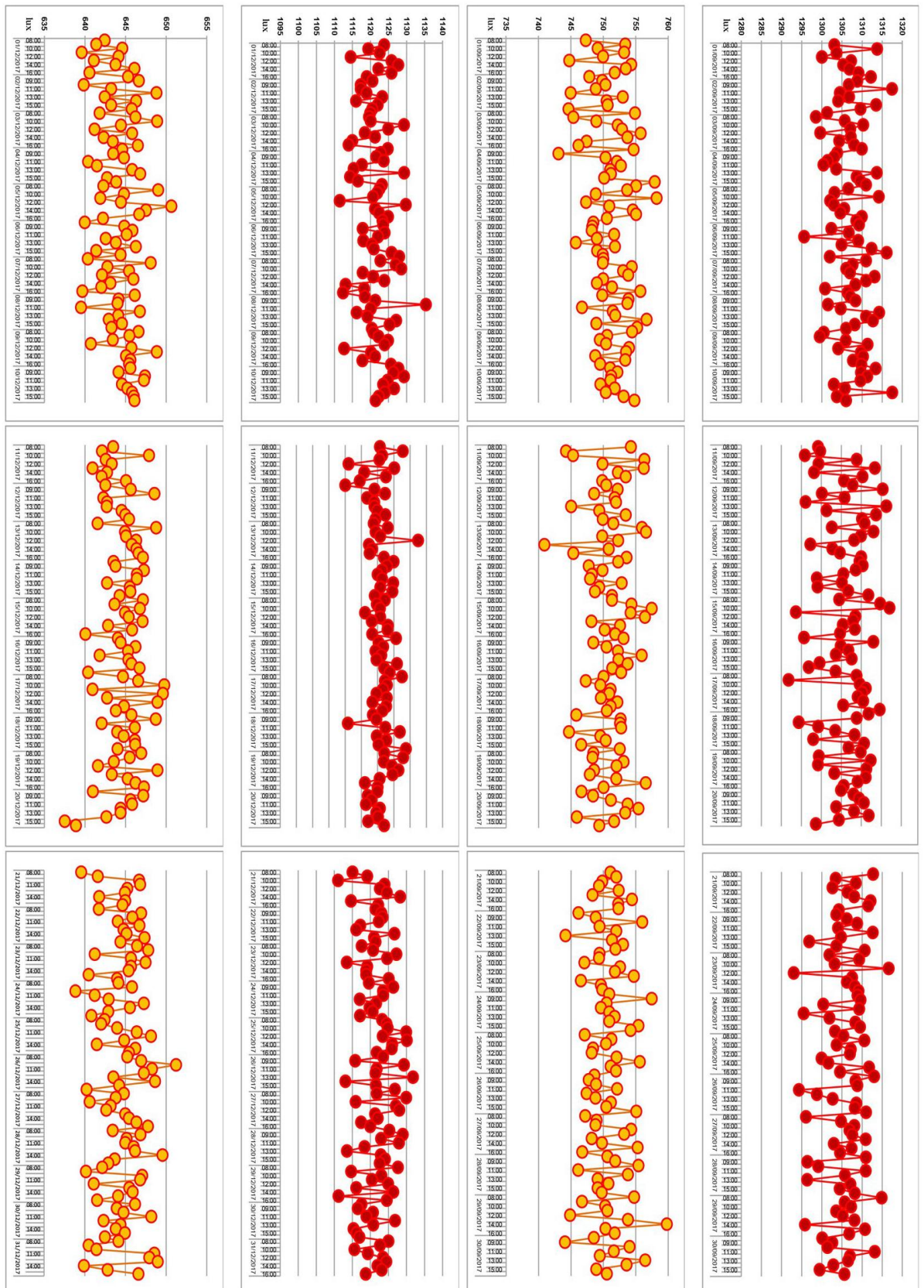


Figure 93 Average illuminance values for Addis Ababa. Respectively, E_{av} in September without (red lines) and with (orange lines) OPVs; E_{av} in December without and with OPVs.

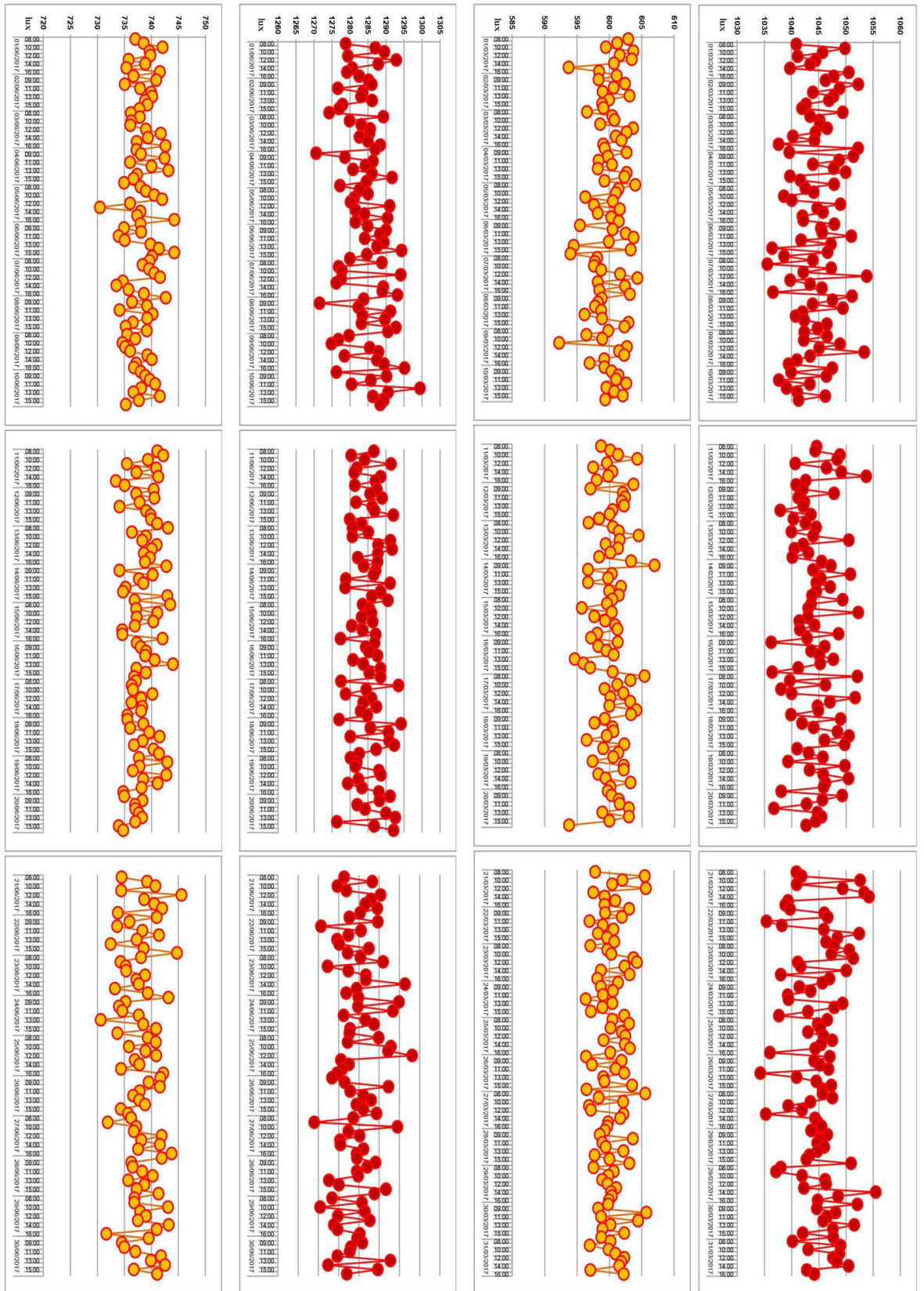


Figure 94 Average illuminance for San Francisco. Respectively, E_{av} in March without (red lines) and with (orange lines) OPVs; E_{av} in June without and with OPVs.

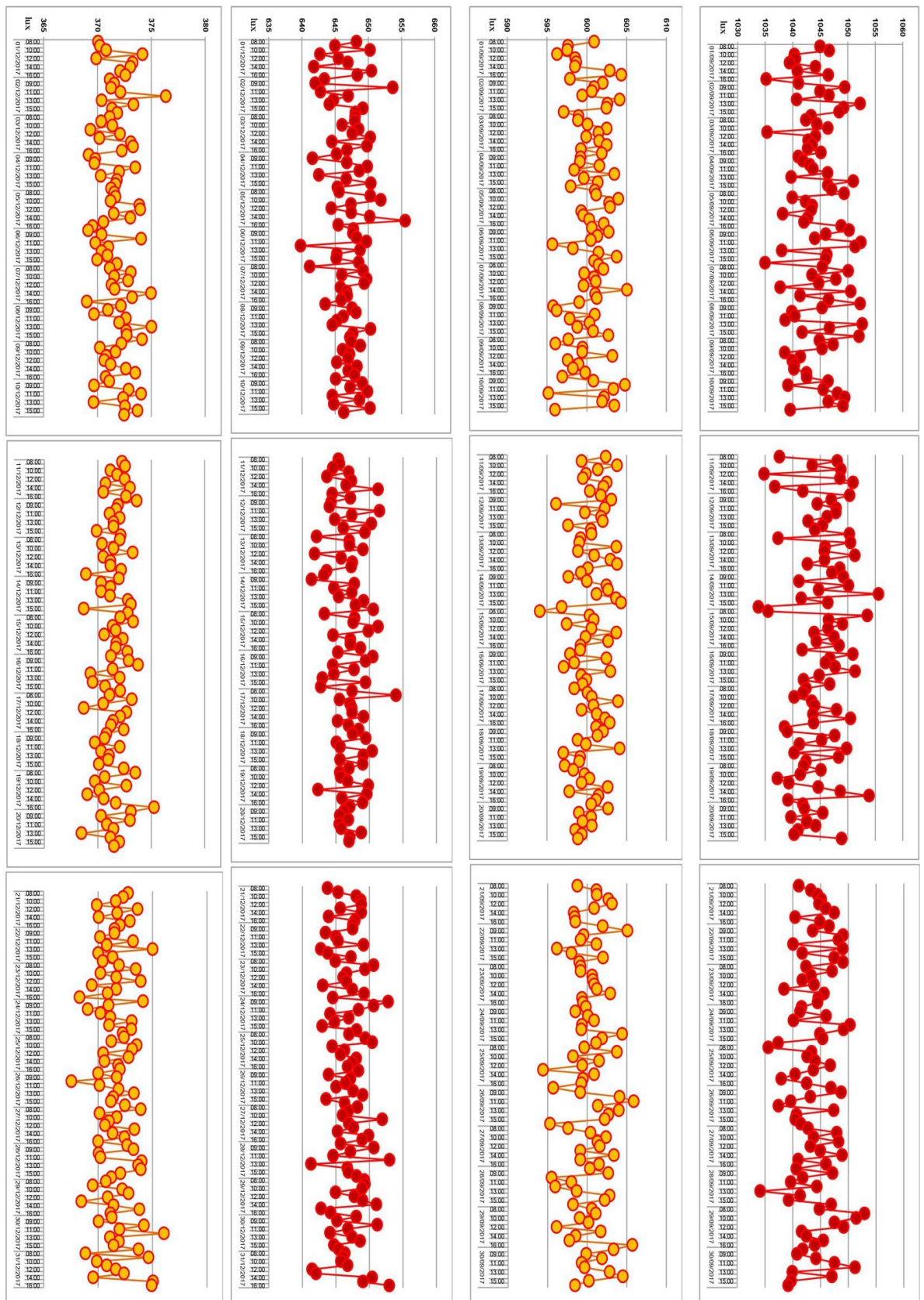


Figure 95 Average illuminance for San Francisco. Respectively, E_{av} in September without (red lines) and with (orange lines) OPVs; E_{av} in December without and with OPVs.

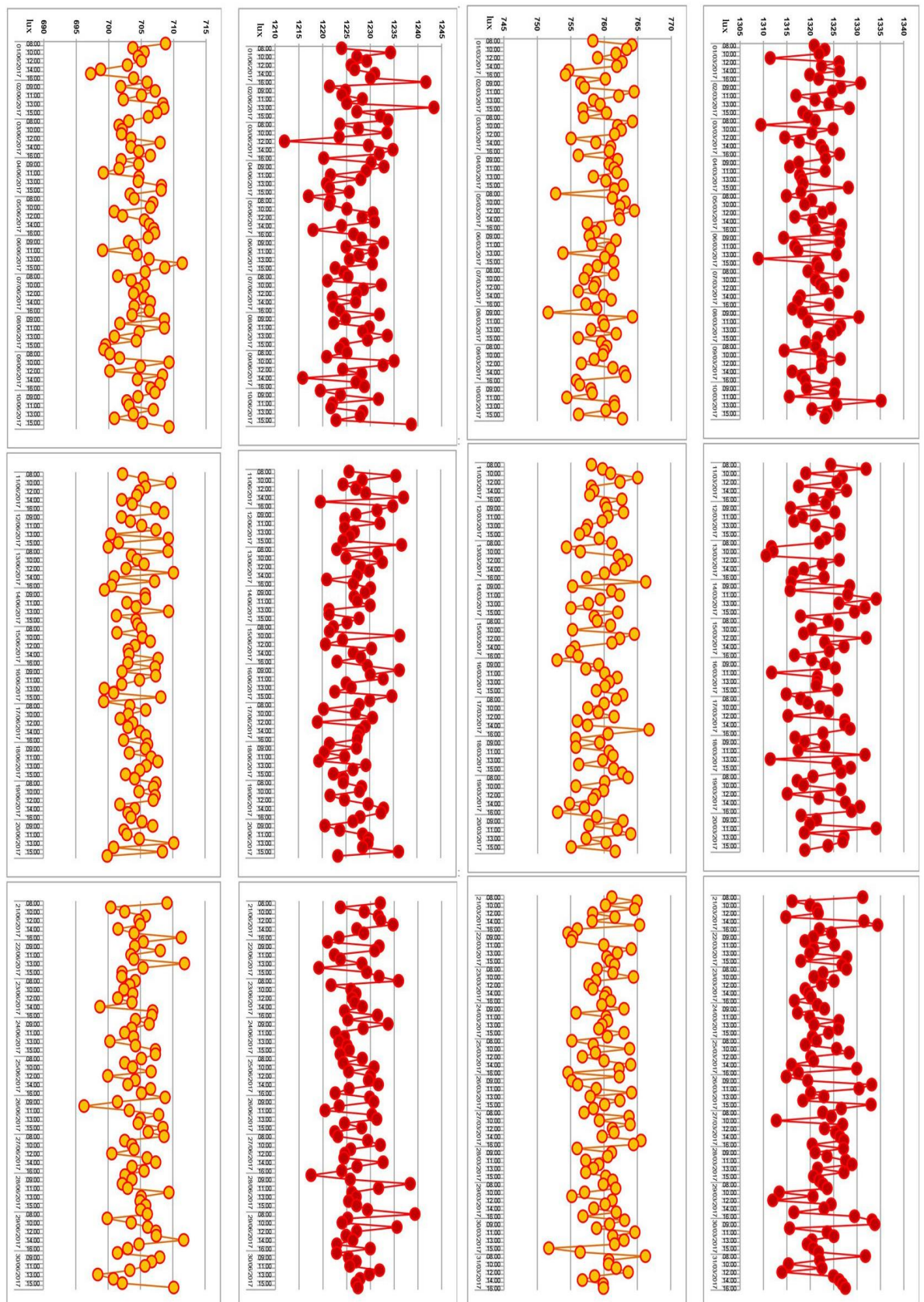


Figure 96 Average illuminance for Singapore. Respectively, E_{av} in March without (red lines) and with (orange lines) OPVs; E_{av} in June without and with OPVs.

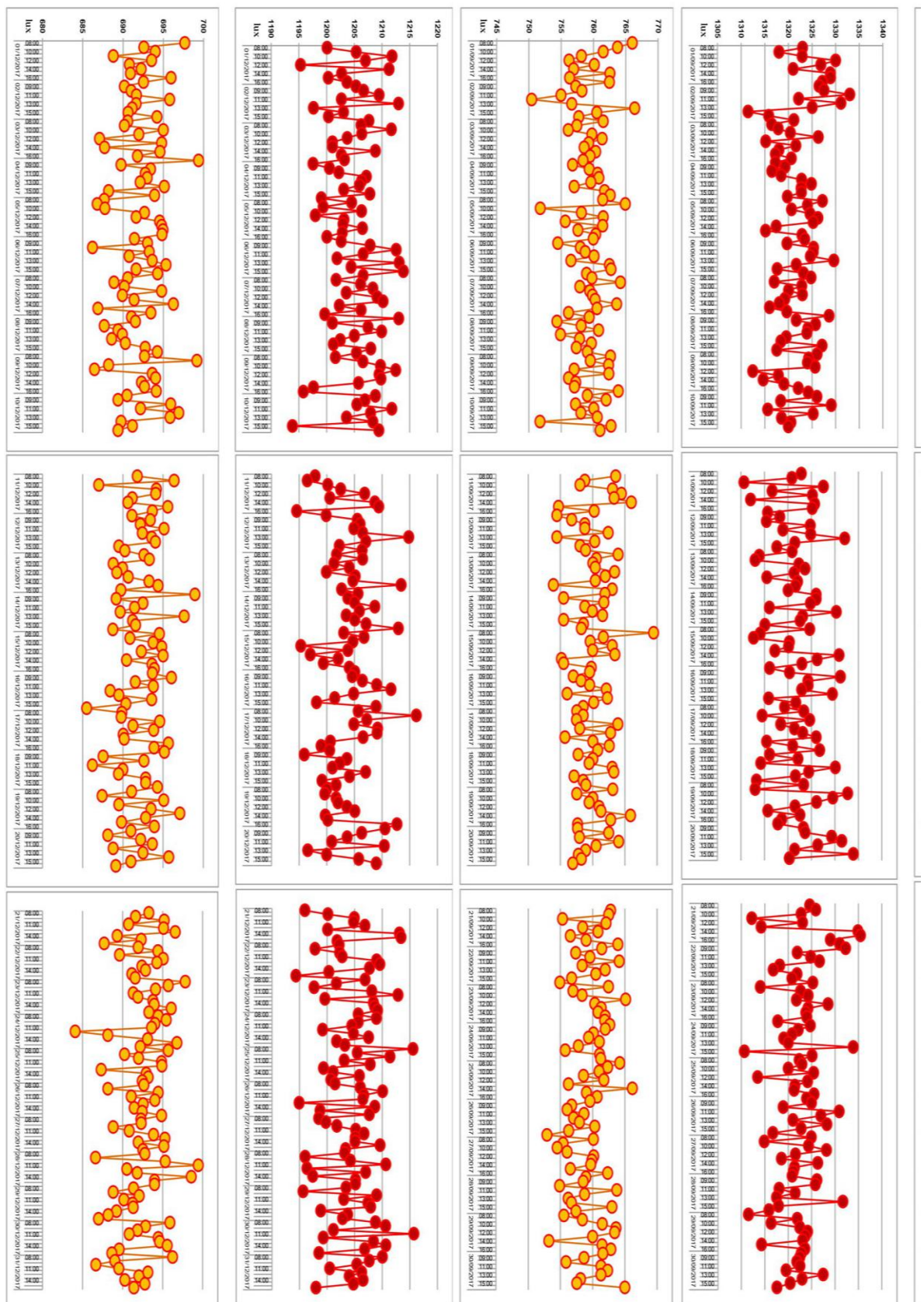


Figure 97 Average illuminance for Singapore. Respectively, E_{av} in September without (red lines) and with (orange lines) OPVs; E_{av} in December without and with OPVs.

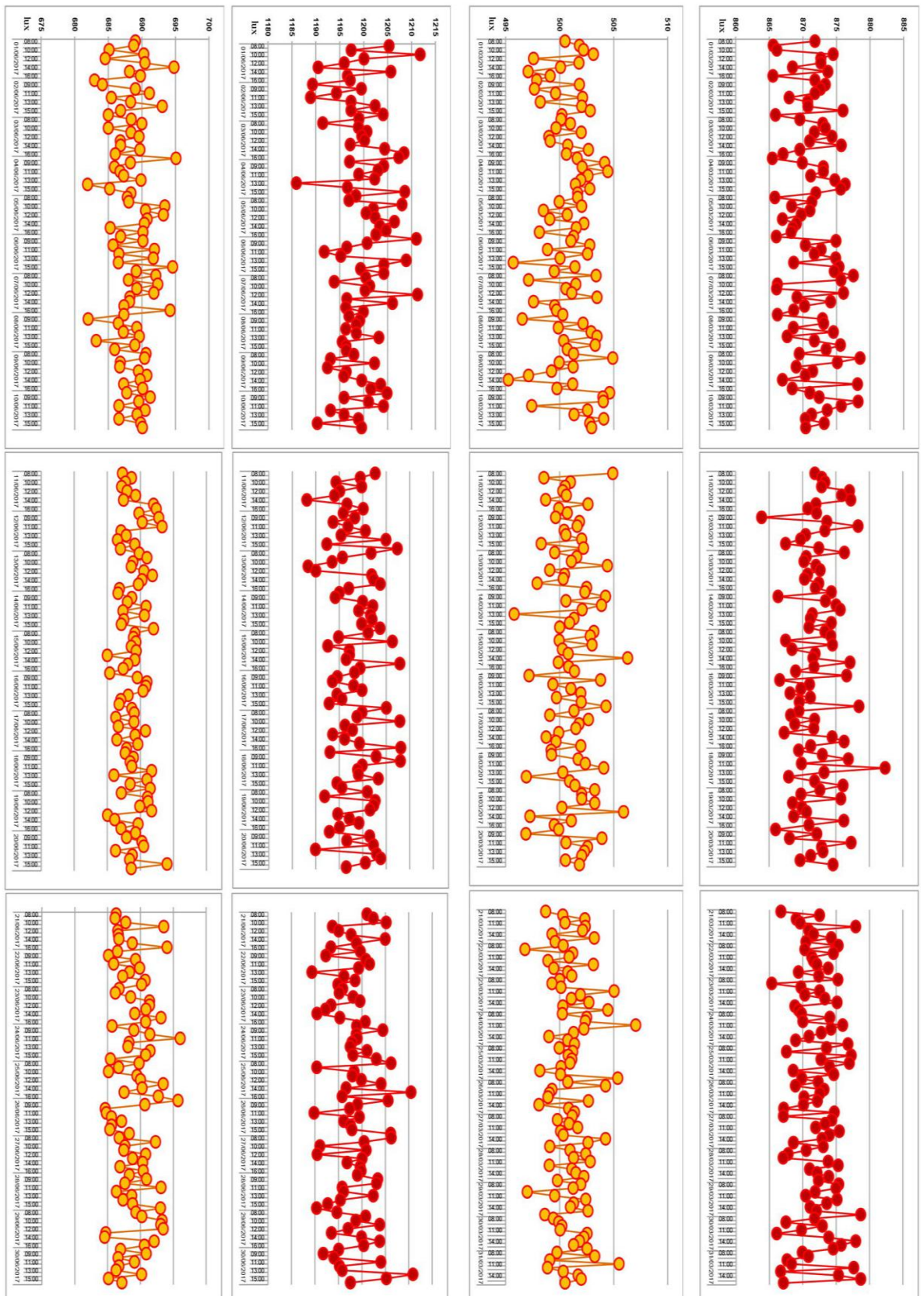


Figure 98 Average illuminance for Stuttgart. Respectively, E_{av} in March without (red lines) and with (orange lines) OPVs; E_{av} in June without and with OPVs.

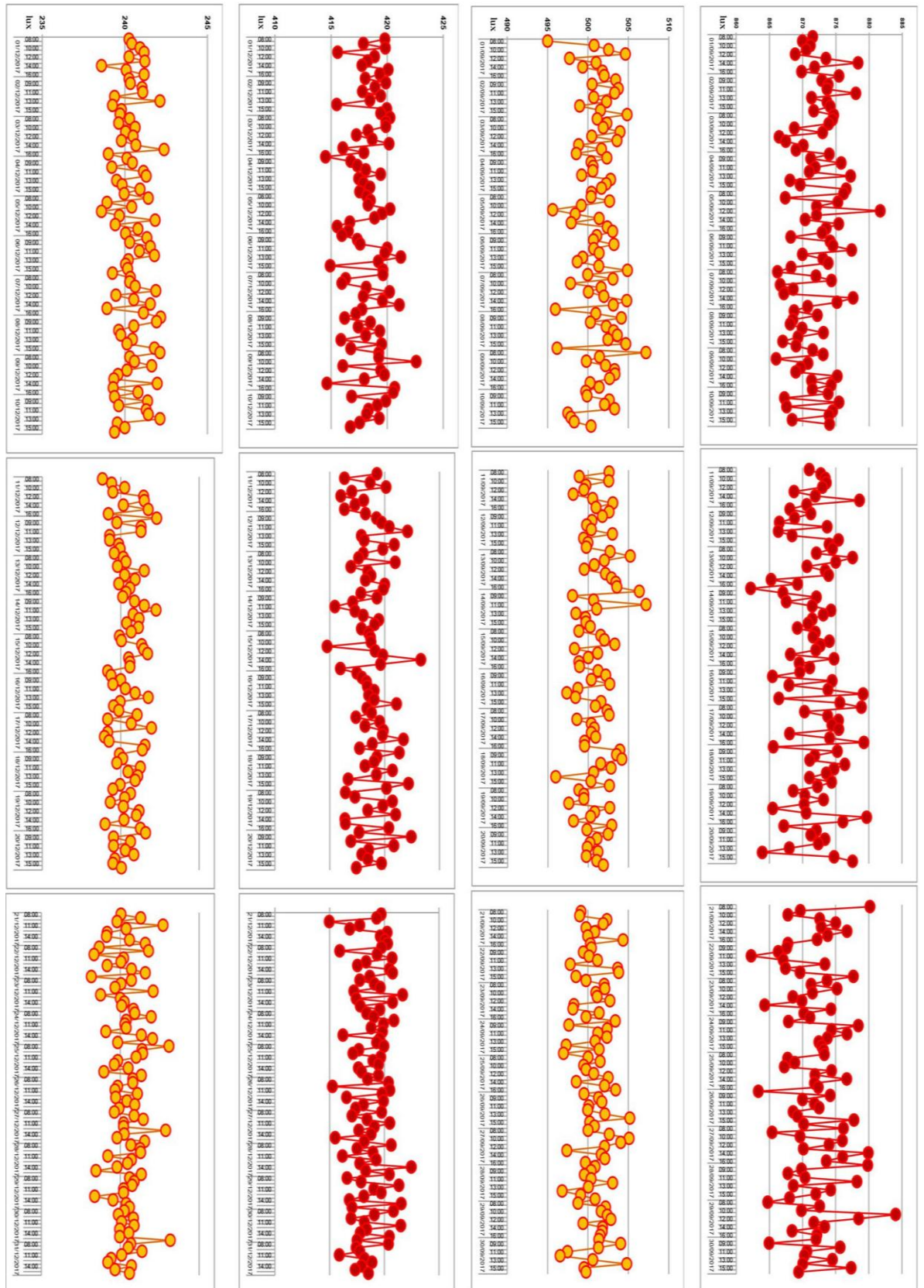


Figure 99 Average illuminance for Stuttgart. Respectively, E_{av} in September without (red lines) and with (orange lines) OPVs; E_{av} in December without and with OPVs.

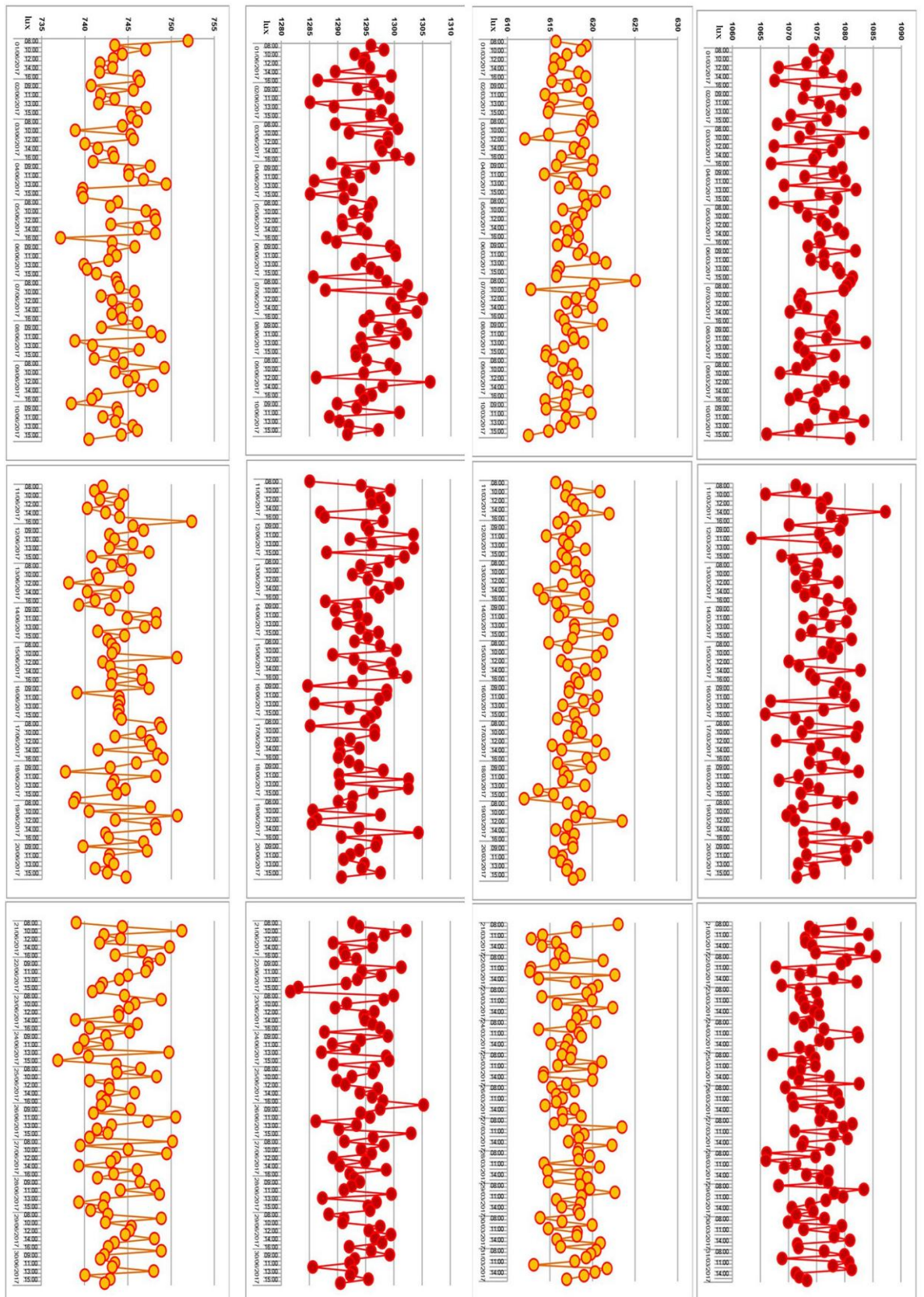


Figure 100 Average illuminance for Tokyo. Respectively, E_{av} in March without (red lines) and with (orange lines) OPVs; E_{av} in June without and with OPVs.

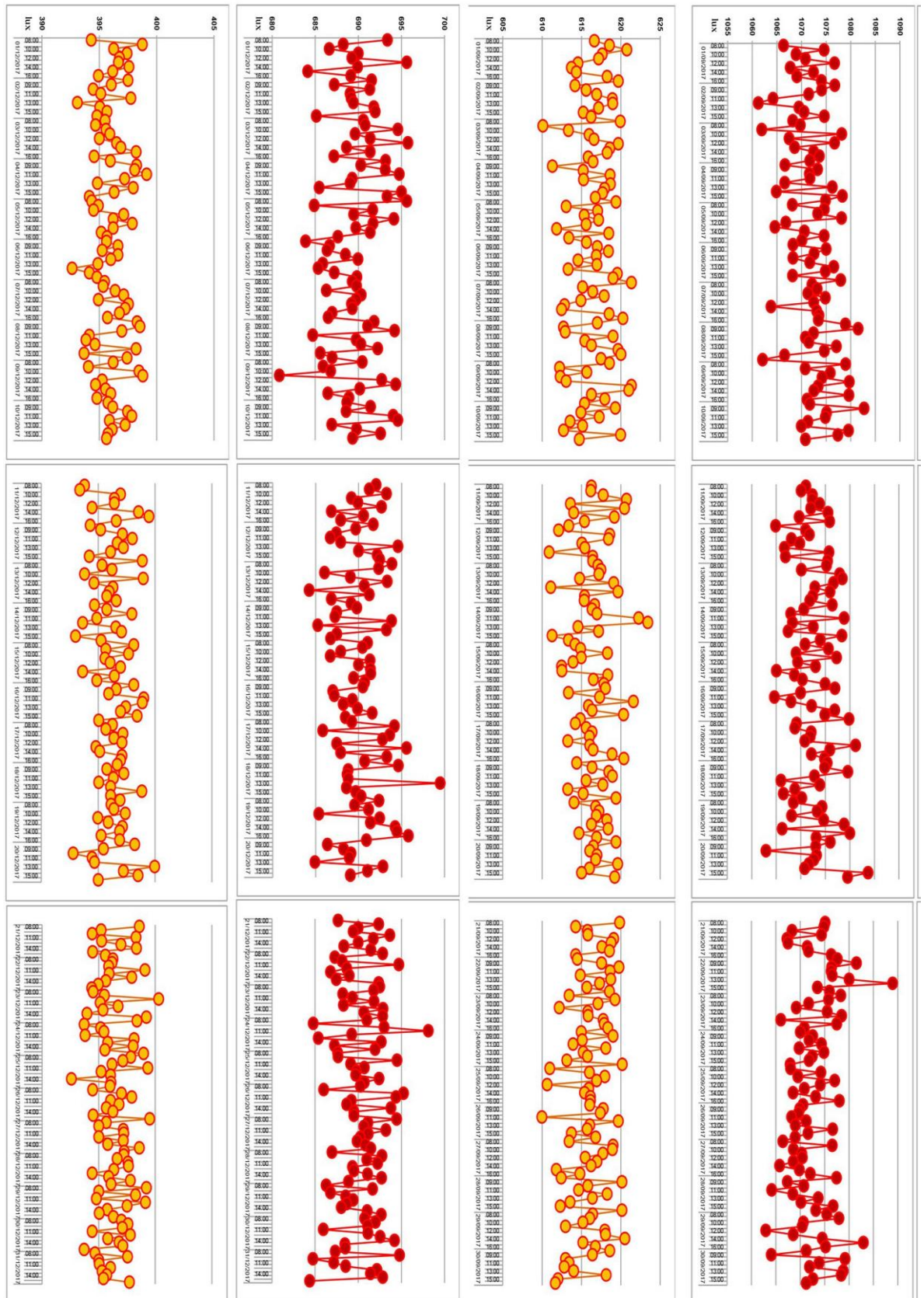
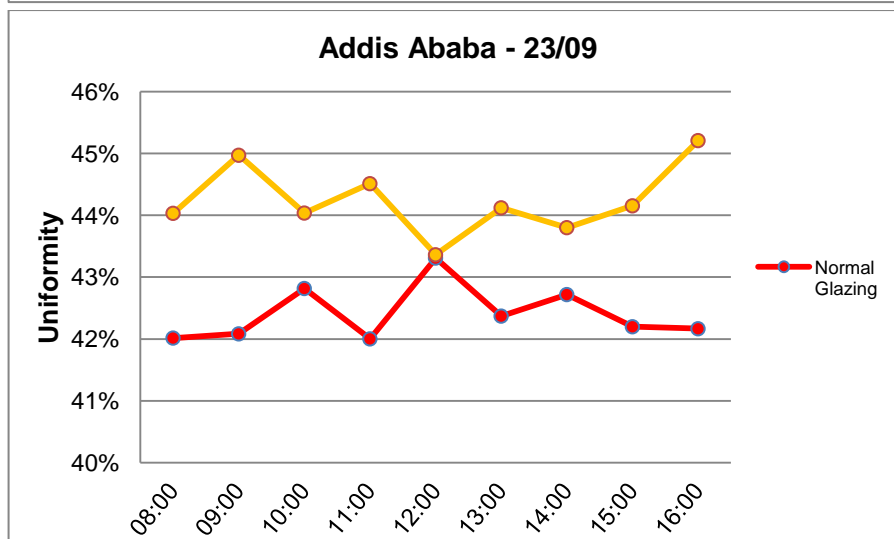
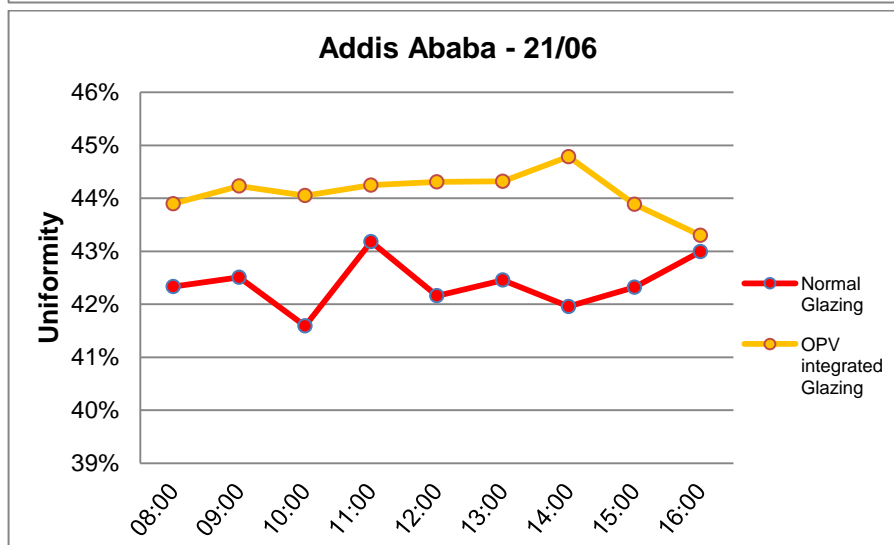
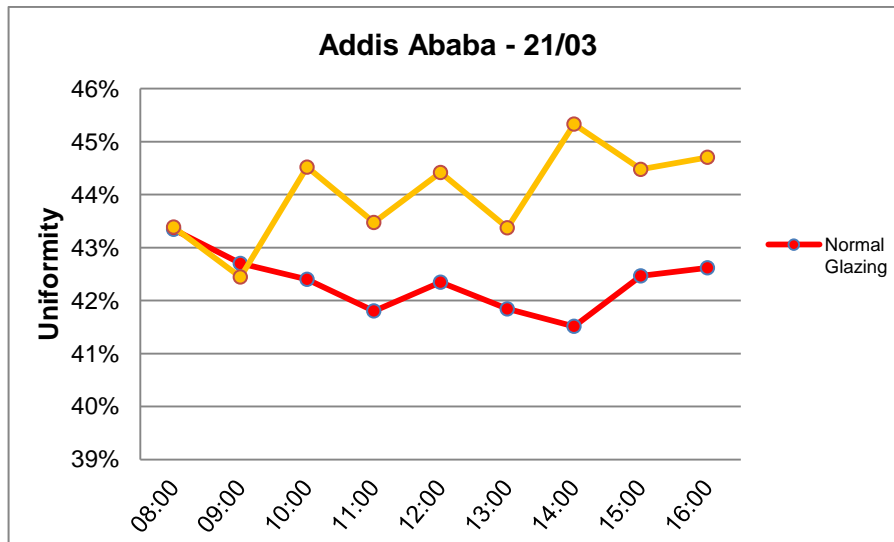


Figura 101 Average illuminance for Tokyo. Respectively, E_{av} in September without (red lines) and with (orange lines) OPVs; E_{av} in December without and with OPVs.



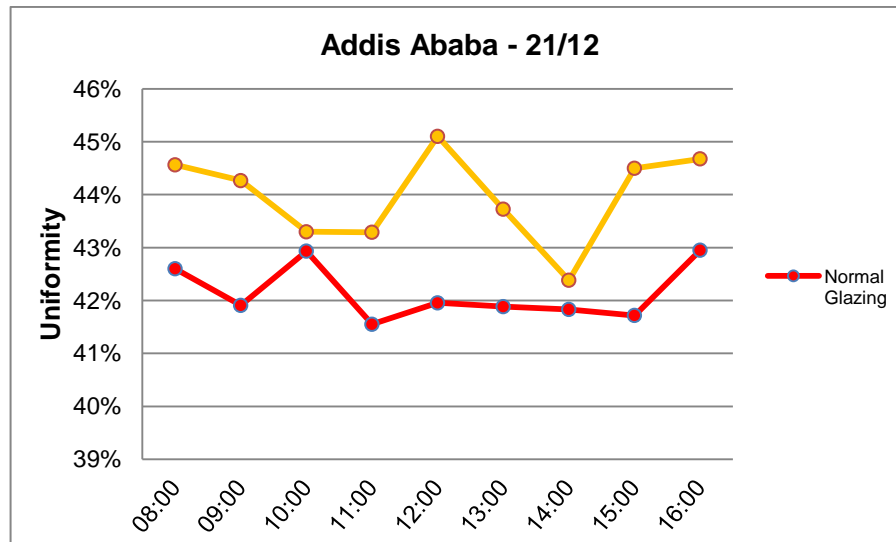
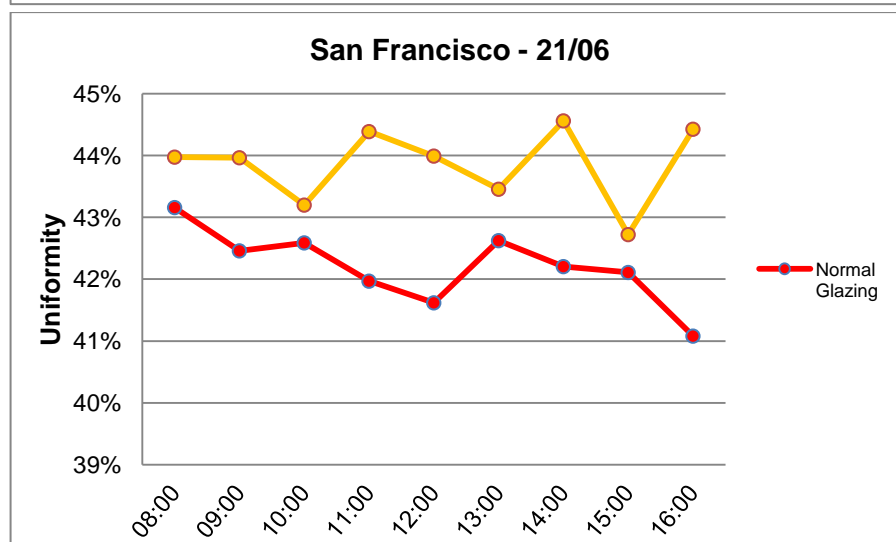
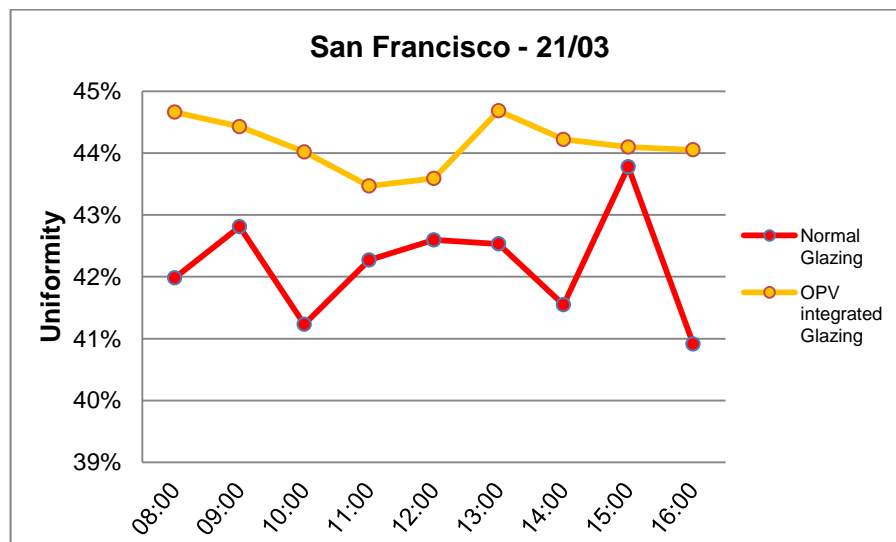


Figure 102 Average illuminance distribution in Addis Ababa for models cases without and with OPVS.



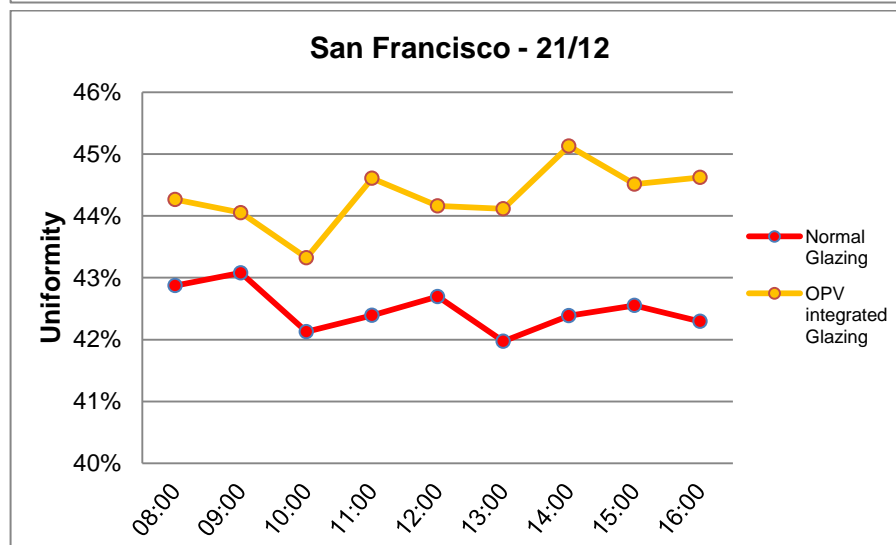
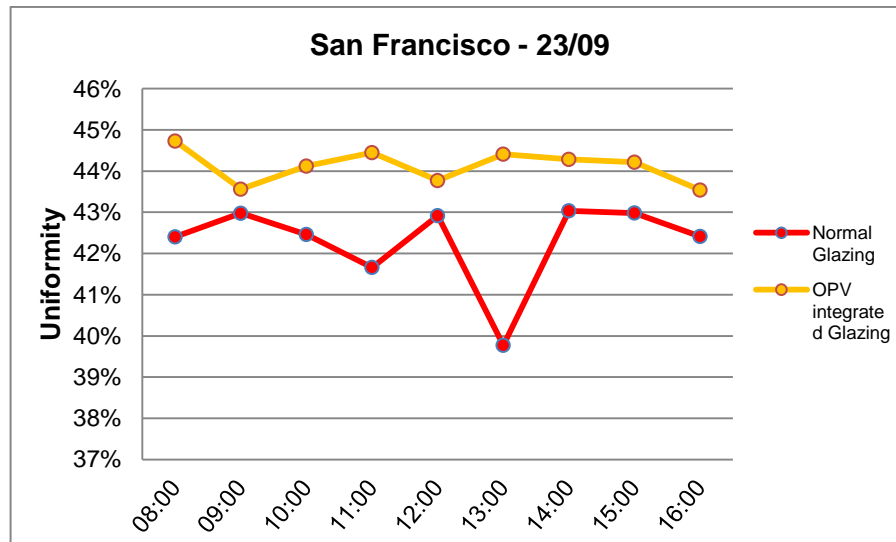
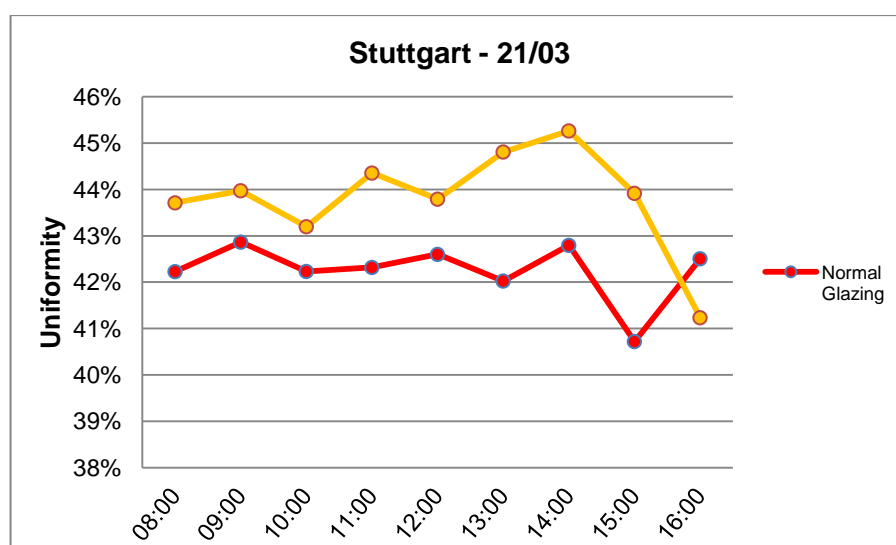


Figure 103 Average illuminance distribution in San Francisco for models cases without and with OPVS.



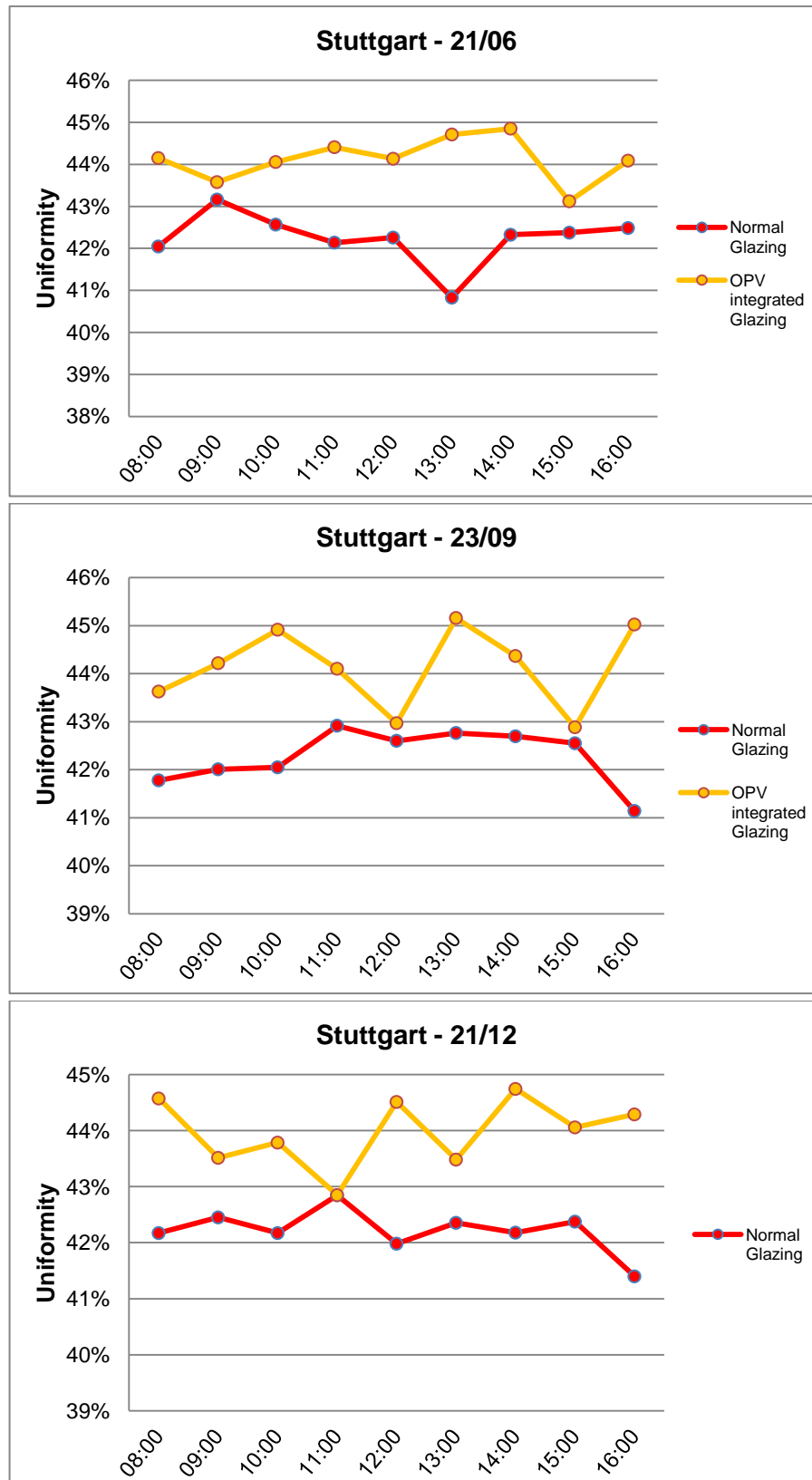
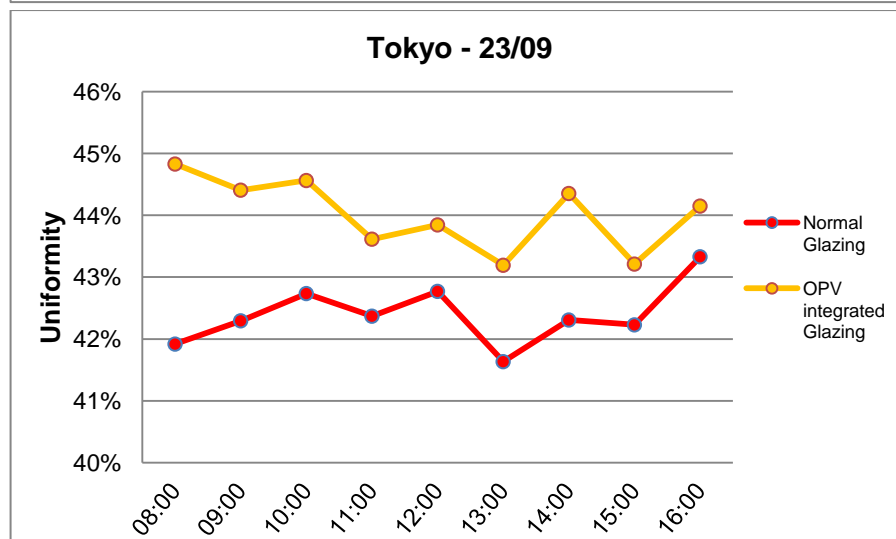
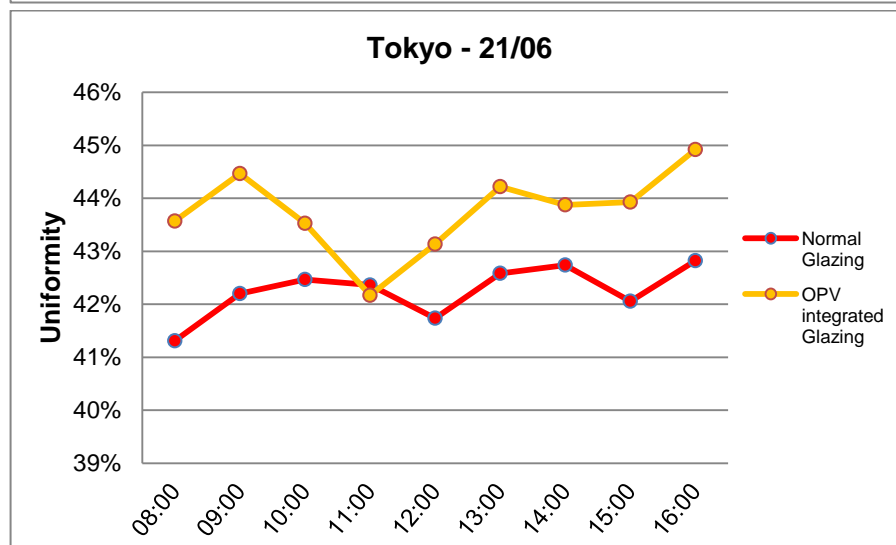
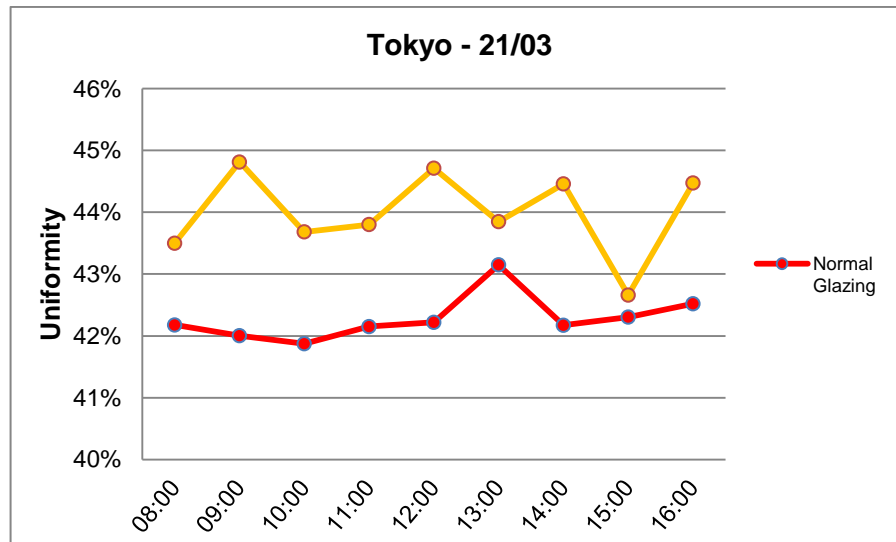


Figure 104 Average illuminance distribution in Stuttgart for models cases without and with OPVS.



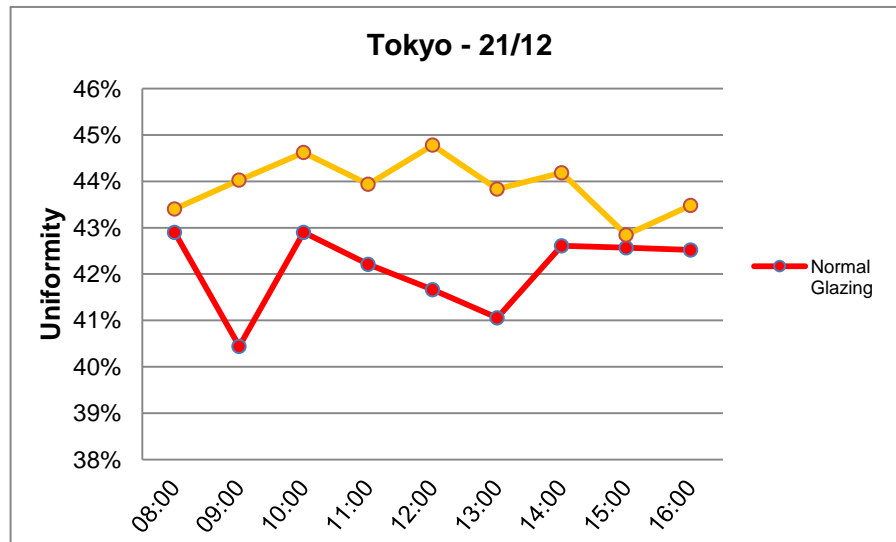


Figura 105 Average illuminance distribution in Tokyo for models cases without and with OPVS.

Table 31 Luminance distribution on 21.03 for every model case.

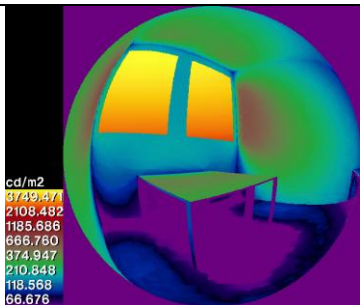
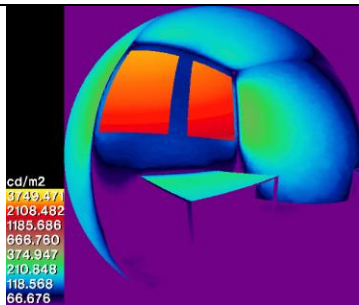
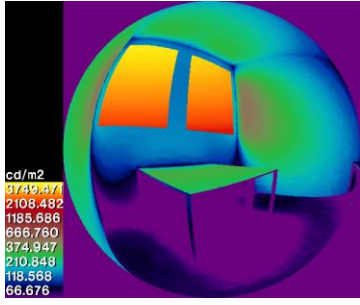
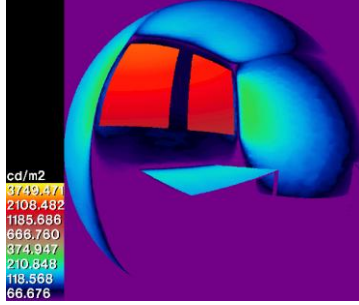
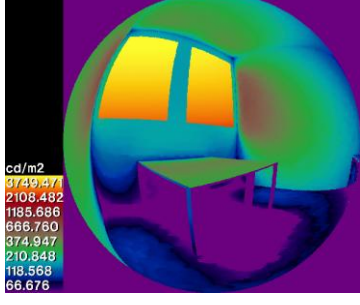
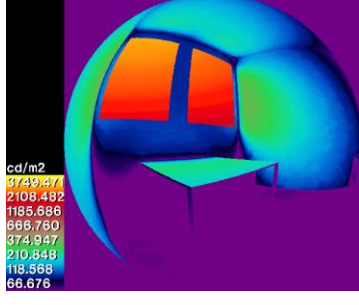
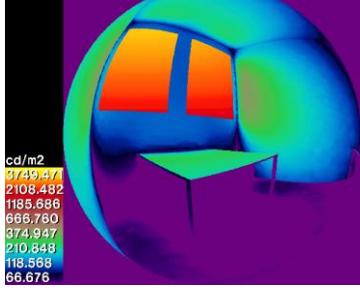
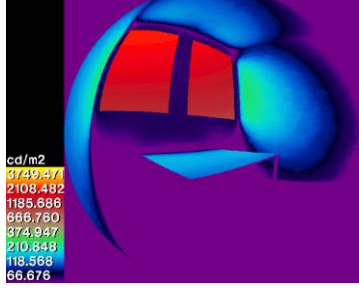
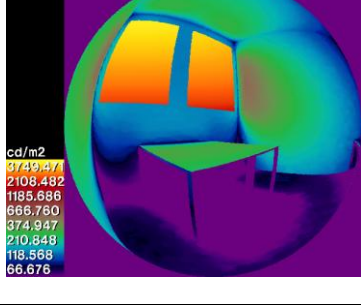
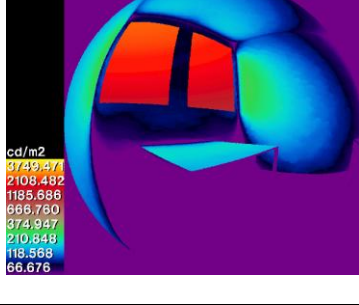
	Scene 3	Scene 3 with OPVs
Addis Ababa		
San Francisco		
Singapore		
Stuttgart		
Tokyo		

Table 32 Luminance distribution on 21.06 for every model case.

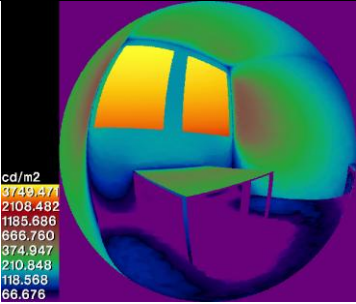
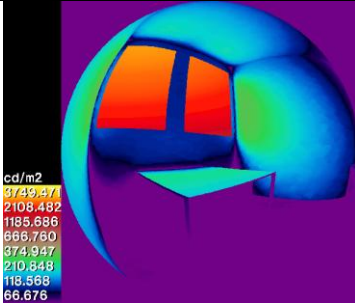
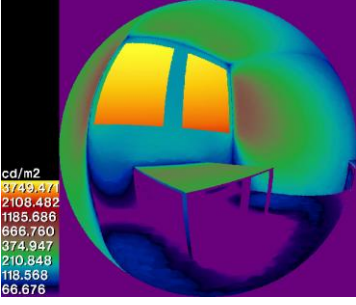
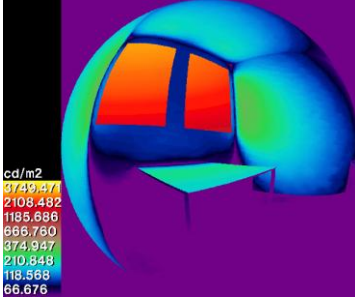
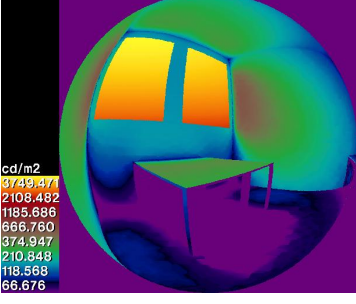
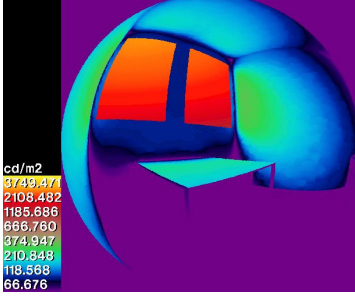
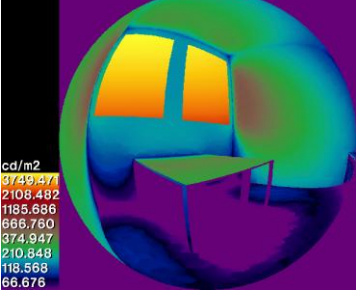
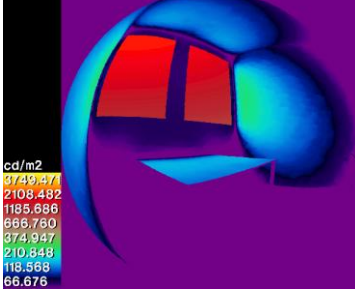
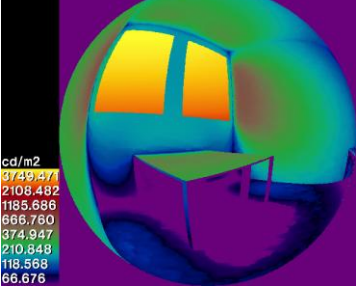
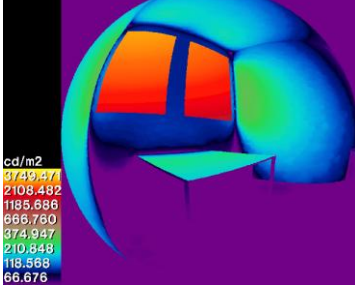
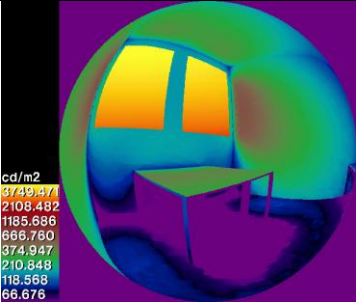
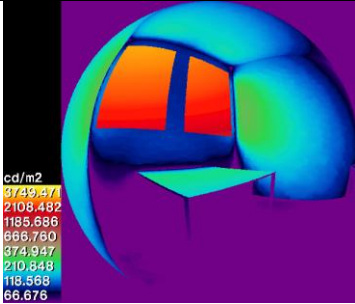
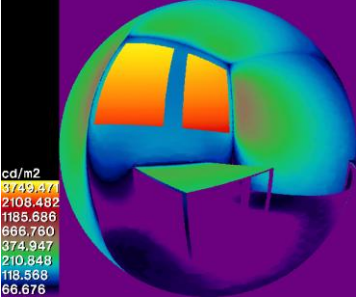
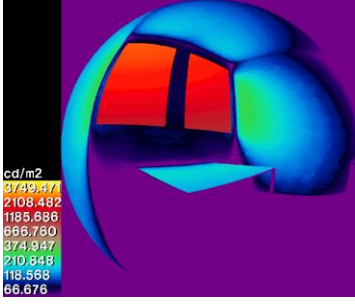
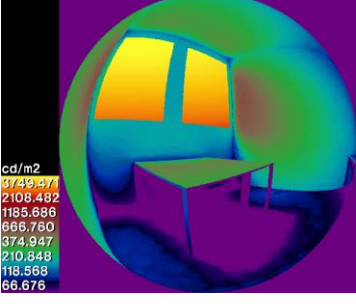
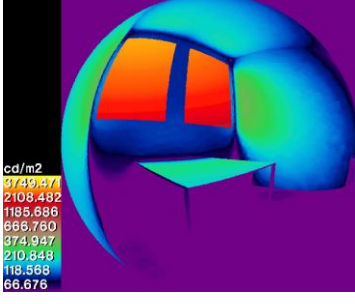
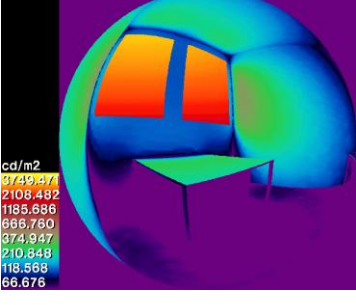
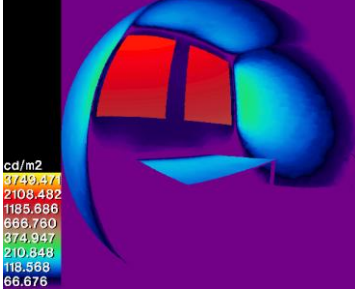
	Scene 3	Scene 3 with OPVs
Addis Ababa		
San Francisco		
Singapore		
Stuttgart		
Tokyo		

Table 33 Luminance distribution on 23.09 for every model case.

	Scene 3	Scene 3 with OPVs
Addis Ababa		
San Francisco		
Singapore		
Stuttgart		
Tokyo	